December 2011

Environmental Technology Verification Report

VERIFICATION OF BUILDING PRESSURE CONTROL AS CONDUCTED BY GSI ENVIRONMENTAL, INC. FOR THE ASSESSMENT OF VAPOR INTRUSION

Prepared by
Battelle

Battelle
The Business of Innovation

Under a cooperative agreement with

EPA **U.S. Environmental Protection Agency**

ETV ETV ETV

December 2011

Environmental Technology Verification Report

ETV Advanced Monitoring Systems Center

VERIFICATION OF BUILDING PRESSURE CONTROL AS CONDUCTED BY GSI ENVIRONMENTAL, INC. FOR THE ASSESSMENT OF VAPOR INTRUSION

by

Ian MacGregor, Mary Prier, Dale Rhoda, and Amy Dindal, Battelle
John McKernan, U.S. EPA

Notice

The U.S. Environmental Protection Agency, through its Office of Research and Development, funded and managed, or partially funded and collaborated in, the research described herein. It has been subjected to the Agency's peer and administrative review. Any opinions expressed in this report are those of the author(s) and do not necessarily reflect the views of the Agency, therefore, no official endorsement should be inferred. Any mention of trade names or commercial products does not constitute endorsement or recommendation for use.

Foreword

The EPA is charged by Congress with protecting the nation's air, water, and land resources. Under a mandate of national environmental laws, the Agency strives to formulate and implement actions leading to a compatible balance between human activities and the ability of natural systems to support and nurture life. To meet this mandate, the EPA's Office of Research and Development provides data and science support that can be used to solve environmental problems and to build the scientific knowledge base needed to manage our ecological resources wisely, to understand how pollutants affect our health, and to prevent or reduce environmental risks.

The Environmental Technology Verification (ETV) Program has been established by the EPA to verify the performance characteristics of innovative environmental technology across all media and to report this objective information to permitters, buyers, and users of the technology, thus substantially accelerating the entrance of new environmental technologies into the marketplace. Verification organizations oversee and report verification activities based on testing and quality assurance protocols developed with input from major stakeholders and customer groups associated with the technology area. ETV consists of six environmental technology centers. Information about each of these centers can be found on the Internet at http://www.epa.gov/etv/.

Effective verifications of monitoring technologies are needed to assess environmental quality and to supply cost and performance data to select the most appropriate technology for that assessment. Under a cooperative agreement, Battelle has received EPA funding to plan, coordinate, and conduct such verification tests for "Advanced Monitoring Systems for Air, Water, and Soil" and report the results to the community at large. Information concerning this specific environmental technology area can be found on the Internet at http://www.epa.gov/etv/centers/center1.html.

Acknowledgments

The authors wish to acknowledge the contribution of the many individuals, without whom this verification testing would not have been possible. Quality assurance oversight was provided by Jonathan Tucker, NAVFAC Atlantic, Michelle Henderson and Laurel Staley, U.S. EPA and Rosanna Buhl, Battelle. We gratefully acknowledge Dr. Bart Chadwick and Dr. Ignacio Rivera-Duarte at SPAWAR Systems Center Pacific for sponsoring this work through the Navy Environmental Sustainability Development to Integration Program, as part of Project 424 on "Improved Assessment Strategies for Vapor Intrusion." This technology was evaluated concurrently in a project sponsored by the Environmental Security Technology Certification Program (ESTCP), and the contribution of effort from ESTCP Project ER-0707 in the implementation of this verification test is also gratefully acknowledged. We thank the various participants on the panel of technical experts who provided input to and reviewed the Quality Assurance Project Plan. Moreover, we thank Dr. Brian Schumacher (U.S. EPA), Ms. Donna Caldwell (NAVFAC Atlantic), and Dr. Ronald Mosley (US EPA, retired) for their review of this verification report. Finally we gratefully acknowledge the work of the technology vendor, Dr. Thomas McHugh and Ms. Lila Beckley, at GSI Environmental, Inc.

Contents

Page

Foreword iii

Acknowledgments iv

List of Abbreviations ix

Chapter 1 Background 1

Chapter 2 Technology Description 2

Chapter 3 Test Design and Procedures 5
3.1 Test Overview 5
3.2 Test Site Descriptions 7
3.2.1 ASU VI Research House 7
3.2.2 Moffett Field Building 107 8
3.3 Experimental Design 9
3.3.1 Decision-making Support 17
3.3.1.1 Building Pressure Differential 18
3.3.1.2 Vapor Intrusion Enhancement and Reduction 18
3.3.1.3 Fractional Contribution of Vapor Intrusion to Indoor CoC Concentrations 20
3.3.2 Comparability 22
3.3.3 Operational Factors 22
3.3.4 Validation of Mosley Model Assumptions 23

Chapter 4 Quality Assurance/Quality Control 25
4.1 Quality Control Results 25
4.2 Data Quality Indicators 29
4.3 Audits 29
4.3.1 Technical Systems Audits 30
4.3.2 Audits of Data Quality 31

Chapter 5 Statistical Methods 34
5.1 Decision-making Support 34
5.1.2 Vapor Intrusion Enhancement And Reduction 35
5.1.3 Fractional Contribution of Vapor Intrusion to indoor CoC concentrations 36
5.2 Comparability 37
5.3 Verification of Model Assumptions 37

Chapter 6 Test Results 40
6.1 Measurement Results From Both Buildings 40
6.1.1 Indoor/Outdoor and Cross-Foundation Pressure Differentials 40
6.1.2 Building Ventilation Rates 41
6.1.3 Concentrations of Compounds in Ambient Air 42
6.1.4 Concentrations of Compounds in Indoor Air 43
6.1.5 Concentrations of Compounds in Sub-Slab Soil Gas 47
6.1.6 Mass Discharges 49
6.2 Decision-making Support 53
6.2.1 Building Pressure Differential 53
6.2.2 Vapor Intrusion Enhancement and Reduction 54
6.2.3 Fractional Contribution of Vapor Intrusion to Indoor CoC Concentrations 56

6.3 Comparability 59
6.4 Operational Factors 59
6.5 Validation of Model Assumptions 60
Chapter 7 Performance Summary 65
Chapter 8 References 69
Appendix A Supplemental Information 72

Tables

Table 1. Mosley Model Notation Used for Description of Several Verification Parameters. 7
Table 2. Days/times for Pressure Control Testing at Each Building 10
Table 3. Types of and Locations for Air Samples Collected During Each of the Three Pressure Perturbation Periods. 14
Table 4. Summary of Sample Types and Timing for Sample Collection at Each Test Building. 15
Table 5. Summary of Results of Various QC Procedures and Samples. 26
Table 6. Summary of Frequency of Measurements Lower Than Estimated MDLs. 29
Table 7. Indoor/outdoor pressure differentials 53
Table 8. Comparison of Radon Mass Discharges from Subsurface Sources to Determine VI Enhancement and Reduction 55
Table 9. Comparison of Indoor and Ambient Air Radon Concentrations under Positive Pressure. 56
Table 10. Fractional Contribution of Ambient Sources, Indoor Sources, and VI to Indoor CoC Concentrations Under Baseline Conditions. 57
Table 11. Comparability of Building Pressure Control Results. 59
Table 12. Validation of Model Assumption 1. 61
Table 13. Validation of Model Assumption 2. 62
Table 14. Validation of Model Assumptions 3, 4, and 5. 62
Table 15. Validation of Model Assumptions 6, 7, and 8. 63
Table 16. Minimum Detectable Differences for Model Assumptions 1 and 2 at Moffett Field Building 107. 64

Figures

Figure 1. Basis of Building Pressure Control Technique for the Assessment of the Impact of VI on Concentrations of CoCs in Indoor Air 3
Figure 2. Delivery of SF_6 to the Building Atmosphere; Collection of SS Air Sample with a PVF Bag; and Collection of an IA Sample into a Stainless Steel Canister. 4
Figure 3. Photographs of the ASU VI Research House 8
Figure 4. Photographs of Moffett Field Building 107 9
Figure 5. Pressure Differential Measurements at ASU House 11
Figure 6. SF_6 Tracer Gas Delivery System as Deployed at Moffett Field Building 107 12
Figure 7. Fan Installed for Building Pressure Control at the ASU House. 13
Figure 8. IA, AA, and SS sampling at ASU House 16
Figure 9. Indoor/Outdoor and Cross-Foundation Differential Pressure Measurements under Three Different Pressure Conditions 41
Figure 10. Building Ventilation Rates Measured under Three Different Pressure Conditions. ... 42
Figure 11. Concentrations of Compounds Measured in Ambient Air 43
Figure 12. Concentrations of Compounds Measured in Indoor Air 44
Figure 13. Average Indoor Air Concentrations Normalized by Ambient Concentrations. 46
Figure 14. Concentrations of Compounds Measured in Sub Slab Soil Gas 47
Figure 15. Average Sub-Slab Concentrations Normalized by Average Indoor Air Concentrations 48
Figure 16. Normalized Mass Discharges at ASU House for Radon, TCE, 1,1-DCE, SF_6, Benzene and Toluene. 51
Figure 17. Normalized Mass Discharges at Moffett Field Building 107 for Radon, TCE, PCE, SF_6, Benzene, and Toluene 52

List of Abbreviations

1,1-DCE	1,1-dichloroethylene
ΔP	differential pressure
ΔF_{VI}	error in F_{VI}
AA	ambient air
AER	air exchange rate
ADQ	audit of data quality
AMS	Advanced Monitoring Systems
ASU	Arizona State University
BL	baseline
COA	certificates of analysis
CoC(s)	contaminant(s) of concern
DQIs	data quality indicators
DQOs	data quality objectives
EPA	U.S. Environmental Protection Agency
ESTCP	Environmental Security Technology Certification Program
ETV	Environmental Technology Verification
F_a	fractional contribution of ambient air to the indoor concentration of a CoC
F_{in}	fractional contribution of indoor sources to the indoor concentration of a CoC
F_{VI}	fractional contribution of vapor intrusion to the indoor concentration of a CoC
GC/ECD	gas chromatography with electron capture detection
GC/MS	gas chromatography/mass spectrometry
H_0	null hypothesis
H_1	alternative hypothesis
Hg	mercury
HVAC	heating, ventilating and air conditioning
IA	indoor air
I/O	indoor/outdoor
LRB	laboratory record book
MDL	method detection limit
MDT	Mountain Daylight Time
NAVFAC	Naval Facilities Engineering Command
NIOSH	National Institute of Occupational Safety and Health
NP	negative pressure
pCi L^{-1}	picocuries per liter
Pa	Pascal
PCE	perchloroethylene (tetrachloroethylene)
PDT	Pacific Daylight Time
PP	positive pressure
PVF	polyvinyl fluoride
QA	quality assurance
QAO	Quality Assurance Officer
QAPP	quality assurance project plan
QC	quality control
QMP	Quality Management Plan
Rn	Radon
RPD	relative percent difference

SF_6	sulfur hexafluoride
SIM	single ion monitoring
SPAWAR	Space and Naval Warfare
SS	subslab
TCE	trichloroethylene
TSA	technical systems audit
$\mu g\ m^{-3}$	microgram per cubic meter
VI	vapor intrusion
VOC	volatile organic compound
VTC	Verification Test Coordinator

Chapter 1
Background

The U.S. Environmental Protection Agency (EPA) supports the Environmental Technology Verification (ETV) Program to facilitate the deployment of innovative environmental technologies through performance verification and dissemination of information. The goal of the ETV Program is to further environmental protection by accelerating the acceptance and use of improved and cost-effective technologies. ETV seeks to achieve this goal by providing high-quality, peer-reviewed data on technology performance to those involved in the design, distribution, financing, permitting, purchase, and use of environmental technologies.

ETV works in partnership with recognized testing organizations; with stakeholder groups consisting of buyers, vendor organizations, and permitters; and with the full participation of individual technology developers. The program evaluates the performance of innovative technologies by developing test plans that are responsive to the needs of stakeholders, conducting field or laboratory tests (as appropriate), collecting and analyzing data, and preparing peer-reviewed reports. All evaluations are conducted in accordance with rigorous quality assurance (QA) protocols to ensure that data of known and adequate quality are generated and that the results are defensible. The definition of ETV verification is to establish or prove the truth of the performance of a technology under specific, pre-determined criteria or protocols and a strong quality management system. The highest-quality data are assured through implementation of the ETV Quality Management Plan. ETV does not endorse, certify, or approve technologies.

The EPA's National Risk Management Research Laboratory (NRMRL) and its verification organization partner, Battelle, operate the Advanced Monitoring Systems (AMS) Center under ETV. The AMS Center recently evaluated the performance of the building pressure control technique for the assessment of the impact of vapor intrusion (VI) on the concentrations of contaminants of concern (CoCs) in indoor air (IA). The pressure control technique was conducted by the technology vendor, GSI Environmental, Inc.

Chapter 2
Technology Description

This report provides results for the verification testing of a building pressure control technique for the assessment of the impact of VI on the concentrations of CoCs in IA. This section provides information on why developing such a technique is important, as well as a description of the pressure control technique itself. GSI Environmental, Inc. was the technology vendor conducting this technique for this verification test.

VI is the migration of volatile chemicals from the subsurface (from soils and/or groundwater) into the air of overlying buildings.[1] Adverse health effects may result from inhalation exposure to certain CoCs such as the volatile organic compounds (VOCs) trichloroethylene (TCE), tetrachloroethylene (perchloroethylene, PCE), 1,1-dichloroethylene (1,1-DCE), and benzene.[i] Reducing or controlling the risk to human health related to inhalation exposure of CoCs due to VI is the stated goal of many regulatory and governmental agencies. That said, many building owners and regulated entities (such as the U.S. Navy)[2,3] have developed policies and guidance to state that they are not responsible for the mitigation of CoCs in the IA of structures in cases where the CoCs are present due to natural or anthropogenic background sources.[ii] Thus, the ability to distinguish concentrations of CoCs in background IA – defined for CoCs as everything unrelated to the vapors that migrate into the overlying structure (from sources such as household activities, consumer products, and building materials)[4] – from CoCs present due to VI is of key importance so that regulated entities can appropriately manage their limited resources when making remediation and mitigation decisions. However, at present little guidance is available to determine the impact of VI compared to the impact of natural or anthropogenic background sources on indoor concentrations of CoCs. One technique that has shown promise for distinguishing background indoor sources of CoCs from those present due to VI is the manipulation of building pressure.[5, 6, 7] Other work[8] in this area has shown that radon occurs naturally in soil gas due to the radioactive decay of uranium, and as a result, in ambient air (AA) at concentrations of 0.2 to 0.7 picocuries per liter (pCi L^{-1}).[9] Therefore, radon may be used to evaluate the VI of CoCs. The performance of the method of measuring radon and CoCs under different building pressures to assess the impact of VI on the concentrations of CoCs in IA (the "building pressure control technique") is the subject of this verification test.

Intentionally inducing negative pressure (NP) or positive pressure (PP) in the building– by use of a fan to drive IA out of the building, or AA into the building, respectively – should enhance or

[i] VOC and CoC are used interchangeably throughout this report.
[ii] Navy guidance states that chemicals from background sources should not be considered CoCs. However, in his report the term CoC may refer to chemicals from either background or VI sources.

reduce VI. This is the conceptual basis for the building pressure control technique and is shown in Figure 1. Under conditions of induced NP (top panel), VI should be enhanced; under induced PP, VI should be stopped or reduced, as shown in the bottom panel. Arrows in the figures indicate the expected direction of air flows. During implementation of the building pressure control method, various types of air samples are collected to demonstrate VI manipulation, as shown by the various symbols in the figure.

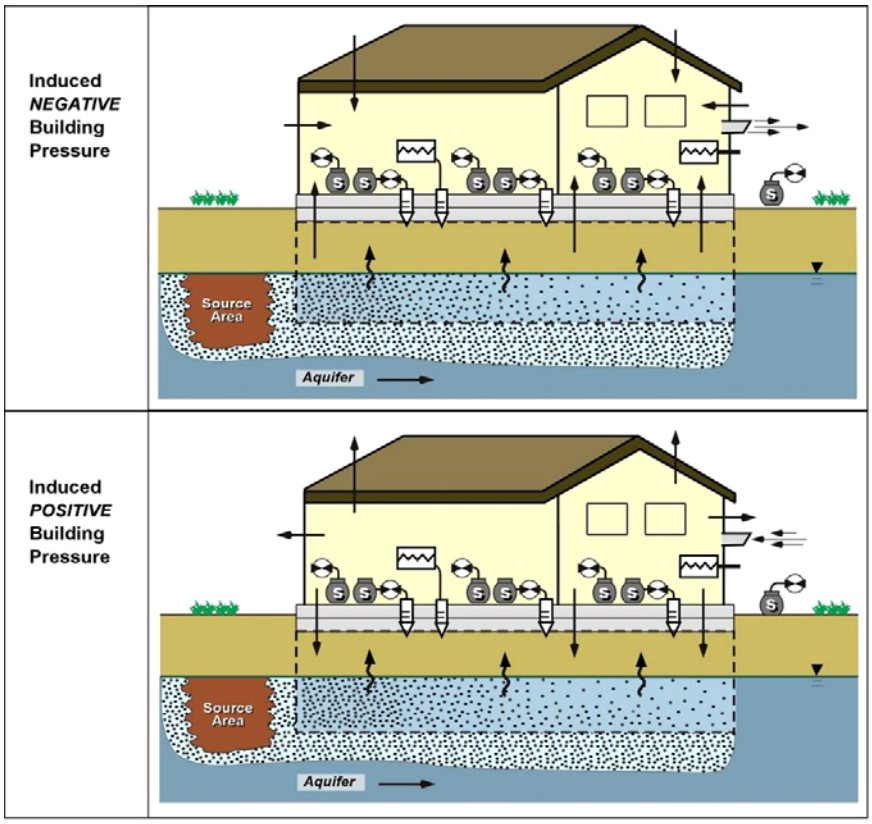

Figure 1. Basis of Building Pressure Control Technique for the Assessment of the Impact of VI on Concentrations of CoCs in Indoor Air. (Figure courtesy of GSI.)

Implementation of the building pressure control technique for the assessment of the impact of VI on the IA at a given building takes place over approximately 3½ days. Over the first half day, the building is prepared for testing. This includes installation of three subslab (SS) sampling points through the building's concrete foundation as well as setting up and verifying the operation of the various air sampling equipment and instrumentation. Over the next 24 hours, the building is maintained under baseline (BL) pressure where the building pressure is not intentionally manipulated. Over the following 24 hours, a NP is induced in the building. Over the final 24 hours, a PP is induced in the building. To accomplish building pressurization and depressurization, windows, and other openings are closed[iii] and a fan is installed in a doorway or window.

During each 24 hour period of BL, NP, and PP testing, a known concentration of the tracer gas, sulfur hexafluoride or SF_6, is released at a known flow rate from a centralized location in the

[iii] Doors and windows are closed, but sealing egresses and vents is not attempted.

building. To the extent possible, indoor doors remain open throughout testing to enhance mixing of the IA. Using the known flow rate of SF_6 and measurements of indoor SF_6 concentrations, the flow rate of AA into the building, that is, the building's air exchange rate (AER) may be determined. Real-time measurement of the differential pressure (ΔP) across the building envelope (the indoor/outdoor (I/O) ΔP) and the building foundation are performed throughout BL, NP, and PP testing.

Finally, several different types of air samples from inside, outside, and below the building – for IA, AA, and SS soil gas, respectively – are also collected and analyzed to characterize concentrations of various CoCs, SF_6, and radon in these three compartments.[iv] Gas samples for analysis of CoCs and SF_6 are collected into stainless steel sampling canisters; whereas samples for radon analysis are collected into polyvinyl fluoride (PVF) DuPont™ Tedlar® gas sampling bags, or measured in near real-time using an instrument designed for this purpose. While the building is under each of the three pressure conditions, IA and SS concentrations of CoCs, SF_6, and radon are measured at three different spatially distributed locations throughout the building and at a single outdoor location. Shown schematically in Figure 2 is the SF_6 delivery system, SS sampling for radon into PVF bags, and IA sampling for VOCs and SF_6 into a stainless steel canister. Canisters and PVF bags are delivered to separate off-site contract analytical laboratories for gas analysis.

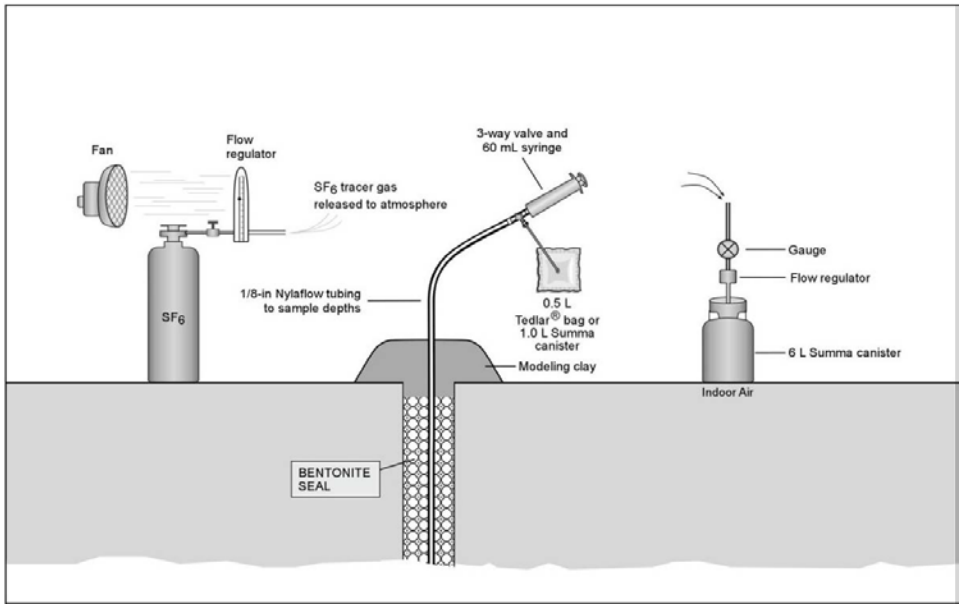

Figure 2. Delivery of SF_6 to the Building Atmosphere; Collection of SS Air Sample with a PVF Bag; and Collection of an IA Sample into a Stainless Steel Canister. (Figure courtesy of GSI.)

[iv] For this verification test, more samples were collected than are needed for routine implementation of this technology. For example, IA, AA, and SS air samples were collected. Routine implementation may be performed without collection of SS samples.

Chapter 3
Test Design and Procedures

3.1 Test Overview

This verification test was conducted according to procedures specified in the *Quality Assurance Project Plan for Verification of Building Pressure Control for the Assessment of Vapor Intrusion*[10] (QAPP) and adhered to the quality system defined in the ETV AMS Center Quality Management Plan (QMP).[11] As indicated in the QAPP, the testing conducted satisfied EPA QA Category III requirements. A panel of technical experts was convened to provide input to the QAPP development. The following experts provided input to the QAPP and provided a peer review of the QAPP and/or this verification report.

- Ms. Donna Caldwell, U.S. Navy, NAVFAC Atlantic
- Mr. Douglas Grosse, EPA, National Risk Management Research Laboratory
- Dr. Ronald Mosley, EPA (retired)
- Dr. Brian Schumacher, EPA, National Exposure Research Laboratory
- Ms. Lynn Spence, Spence Environmental Consulting

In addition, the VI technology category was reviewed with the broader AMS Center Stakeholder Committees during regular stakeholder teleconferences, including the November 5 and 12, 2009 meetings, and input from those committees was solicited.

Battelle conducted this verification test with funding support from the U.S. Navy SPAWAR Systems Center Pacific through funding from the Navy Environmental Sustainability Development to Integration Program, as part of Project 424 on "Improved Assessment Strategies for Vapor Intrusion". The subject technology is concurrently being evaluated in project ER-0707 sponsored by ESTCP.

The purpose of this verification test was to generate performance data on the use of the building pressure control technique as a method to understand the impact of VI on the concentrations of CoCs in IA. In general, the data generated from this verification test are intended to provide organizations and users with information on the ability of this methodology to assess VI impacts.

GSI Environmental staff, with oversight from Battelle, implemented the building pressure control technique at two different buildings (described later in this Chapter); testing was executed in the autumn of 2010, over the course of 3.5 days at each building. The pressure

control technique was evaluated at the two buildings using the following types of performance parameters:

- Decision-making support
- Comparability
- Operational factors

The overall goal of implementing the building pressure control method is to obtain a better understanding of VI in a building. For instance, if the control of building pressure results in clear changes in building pressures and CoC and radon concentrations, the pressure control method may yield results that are useful for decision-making (i.e., is VI a concern for this building?). The effectiveness of the building pressure control method to support decision-making was evaluated through three different metrics. The first metric under decision-making support is to understand if the building pressure can be decreased and controlled and subsequently elevated and controlled at each of the two buildings under induced NP and PP conditions, respectively. The next metric was to determine, by inspection of the mass discharge of radon from subsurface sources whether VI was in fact enhanced under NP and reduced (or stopped) under PP. Demonstration of control of radon VI by manipulation of building pressure is important since it should allow for concomitant control of CoC VI. The last sub-parameter under decision-making support is the calculation of the fractional contribution of VI (F_{VI}) for each of several different concentrations of indoor CoCs. F_{VI} was calculated for four different CoCs at each of the two test buildings. Of the four CoCs, two were among those expected to have subsurface sources [trichloroethylene (TCE), and either 1,1-dichloroethylene (1,1-DCE) or tetrachloroethylene (PCE)], and two others were CoCs not expected to be present in IA as a result of VI (benzene and toluene). F_{VI} for each CoC was calculated at each of the two buildings under both NP and PP conditions according to an indoor air quality model developed by Dr. Ronald Mosley (i.e., the Mosley Model).[12] The error in each F_{VI} (ΔF_{VI}) calculation was also estimated based on a Monte Carlo error estimation technique. Given $F_{VI} \pm \Delta F_{VI}$, decision-makers may evaluate the impact of VI on the indoor atmosphere by calculation of the indoor concentration of each CoC attributable to VI and comparison of this result to appropriate regulatory criteria. Additional support to decision-makers was also provided by qualitative trends, with respect to changes in building pressure, in concentrations of compounds in IA as well as trends in the changes of compound mass discharges.

F_{VI} was calculated using the Mosley Model that is presented and described in its entirety in the QAPP.[10] The Mosley Model notation is used throughout this report since this facilitates the presentation of various results and verification metrics. Other notation was also developed based on Mosley's use of superscripts and subscripts to specify building pressure, as shown in Table 1.

Table 1. Mosley Model Notation Used for Description of Several Verification Parameters.

Parameter, units	Subscripts	Superscripts
R = radon concentration, pCi L^{-1} or pCi m^{-3}	i = indoor air	+ = positive pressure
Q = flow rate, $m^3 h^{-1}$	a = ambient air	- = negative pressure
C = CoC concentration, μg m^{-3}	s = soil gas	(no superscript) = baseline conditions (no pressure perturbation)
T = tracer gas concentration, μg m^{-3}	T = tracer	
G = generation rate of a compound by indoor sources, μg h^{-1} or pCi h^{-1}	C = CoC	
E = entry rate of a compound from a subsurface source, μg h^{-1} or pCi h^{-1}	R = radon	
F = fractional contribution of the concentration of a CoC, unitless	VI = vapor intrusion	

Other symbols and values:
V = building volume, m^3
λ = radioactive decay constant for ^{222}Rn, 0.1813 d^{-1} = 0.007555 h^{-1} (half life = 3.823 d; reference 13)
Q_i/V = building air exchange rate (AER), h^{-1}

Beyond the three metrics comprising decision-making support, the metric of comparability was assessed for the pressure control technique as the similarity of the building envelop differential pressures achieved under induced NP and PP conditions at each of two buildings. The final performance metric was comprised of an assessment of operational factors such as ease of implementation of the pressure control technology, the expertise required to carry out the field work and interpret the results, and costs to perform the testing.

3.2 Test Site Descriptions

3.2.1 ASU VI Research House

Arizona State University (ASU) purchased this research house (referred to as the "ASU House") near Hill Air Force Base in Layton, UT, for use on Strategic Environmental Research and Development Program Project ER-1686. This building overlies a dissolved plume of TCE and 1,1-DCE and as part of the work on ER-1686, ASU has confirmed that VI of these compounds is occurring at this building. Hill Air Force Base has deployed a near real-time gas chromatograph mass spectrometer (GC/MS), the HAPSITE® Smart Chemical Identification System (Inficon, East Syracuse, New York), that measures the IA concentrations of CoCs every hour.

Photographs of the house are shown in Figure 3. The floor plan of the home is shown in Figure A1 in Appendix A. The building is an unoccupied single-family dwelling with a partially below-grade finished basement and a single story living space above the basement. The area and

volume of the living space in the building, determined by measurement of the inner building dimensions, are 114 m^2 and 273.5 m^3, respectively. The area and volume calculations exclude the garage, since during testing the door between the living space and garage generally remained closed. The volume also excludes any attic space. During testing field staff were present in the home between the hours of ~ 06:30 and 18:00 Mountain Daylight Time (MDT). During all testing interior doors remained open (other than the door between the living space and garage), windows were closed, the fan to induce the pressure perturbation was kept running, and the building's heating, ventilation and air conditioning (HVAC) system operated normally. The external garage door (that would allow ingress/egress of vehicles) remained closed during testing, but otherwise building egresses were not strictly controlled and testing staff moved about freely.

Figure 3. Photographs of the ASU VI Research House. Panel A, Front, and Panel B, Rear of the Building.

3.2.2 Moffett Field Building 107

A number of buildings at Naval Air Station Moffett Field, near Palo Alto, CA, are impacted by subsurface sources of TCE and PCE.[14] The building selected for this verification test was Building 107, used by the U.S. Navy. It is a single story slab-on-grade structure and is shown in the photographs in Figure 4. The floor plan of the building is shown in Figure A2 in Appendix A. The area and volume of the usable space of the building, determined by measurement of its inner dimensions, are approximately 154 m^2 and 365 m^3, respectively. The volume calculation excluded the void space between the drop ceiling and roof. The building was occupied by Navy personnel and verification testing staff between the hours of ~ 06:30 and 18:00 Pacific Daylight Time (PDT) on test days. During all testing interior doors remained open, the fan to induce the appropriate pressure perturbation was kept running, exterior windows were closed, and the building's HVAC system operated normally, but building egresses were not controlled and building occupants were allowed to come and go freely.

Figure 4. Photographs of Moffett Field Building 107. Panel A Shows the West Side of Building, Panel B the Southeast Corner, and Panel C the Northeast Corner.

3.3 Experimental Design

The test schedule and experimental procedures are discussed in detail in the QAPP. Two back-to-back pressure control tests were conducted at each building. Both tests at each building were included as part of GSI Environmental's ESTCP project ER-0707. Only the second pressure control test at each building was included in the present verification. The initial pressure control test that occurred at each building was nominally identical with respect to duration, types of sampling performed, pressure control sequence, etc., to the ETV test that followed.[v] The ETV portions of the field work were conducted Monday, October 4 through Thursday, October 7, 2010 at the ASU House and Sunday, October 31 through Wednesday, November 3, 2010 at Moffett Field Building 107. Beginning late in the afternoon on the first day of testing, and lasting over the next three consecutive days, each building was maintained for 24 hours at each of the three pressure perturbation conditions (BL, NP, and PP). During the first 12 hours at each

[v] Conducting back-to-back building pressure tests may result in anomalous BL building conditions during the second set of tests. However, results generated during the ESTCP-only tests demonstrate that contaminant concentrations and mass discharges under BL conditions were similar for both this initial test and subsequent ETV test. This outcome is consistent with the conclusion that BL results for the ETV test are representative of normal building conditions.

pressure condition, the building atmosphere was allowed to come to equilibrium, after which the next 8 to 12 hours was taken to characterize the concentrations of various species in the building atmosphere.[vi] Table 2 shows the timing for each of the pressure control tests at each of the two buildings.

Table 2. Days/times for Pressure Control Testing at Each Building

ASU VI Research House (times MDT)		
Pressure condition	Begin	End
BL	10/04/2010 16:40	10/05/2010 17:50
NP	10/05/2010 17:50	10/06/2010 18:00
PP	10/06/2010 18:00	10/07/2010 18:05
Moffett Field Building 107 (times PDT)		
Pressure condition	Begin	End
BL	10/31/2010 16:16	11/01/2010 16:21
NP	11/01/2010 16:36	11/02/2010 17:13
PP	11/02/2010 17:13	11/03/2010 16:00

As shown in the building floor plans in Appendix A, air sampling was conducted at various locations interspersed throughout each of the two buildings. Before testing could begin, SS sampling points needed to be installed. SS sampling points were already installed and available on the lower level of the ASU House; at Moffett, SS sampling points were installed following specifications provided in the QAPP. SS sampling points were spatially separated throughout the building and located in unobtrusive areas. Installation at Moffett occurred on October 28, 2010, prior to commencement of the ESTCP portion of the field work.

At one of the SS sampling points, shown as "Foundation Pressure" in the floor plans, the cross-foundation SS ΔP was measured over the entire test interval (approximately 72 hours). At the location given as "Building Pressure Measurement" in the floor plans, the I/O ΔP was determined over approximately the same time interval. Each differential pressure measurement was performed using a separate calibrated Omniguard 4® (Engineering Solutions Inc., Tukwila, WA) real-time differential pressure instrument. For the SS measurement, the reference port was open to the building atmosphere and the other port was connected with ¼ inch semi-rigid walled tubing to the SS sampling port. For the I/O measurement, the reference pressure port on the Omniguard 4® was open to the indoor atmosphere and the other port was connected to ¼ inch semi-rigid-walled tubing placed outside of the building envelope through a slightly opened window. The open end of the tubing extended approximately 2 inches from the building. Following installation through the open window, the window opening was sealed with tape. The

[vi] Twelve hours is the minimum time for equilibration following a change in building pressure: at a minimum air exchange rate of 0.25 h^{-1}, 3 air changes would occur over 12 hours, after which indoor air concentrations would be $(1 - e^{-3})*100\% = 95\%$ of their expected final equilibrium concentrations. Moreover, given that integrated and other air sampling must occur over the next twelve hours following establishment of the new indoor equilibrium concentrations, twenty-four hours may be interpreted as the minimum required time for testing at each pressure condition.

same connections to the instruments were maintained throughout testing at both buildings so that consistency of the observed sign of ΔP was maintained.[vii] Figure 5 shows the SS and I/O pressure differential measurements at ASU House. Before and after each pressure condition, the zero reading of each pressure transducer was verified. The minimum and maximum measured pressure differential was recorded to an internal instrument datalogger every five minutes for the duration of testing. Note that at the ASU House, I/O pressure differentials were not measured under BL conditions. This issue was documented in QAPP Deviation 1; the lack of BL ΔP at ASU House had only a minimal impact on test outcomes, given that these measurements were not included specifically in any of the verification parameters.

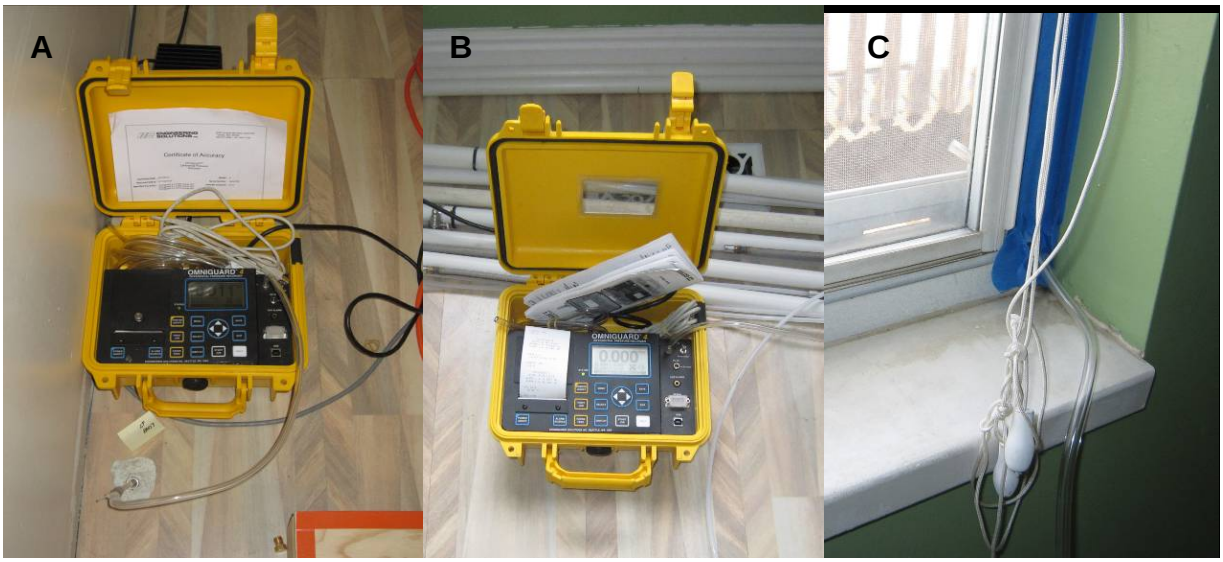

Figure 5. Pressure Differential Measurements at ASU House. Panel A, SS ΔP Monitoring, Showing Connection to SS Sampling Point; Panel B, I/O monitor; Panel C, Tube Extended Outside Window for I/O ΔP Monitoring.

In order to measure building ventilation rates (air exchange rates, AERs), SF_6 tracer gas was released at each building (at the locations shown as "SF_6 release" in the building floor plans in Appendix A) over the entire duration of pressure testing at each building. Pure (> 99.8%) SF_6 was delivered continuously; delivery was initiated at the start of the ESTCP testing that preceded the ETV tests at each building, and delivery of the tracer continued uninterrupted until the conclusion of the final PP test on October 7 and November 3, 2010, at ASU House and Moffett Field Building 107, respectively. Tracer gas delivery was controlled using a rotameter, and based on previous work and guidance in the QAPP, the target release rate of pure SF_6 was approximately 0.5 mL min^{-1}. Figure 6 shows the tracer gas delivery system as deployed during testing at Moffett Field Building 107.

Maintaining a steady tracer gas release rate is critical in order to obtain accurate estimates of the building ventilation rates. Thus, the SF_6 release rate, as indicated by the rotameter, was checked approximately every 16 hours and adjusted if found to have drifted by more than 10%.

[vii] With the reference port open to the interior of the building, ΔP was positive under NP conditions, and negative under PP conditions.

Furthermore, the SF_6 flow rate was independently verified, before and after each of the three pressure conditions at each building, using a DryCal® DC-2 (Bios International Corporation, Butler, NJ). Whereas the rotameter indicated that the delivery of SF_6 flow rate remained relatively constant over the duration of testing at both buildings (as evidenced by fairly invariant rotameter readings), the rotameter-determined flow rate differed from the DryCal®-determined flow rate by more than the 10% acceptance criteria established in the QAPP. As documented in QAPP Deviation 2, and described in more detail in Section 4.2, the flow rate of tracer gas as measured by the DryCal® was substituted for that indicated by the rotameter. Such a deviation from the QAPP positively impacted the test given that more accurate building ventilation rates were obtained by using the DryCal-determined SF_6 flow rates. This was important, given that the accuracy of the tracer gas flow rate measurement is one of the Data Quality Indicators (DQIs) discussed in Section 4.2.

Figure 6. SF_6 Tracer Gas Delivery System as Deployed at Moffett Field Building 107.

Under BL pressure conditions, each building's pressure was not intentionally manipulated. However, in the late afternoon on Days 2 and 3 of testing at each building, the building pressure was decreased (to induce a NP) or increased (to induce a PP). This was accomplished using a Lasco® Model 3733 20" box fan installed in a window, either pushing air out of, or into, the building, respectively. At ASU House, the fan was set to speed 2 (medium); at Moffett Field Building 107, the fan was operated at its highest speed, speed 3.[viii] Fan locations at each building are indicated on the floor plans in Appendix A by "Fan for pressure control." Figure 7 shows the fans as installed at the ASU House. NP and PP pressure conditions were maintained for at least 12 hours before collection of AA, IA, or SS gas began the next morning, so as to best ensure that the building atmosphere became well-mixed and to allow concentrations of the various gas-phase

[viii] At Moffett Field Building 107 the BL I/O ΔP was slightly negative due to the action of the building's HVAC system. The fan was operated at its highest setting to better ensure that it could overcome the inherent negative I/O ΔP and induce a positive pressure in the building.

species to come to equilibrium. At the ASU House, the attainment of new equilibrium concentrations of TCE and 1,1-DCE was investigated by inspection of measurements performed by the on-site portable near-real time HAPSITE® GC/MS. Data generated from the HAPSITE® GC/MS were only for diagnostic purposes and were not included in any verification parameters. These data are discussed in subsequent Chapters.

Figure 7. Fan Installed for Building Pressure Control at the ASU House.

Beginning on the morning of the second, third and fourth days of testing; corresponding to October 5, 6, and 7 at ASU House and November 1, 2, and 3 at Moffett Field Building 107; and corresponding to BL, NP, and PP conditions, respectively; IA, AA and SS gas was collected to measure various CoCs (VOCs), SF_6, and radon. Given in Table 3 is the number of discrete samples collected for each matrix. Also given are the locations where each of the three discrete samples was collected; these locations correspond to those shown in the building floor plans in Appendix A. Specific indoor sampling points were selected as a compromise between attaining spatial representativeness while minimizing disturbance to building occupants and activities. Ambient sampling locations were selected nominally upwind of the test building, away from obvious VOC sources. Sampling procedures and types of samples collected are described in additional detail below. Times when each type of sample was collected, and total numbers of samples collected, are given in Table 4.

Table 3. Types of and Locations for Air Samples Collected During Each of the Three Pressure Perturbation Periods. VOCs, SF_6, and Radon Were Measured in Each Matrix and Location.

Matrix	Number of Locations	Location
Indoor air	3	Open area on lowest building level plus two additional samples based on building layout; IA-1, IA-2, IA-3
Ambient air	1	Upwind location; AA-1
Subslab soil gas	3	Three locations distributed across the building foundation; SS-1, SS-2, SS-3

In order to characterize the concentrations of VOCs, SF_6, and radon in IA and AA, two different types of air samples were collected, one each at IA-1, IA-2, IA-3, and AA-1. One 8-hour time-integrated air sample for analysis of trace level VOCs/SF_6 (for IA and AA) was collected into an evacuated 6-L stainless steel canister at each of the four sampling locations. IA and AA air canister sampling is shown in Figure 8. Sampling commenced in the early morning and ended in the early afternoon on each day. Three to four times throughout the day during sampling, canister pressures were checked to ensure that each was filling at an approximately constant rate. In one instance, under PP conditions at ASU House, the AA canister was found to be filling too quickly. The rate of vacuum decrease indicated a leak in the canister valve or flow control device. Thus another AA sample was collected; analysis results from this recollected sample have been used for data interpretation and analysis.

At each IA and AA sampling location, a grab sample for radon analysis was collected into a 500-mL PVF bag using a 50-mL polyethylene syringe connected to a polymer three-way valve. Each PVF bag was filled with approximately 300 mL (6 syringes full) of air in approximately one minute. A new syringe was used on each sampling day; AA samples were collected first, followed by IA samples. Before collection of matrix into the bag, the syringe was purged three times with the matrix.

Table 4. Summary of Sample Types and Timing for Sample Collection at Each Test Building.

ASU House (times MDT)

Sample name	Sample type	Pressure Condition, Date	Time Start	Time Stop	Pressure Condition, Date	Time Start	Time Stop	Pressure Condition, Date	Time Start	Time Stop	Total samples[a]
IA, AA ($VOCs/SF_6$)	Integrated	BL, 10/5/2010	06:50	14:47	NP, 10/6/2010	06:55	15:06	PP, 10/7/2010	06:46	16:18	24[c]
SS ($VOCs/SF_6$)	Grab[b]		14:54	15:18		15:15	15:40		15:29	15:50	
IA, AA (Rn)	Grab		13:52	14:08		13:15	13:23		14:12	14:19	24[e,f]
SS (Rn)[d]	Grab		15:00	16:59		15:20	17:10		15:33	17:41	

Moffett Field Building 107 (times PDT)

Sample name	Sample type	Pressure Condition, Date	Time Start	Time Stop	Pressure Condition, Date	Time Start	Time Stop	Pressure Condition, Date	Time Start	Time Stop	Total samples[a]
IA, AA ($VOCs/SF_6$)	Integrated	BL, 11/1/2010	07:00	15:00	NP, 11/2/2010	06:58	15:00	PP, 11/3/2010	06:25	14:25	23[g]
SS ($VOCs/SF_6$)	Grab		15:06	15:23		15:01	15:27		14:30	14:44	
IA, AA (Rn)	Grab		12:45	12:50		13:15	13:23		13:59	14:03	24[e,f]
SS (Rn)	Grab		15:10	16:33		15:05	17:02		14:31	15:52	

[a]Total number of samples includes those collected for quality control purposes
[b]Collection of individual grab samples was generally complete in under one minute; start/stop times indicate when each type of grab sampling was initiated and completed, respectively
[c]Total canisters collected include: 9 IA, 3 AA, 9 SS, 1 IA/AA duplicate, 1 SS duplicate, and 1 additional AA under PP conditions
[d]SS Rn measured both by sampling into PVF bags and onsite analysis using the RAD7
[e]Total number of PVF bags collected include: 9 IA, 3 AA, 9 SS, 1 field blank, 1 IA/AA duplicate, 1 SS duplicate
[f]Total number of Rn samples does not include onsite sampling and analysis by RAD7
[g]Total canisters collected include: 9 IA, 3 AA, 9 SS, 1 IA/AA duplicate, and 1 SS duplicate

The measurement of the concentrations of VOCs, SF_6, and radon in SS gas required collection of several different types of samples. For the determination of VOC and SF_6 concentrations, one grab sample each was collected at SS-1, SS-2, and SS-3 into individual evacuated 1-L stainless steel canisters. Each canister grab sample at each location was filled in less than one minute. Following the procedures used for grab sampling in IA and AA, grab samples were also collected in PVF bags at each SS location for radon measurement. Prior to initiating SS sampling at a given sample point, approximately 50 mL of gas was withdrawn from the sample point using a polyethylene syringe. This SS purge gas was injected into a separate PVF bag for discharge outdoors at a later time so as to avoid artificially elevating IA radon concentrations. Also, before collection of each canister grab sample, the integrity of the plumbing connecting the canister and three-way valve to the SS sampling line was confirmed by verifying, by inspection of the canister pressure gauge, that a vacuum could be pulled using the polyethylene syringe.

SS radon was also determined using a near real-time instrument, the Durridge RAD7® radon detector (Bedford, MA). A total of five RAD7® readings were performed at each sampling point, each lasting 5 minutes. The average of the final three readings was taken as the radon concentration at that sampling point. Whereas SS radon was measured using both sampling into PVF bags and near-real time monitoring with the RAD7®, per the QAPP, the RAD7® will be used for data interpretation in this verification test. SS sampling using the RAD7® is shown in Figure 8.

Figure 8. IA, AA, and SS sampling at ASU House (Panels A, B, and C, respectively).

Before canister sampling commenced, canisters were checked for leaks by inspection of initial canister vacuum. Following collection, final canister pressures were also recorded so that canister integrity could be tracked until analysis. No canisters were rejected based on out-of-bounds initial pressure; however, three canisters leaked between shipment and analysis (this is subject of Deviation 3, that is discussed in more detail in Chapter 4). At each test building, two duplicate canisters, one for IA/AA and one for SS gas, were collected. Details of the various QC measures to ensure the validity of the canister sampling are given in Chapter 4.

All PVF bags were leak-checked prior to sampling by pulling a vacuum on the empty bag using the polyethylene syringe. Each bag was checked again following sample collection, this time by gently squeezing each bag to verify absence of leaks. Two PVF bags failed initial leak checks and were discarded. At each test building, one field blank was generated by filling a bag with

aged AA, and two duplicate PVF bags, one for IA/AA and one for SS gas, were collected. More details of the various QC measures employed to ensure validity of the PVF bag sampling are presented in Chapter 4.

At the completion of each day of testing, the canister samples were shipped by common carrier to Columbia Analytical Services (Simi Valley, California) for analysis of VOCs and SF_6, and the PVF bags were similarly shipped to the University of Southern California, Department of Earth Sciences, for radon analysis. Analyses were performed as specified in the QAPP. Briefly, analysis of canister samples for VOCs was performed using cryogenic preconcentration GC/MS according to the procedures outlined in EPA Compendium Method TO-15[15], with TO-15 scan for VOCs in SS gas and TO-15 with selected ion monitoring (SIM) for VOCs in IA/AA. Canister samples for SF_6 were analyzed using GC/electron capture detection (ECD) according to procedures in National Institute of Occupational Safety and Health (NIOSH) Method 6602.[16] Radon concentrations were measured by way of alpha scintillation counting following established EPA protocols.[17] Additional details of the radon analysis method are given in McHugh et al.[8]

The various verification parameters are described in the next several sections.

3.3.1 Decision-making Support

The goal of implementing the building pressure control method is to obtain a better understanding of VI in a building. If the control of building pressure results in clear changes in building conditions, such as I/O differential pressures and concentrations of radon and CoCs, then the pressure control method may yield results that are useful for decision-making (i.e., is VI a concern for this building?). The effectiveness of the building pressure control method to support decision-making was evaluated through three metrics:

1. Building Pressure Differential: Did the pressure control method control building pressure?

2. Vapor Intrusion Enhancement and Reduction: Did the pressure control method increase the mass discharge of radon from subsurface sources through the building foundation under induced NP conditions and/or decrease the mass discharge of radon from subsurface sources through the building foundation under induced PP conditions?

3. Fractional Contribution of Vapor Intrusion to Indoor CoC Concentrations: Did the pressure control method provide an improved understanding of the contribution of VI to the concentration of individual CoCs detected in IA?

Each of these three quantitative verification metrics comprising decision-making support is described in more detail in the following sections. In addition, qualitative metrics related to providing support to decision-makers, metrics based on the inspection of trends in concentrations of compounds in IA as well as mass discharges with respect to changing building pressure, are described along with the presentation of the test results in Section 6.1.

3.3.1.1 Building Pressure Differential

The first metric for the verification of the performance of the building pressure control methodology is whether the building pressure could be decreased and subsequently elevated at each of the two buildings under induced NP and PP conditions, respectively. The Omniguard 4® pressure differential instrument measured the minimum and maximum I/O ΔP every five minutes. The average ΔP for each five minute time interval was calculated as the arithmetic mean of the minimum and maximum ΔP. Observed mean ΔPs of less than -1 Pa (under NP conditions) and greater than 1 Pa (under PP conditions) would verify that some degree of building pressure control had been attained. More details of the data manipulation and statistical tests applied to these data are described in Chapter 5.

3.3.1.2 Vapor Intrusion Enhancement and Reduction

The second verification metric under decision-making support is the effect of the pressure control method on enhancement and reduction of radon VI. This metric was evaluated by comparison of the mass discharge of radon from subsurface sources through the building foundation under different building pressure conditions.[18,ix] For instance, under induced NP, the mass discharge of chemicals with subsurface sources, including radon and CoCs, through the building foundation and into IA may be enhanced. Similarly, under induced PP conditions, mass discharge of radon and CoCs from subsurface sources into IA may either be reduced or eliminated, where the latter condition indicates that VI has effectively been 'turned off' by the induction of PP.

Direct measurement of SS-to-IA flow rates is quite difficult; consequently, it is difficult to directly measure the mass discharge of chemicals from subsurface sources. Nonetheless, the mass discharge of radon (and by extension, CoCs) from subsurface sources may be estimated as follows. The total mass discharge from the building of radon from all possible sources –indoor, ambient, and subsurface – is calculated as in Equation 1 from the radon concentration in IA (R_i, pCi m^{-3}) and the building ventilation rate, i.e., the flow of IA out of the building (Q_i, m^3 h^{-1}).

$$Q_i \cdot R_i \qquad (1)$$

Similarly, the approximate mass discharge of radon from ambient sources into IA is found using Equation 2.

$$Q_a \cdot R_a \approx Q_i \cdot R_a \qquad (2)$$

Where Q_a is the flow rate of AA into the building and R_a is the ambient radon concentration.[x] If the mass discharge of radon into IA from indoor, but not ambient, sources is negligible,[xi] then by

[ix] Mass discharge is defined in Reference 18 as the strength of a source at a given time and location; it is actually a rate and is defined in units of mass/time. In this report it is convenient to use mass discharge more generically for both radon and CoCs given the utility of the comparisons in the observed trends of radon and CoC mass discharges, even though a mass discharge of radon has units of activity/time rather than mass/time. Furthermore, mass discharge may refer to the generation rate of radon/CoCs from indoor source(s), the entry rate of radon/CoCs from subsurface and/or ambient sources into the building, or the total discharge of radon/CoCs from the building.

[x] As described in the Mosley Model, this calculation assumes that $Q_a \approx Q_i$, i.e., that the building ventilation rate is

mass balance the mass discharge from subsurface sources through the building foundation into IA may be estimated by subtraction of Equation 2 from 1:

$$Q_i \cdot (R_i - R_a) \quad (3)$$

Note that the notation for Equations 1, 2, and 3 is appropriate for BL conditions.

For each building, three IA radon concentrations were measured at each pressure condition; the mean of these three measurements was the mass discharge calculations; under BL conditions, this concentration is given as R_i. A single AA radon measurement was also taken at each building under each pressure condition; under BL conditions this is denoted by R_a. Also, at each building under each pressure condition, the building air flow rate between indoors and ambient (the building ventilation rate) was determined at all three pressure conditions as (using the notation appropriate for BL conditions) $Q_i = C_T \cdot Q_T / T_i$, where Q_i is the building ventilation rate, C_T is the concentration of SF_6 ($\mu g\ m^{-3}$), Q_T is the flow rate of the tracer gas ($m^3\ h^{-1}$), and T_i is the mean of three spatially distributed measurements of the indoor concentration ($\mu g\ m^{-3}$) of SF_6. C_T was known (99.8% and converted to $\mu g\ m^{-3}$ assuming T = 25°C, P = 1 atm; all concentrations were converted to this same T/P scale) and for each pressure control test at each building, the SF_6 flow rate was determined as the mean of two (one pre- and one post-test) DryCal measurements.

The degree that VI was enhanced under induced NP conditions was determined by comparison of $Q_i^- \cdot (R_i^- - R_a^-)$ to $Q_i \cdot (R_i - R_a)$. If $Q_i^- \cdot (R_i^- - R_a^-) > Q_i \cdot (R_i - R_a)$, that is, if the mass discharge of radon from subsurface sources increased under induced NP compared to BL, then under induced NP some degree of enhancement of VI has been verified. Similarly, the degree that VI was reduced under induced PP conditions was determined by comparison of $Q_i^+ \cdot (R_i^+ - R_a^+)$ to $Q_i \cdot (R_i - R_a)$. If $Q_i^+ \cdot (R_i^+ - R_a^+) < Q_i \cdot (R_i - R_a)$, that is, if the mass discharge of radon from subsurface sources decreased under induced PP compared to BL, then under induced PP conditions some degree of reduction of VI has been verified.

Under PP conditions, VI may also be reduced to the point that it has been 'turned off.' If under PP conditions the radon concentration in IA (R_i^+) equals the radon concentration in AA (R_a^+), then there is some degree of confidence that VI has been stopped or 'turned off' by the induction of PP. As will be shown in Section 6.2, the mass discharge of radon from subsurface sources into IA decreased at both buildings under PP compared to BL, thus $R_i^+ = R_a^+$ was also checked for both buildings. For each building, R_i^+ was calculated as the mean of the three IA radon measurements and R_a^+ was the single AA radon measurement.

much greater than the flow rate of soil gas through the foundation into the building, an assumption that is generally valid.

[xi] Under induced PP conditions, the mass discharge of radon from ambient sources into IA was greater than 75% of the total mass discharge, indicating that AA was a non-negligible source of radon. As a result, VI enhancement and reduction were evaluated as the mass discharge from subsurface sources through the building foundation using Equation 3. This interpretation results from the assumption that radon emission from indoor sources is negligible compared to subsurface sources (an assumption supported by the radon literature).[19]

For all calculations, MDLs were substituted where concentrations were reported as either zero or not detectable. Such substitutions were only performed for SF_6 and CoC concentrations since in all cases a measureable concentration of radon was determined in all IA and AA samples. Further details of MDL substitutions may be found in Section 4. Additional details of the data manipulation and statistical tests applied to these data are presented in Chapter 5.

3.3.1.3 Fractional Contribution of Vapor Intrusion to Indoor CoC Concentrations

The third verification metric that comprises decision-making support is the ability of the pressure control technique to determine the fractional contribution of VI (F_{VI}) to the IA concentration of several different CoCs. At each test building, two CoCs were selected that were expected to have subsurface sources, and two CoCs were selected that were not expected to be present in the subsurface but instead were expected to have only indoor, or potentially predominantly ambient sources. At the ASU House, the four CoCs were TCE and 1,1-DCE (expected in the subsurface) and benzene and toluene (not expected in the subsurface). At Moffett Field Building 107, the four CoCs were TCE and PCE (expected in the subsurface) and benzene and toluene (not expected in the subsurface).

The F_{VI} calculation combines building ventilation rates and compound concentrations from either (i) BL and NP (F_{VI}^-), or (ii) BL and PP (F_{VI}^+). In both cases, the calculation yields an estimate of the fractional contribution of VI to a CoC's concentration under BL conditions. Both F_{VI}^- and F_{VI}^+ and the error in each F_{VI} (denoted as ΔF_{VI}) were calculated for the four CoCs for each building. Thus, a total of 16 different $F_{VI} \pm \Delta F_{VI}$ combinations were calculated (2 buildings · 2 pressure conditions · 4 CoCs).

At each of the two buildings, F_{VI}^- for each of the four CoCs was calculated according to the Mosley Model using BL and NP results by combining Equations 4 and 5. More detail of the Mosley Model is provided in the QAPP.

$$E_C = \frac{[Q_i^-(C_i^- - C_a^-) - Q_i(C_i - C_a)][Q_i(R_i - R_a)]}{[Q_i^-(R_i^- - R_a^-)] - [Q_i(R_i - R_a)]} \quad (4)$$

$$F_{VI} = \frac{E_C}{Q_i C_i} \quad (5)$$

Q_i and Q_i^- were calculated as described in Section 3.3.1.2. For each building, mean IA concentrations under BL and NP (R_i and R_i^-), AA radon concentrations under BL and NP (R_a and R_a^-), and the corresponding building ventilation rates under BL and NP (Q_i and Q_i^-) were calculated as described in Section 3.3.1.2. C_i and C_i^- were calculated for each of the four CoCs at each building as the arithmetic mean of the three IA concentration measurements under BL and NP conditions, respectively. C_a and C_a^- were the concentrations of each of the CoCs in the single AA sample collected under BL and NP conditions, respectively.

F_{VI}^{+} may be determined by way of two different methods. One assumes that VI has been reduced (but not stopped completely), and employs a calculation of complexity similar to that under NP. The other is a more simplified calculation, where VI is assumed to have been halted under PP. As is shown in Chapter 6, $R_i^{+} = R_a^{+}$ at both buildings, indicating that the more simplified F_{VI}^{+} calculation was the most appropriate for this verification test. Thus, at each of the two buildings, the F_{VI}^{+} values for each of the four CoCs were found according to the Mosley Model using BL and PP results by combining Equations 5 and 6.

$$E_C = Q_i(C_i - C_a) - Q_i^{+}(C_i^{+} - C_a^{+}) \quad (6)$$

Q_i^{+} was determined similarly to Q_i and Q_i^{-}. C_i^{+} was calculated for each of the four CoCs at each building as the arithmetic mean of the three IA concentration measurements under PP conditions. C_a^{+} was the concentration of each of the CoCs in the single AA sample collected under PP conditions.

Not only may CoCs be present in indoor air due to contributions as a result of VI (i.e., from subsurface sources), they may also be present due to emissions from ambient and indoor sources. Thus, in addition to calculating F_{VI}, the fraction of each CoC's concentration in IA that was due to ambient and indoor sources, F_a and F_{in}, respectively, were calculated for both NP and PP for the four CoCs at each building. According to the Mosley Model, F_a is calculated using Equation 7.

$$F_a = \frac{Q_i C_a}{Q_i C_i} = \frac{C_a}{C_i} \quad (7)$$

Note that the expression simplifies to the ratio of the CoC's concentration in AA to its concentration in IA, both under BL conditions. Thus only a single estimate of F_a is determined using the pressure control technique.

Similar to F_{VI}, F_{in} may be estimated two different ways. F_{in}^{-} is found by combining Equations 4 and 8; F_{in}^{+} is calculated using Equations 6 and 8.

$$F_{in} = \frac{Q_i(C_i - C_a) - E_C}{Q_i C_i} \quad (8)$$

Note that for each of the two independent sets of fractional contribution calculations, $F_a + F_{in} + F_{VI} = 1$.

The error in each F_{VI}, ΔF_{VI}, was estimated using a Monte Carlo technique described in Chapter 5. Notionally, the F_{VI}s for each CoC under NP and PP should be independent estimates of the same quantity, and $0 < F_{VI} < 1$. Inspection of the F_{VI}s and associated error intervals allows the degree of confidence that the pressure control technique can ascribe a CoC's indoor concentration to VI to be determined.

As with the calculations in Section 3.3.1.2, where concentrations were reported as either zero or not detectable, estimated detection limits were substituted. Such substitutions were only

performed for SF_6 and CoC concentrations since in all cases a measurable concentration of radon was determined in all samples. Further details of MDL substitutions may be found in Section 4. Additional details of the data manipulation and statistical tests applied to these data are presented in Chapter 5.

3.3.2 Comparability

The verification metric of comparability is intended to evaluate the consistency of the pressure control that was attained in different buildings.

The arithmetic mean of each time series of I/O pressure differentials was calculated according to Section 3.3.1.1 to determine a total of four mean overall pressure differentials at the two different buildings: (1) ΔP_1^- and ΔP_2^-, the mean differential pressure under induced NP at the ASU House and Moffett Field Building 107, respectively; and (2) ΔP_1^+ and ΔP_2^+, the mean differential pressure under induced PP conditions at ASU House and Moffett Field Building 107, respectively. The comparability of the building pressure control methodology was assessed by comparison of the two NP differential pressures and the two PP differential pressures according to the statistical calculations described in Chapter 5.

3.3.3 Operational Factors

Metrics related to operational factors are intended to evaluate primarily the cost and level of effort associated with implementation of the pressure control method. Operational factors for implementation of the entire building pressure control technology were evaluated based on Battelle's observations and input from the technology vendor. General operational factors include the knowledge, expertise, training, and costs required to carry out all aspects of the field sampling campaign, including installation of the SS sampling points, measurement of pressure differentials, and collection of all of the various air samples. The vendor provided cost information, including information on purchase prices for the Omniguard 4® and RAD7® real-time monitors, charges for off-site analysis of VOCs and SF_6 and radon, and costs for the vendor's time in the field to plan and carry out the field work. Other factors included the maintenance needs, calibration requirements and frequencies for the real-time pressure differential and radon instruments, data output and analysis, and sustainability factors, such as consumables required and used (if any), ease of use, and repair requirements (if any) of the real-time monitors. Examples of other pertinent information include the number of canisters received from the analytical laboratory, and number of PVF bags that were deemed unacceptable for sample collection; the effort and/or cost associated with maintenance or repair of real-time instruments; vendor effort (e.g., time on site) for repair or maintenance; the duration and causes of any downtime for real-time instruments; Battelle's observations about ease of use, clarity of the vendor's instruction manual; and overall convenience of the technologies and accessories/consumables. During testing at the ASU House Battelle testing staff documented observations in a laboratory record book (LRB). These observations were summarized to aid in describing the technology performance.

3.3.4 Validation of Mosley Model Assumptions

The Mosley Model was used for quantitative evaluation of the third decision-making metric (i.e., the fractional contribution of VI to CoC concentrations in IA, F_{VI}). A number of different assumptions are stated in the Mosley Model, several were explicitly tested using the data collected in this verification of the pressure control methodology. Verifying the validity of the assumptions helped to explain the outcomes of the F_{VI} calculations.[xii] As described below, three different groups of assumptions, with eight assumptions in total, were explicitly tested at each building.

Group 1: Building pressure control has no significant effect on CoC and radon concentrations in SS soil gas below the building foundation.

1. $C_s = C_s^-$
2. $R_s = R_s^-$

C_s and C_s^- for each CoC and R_s and R_s^- were calculated as the mean of the three SS concentration measurements under BL and induced NP conditions, respectively.[xiii]

Group 2: Radon concentrations in AA are much lower than those in SS soil gas below the building foundation.

3. $R_a << R_s$
4. $R_a^- << R_s^-$
5. $R_a^+ << R_s^+$

The values of R_a, R_a^-, and R_a^+ were based on single grab samples of AA. R_s^+ was found as the mean of the three SS concentration measurements under induced PP conditions.

Group 3: In IA, the loss of radon through building ventilation is much greater than the loss due to radioactive decay.

6. $Q_i >> \lambda V$
7. $Q_i^- >> \lambda V$
8. $Q_i^+ >> \lambda V$

Building volumes were estimated based on interior dimensions and are given in Section 3.1. The values of Q_i, Q_i^-, and Q_i^+ were calculated as in section 3.3.1.2.

[xii] It should be noted, however, that some of the model assumptions cannot be verified using the data collected during this verification test. For example, the Mosley Model assumes that the change in the magnitude of mass transport though the building foundation under induced NP will be the same for radon and the CoCs.

[xiii] Note that it is unnecessary to validate assumptions 1 and 2 above under PP conditions when it is determined that VI has been 'turned off', i.e. when $R_i^+ = R_a^+$, since the calculation of F_{VI} no longer depends on the simplifying assumption that $C_s = C_s^+$ and $R_s = R_s^+$.

Estimated detection limits were substituted where concentrations were reported as either zero or not detectable. Errors in the various parameters were estimated as described in Chapter 5 along with additional details of the statistical comparisons.

Chapter 4
Quality Assurance/Quality Control

QA/quality control (QC) procedures were performed in accordance with the QMP[11] for the AMS Center and the QAPP for this verification test. There were a total of five deviations from the QAPP. A deviation is an action or QC outcome that differs from QAPP procedures and specifications. As detailed in the discussion of each deviation, there was little to no negative impact on this verification test from any of the five deviations. Two deviations (1 and 2) were described in Chapter 3 and related directly to the field testing, and the remaining three (3, 4, and 6); are described in this Chapter, along with the rationale for vacating Deviation 5. Also covered here are the general QA/QC procedures employed for this verification test.

4.1 Quality Control Results

A variety of QC measures were implemented to ensure that data of the highest quality were generated during this verification test. QC procedures were carried both in the field and at the analytical laboratory, ranging from basic checks of instrument functionality to analytical instrument calibrations; a number of different field QC samples were also generated for subsequent laboratory analysis, including field blanks and duplicate samples; and various lab QC samples were analyzed, such as replicates and method blanks. The specific QC procedures and samples generated during the performance of this verification test, as well as applicable acceptance criteria, are described in detail in the QAPP. The results of the implementation of this verification test's QA/QC program are summarized in Table 5. In general nearly all of the various QC measures were found to be within acceptable limits. Those that were not found to be acceptable were the subject of findings or observations in one of two Technical Systems Audits (TSAs) or Audits of Data Quality (ADQs). Findings were written up as QAPP deviations. The impact of QAPP deviations 3, 4, and 6, as well as the observations from the first Audit of Data Quality (ADQ), as referenced in Table 5, are described in more detail in Section 4.3.

Table 5. Summary of Results of Various QC Procedures and Samples.

QC Sample Type	Lab/ field	Quantity reviewed	Quantity acceptable	Quantity unacceptable	Notes
Instrument Calibration (VOC) IA/AA	L	4	4	0	closing CCVs not performed; QAPP deviation 4, no impact to test, see text
Instrument Calibration (VOC) SS	L	5	5	0	closing CCVs not performed; QAPP deviation 4, no impact to test, see text
Instrument Calibration (SF_6)	L	5	5	0	
Continuing Calibration Verification (VOC) IA/AA	L	4	4	0	
Continuing Calibration Verification (VOC) SS	L	5	5	0	
Continuing Calibration Verification (SF_6)	L	17	17	0	
Method Blank (VOC) IA/AA	L	4	4	0	
Method Blank (VOC) SS	L	5	5	0	
Method Blank (SF_6)	L	5	5	0	
Method Blank (radon)	L	various	all	0	QAPP deviation 6: no impact to test, see text
Laboratory Replicate (VOC) IA/AA	L	4	4	0	
Laboratory Replicate (VOC) SS	L	5	5	0	
Laboratory Replicate (SF_6)	L	5	5	0	
Laboratory Replicate (radon)	L	10	10	0	
Laboratory Replicate (IA/AA radon)	L	2	1	1	ADQ 1 observation 2; potential increased radon variability at low concentrations, no corrective action necessary, see text
Laboratory Replicate (SS radon)	L	11	11	0	SS radon in PVF bags not used for ETV test
Calibration of radon counting cells	L	various	all	0	QAPP deviation 6; no impact to test, see text
Differential Pressure Zero Check	F	15	15	0	QAPP deviation 1; minimal impact to test, see text
Canister Pressure Pre-use Check	F	47	47	0	
Canister Pressure Receipt Check	L	47	11	36	QAPP deviation 3; 44 pass revised acceptance criterion, minimal impact to test, see text
Canister Cleanliness Certification	F	47	47	0	
Canister (Analytical) Hold Time (VOC)	L	47	47	0	
Canister (Analytical) Hold Time (SF_6)	L	47	47	0	
PVF Bag (Analytical) Hold Time (radon)	L	48	48	0	
PVF Bag (Analytical) Hold Time (IA/AA radon)	L	28	28	0	
PVF Bag (Analytical) Hold Time (SS radon)	L	20	20	0	SS radon in PVF bags not used for ETV test

Table 5. Summary of Results of Various QC Procedures and Samples (Continued)

QC Sample Type	Lab/ field	Quantity reviewed	Quantity acceptable	Quantity unacceptable	Notes
Canister (Field) Duplicates (VOC) IA/AA	F	2	1	1	ADQ 1 observation 4; potential increased toluene variability at low concentrations; no corrective action required, see text
Canister (Field) Duplicates (VOC) SS	F	2	1	1	ADQ 1 observation 4; potential increased PCE variability at low concentrations; no corrective action required, see text
Canister (Field) Duplicates (SF_6)	F	2	2	0	
PVF Bag (Field) Duplicates (radon) IA/AA	F	2	1	1	ADQ 1 observation 5; potential increased variability at low concentrations; no corrective action required, see text
PVF Bag (Field) Duplicates (radon) SS	F	2	2	0	SS radon in PVF bags not used for ETV test
PVF Bag (Field) Blank (radon)	F	2	2	0	ADQ 1 observation 3; minimal data quality impact, see text
Canister Matrix Spike (VOC) IA/AA	L	4	4	0	Data Quality Indicator, see text
Canister Matrix Spike (VOC) SS	L	5	5	0	
Canister Matrix Spike (SF_6)	L	5	5	0	Data Quality Indicator, see text
Radon matrix spike	L	various	all	0	QAPP deviation 6; no impact on test, see text

Another aspect of the quality system is the selection, use, and number of observations below selected method detection limits (MDLs). Estimates of VOC and SF_6 MDLs used in this report were those provided by the analytical laboratory. For radon, the selection of an appropriate and applicable MDL is described below.

The analytical laboratory estimated that the lower limit of detection (LLD) for radon was approximately 0.14 pCi L^{-1}, that was estimated using procedures promulgated by the EPA.[19] This guidance stated that the LLD is an "a priori estimate of the quantity of activity that will be detected with a given confidence." However, the LLD "is [only] a prediction of measurement capability;" to evaluate whether a radon measurement is greater than background, another metric, the minimum significant measured activity (MSMA), defined as "the smallest measurement interpreted to demonstrate the presence of activity in the sample," should be employed. In general, both LLD and MSMA are calculated at a 95% confidence level where a 5% false positive rate is deemed acceptable. MSMA varies on a per sample basis and depends on, for example, the cell that the radon activity is measured (and specifically the cell volume, background count rate, and efficiency factor), the count time, and the sample hold time. Including counting cell-specific information to estimate the MSMA is important given that certain counting cells have higher background count rates than others, and counting cells are segregated on this basis. To effectively measure IA/AA radon, only those cells with the lowest background counts (and lowest MDLs) may be used. MSMA is defined as $2.77 \cdot s_b$, where s_b = standard deviation of the background activity. The analytical laboratory provided s_b for each radon measurement, and the radon MDL was set equal to the MSMA.

Where measured values of SF_6 and CoCs were reported as zero (below the applicable MDL), the value of the MDL was substituted for the zero measurement in all calculations (of averages, standard deviations, etc.). Radon concentrations were never reported as zero; thus, the actual reported radon concentrations were used in all calculations. Although a reported result that is below the MDL has a higher uncertainty than a reported result at a higher concentration, the reported result is a more accurate characterization of the actual radon concentration in the sample as compared to the estimated MDL. Such treatment of radon data is consistent with EPA guidance.[20, xiv]

In general, MDL substitutions negatively impacted the statistical calculations, for instance, by precluding post-hoc power analysis. The impact of these substitutions is described in more detail in Chapter 6. Specific instances where the reported concentrations were less than applicable MDLs are shown in yellow highlight in the raw data that are presented in Tables A2 through A7 in Appendix A.

[xiv] Reference 20, Appendix A states: "The result obtained in a measurement, which is a sample of the infinite population of possible results, is the best estimate of the mean value of the population. These actual results, whether greater than or less than the LLD, and whether positive, negative, or zero, should be used in averaging. Elimination of results less than the LLD, or of results less than zero, introduces a bias into the overall average value."

Table 6. Summary of Frequency of Measurements Lower Than Estimated MDLs.

Measurement	Total #[a]	# < MDL	% < MDL
IA/AA VOC	96[b]	6	6%
SS VOC	72[c]	13	18%
IA/AA/SS SF_6	42[d]	3	7%
IA/AA Rn	24[e]	5	21%
SS Rn	54[f]	11	20%

[a]Totals exclude results of duplicate and replicate analyses
[b]4 total cans (3 IA and 1 AA)/pressure condition; 3 pressure conditions; 4 compounds/building; 2 buildings
[c]3 SS cans/pressure condition; 3 pressure conditions; 4 compounds/building; 2 buildings
[d]7 total cans (3 IA, 1 AA, and 3 SS)/pressure condition; 3 pressure conditions; 2 buildings
[e]4 total PVF bags (3 IA and 1 AA)/pressure condition; 3 pressure conditions; 2 buildings
[f]3 measurements/SS point; 3 SS points/pressure condition; 3 pressure conditions; 2 buildings

4.2 Data Quality Indicators

The primary objective of this verification test was to evaluate the capability of the building pressure control technique to provide decision-makers with the quantitative information required to determine the extent that CoCs are present in IA as a result of VI. To ensure that this verification test provided suitable data for a robust evaluation of performance, a data quality objective (DQO) was established. This DQO was that F_{VI} be greater than ΔF_{VI}. To maximize the likelihood that the DQO be attained, three different data quality indicators (DQIs) were established. Two are indicated in Table 5 above, that is, that canisters spiked with either CoCs or SF_6, approximately at levels expected to be found in IA, were recovered between 70 to 130 % and 80 to 120% for CoCs and SF_6, respectively. These two DQIs were achieved. The other DQI, the accuracy of the delivery rate of the SF_6 tracer gas, was also achieved, but only after the flow rates as measured by an independent flow transfer standard, the DryCal® DC-2, were substituted for those indicated by the rotameter. Although the rotameter provided stable, constant delivery of SF6, the agreement in measured flow rate between the rotameter and the DryCal® did not meet acceptance criterion specified in the QAPP. Therefore, following the conclusion of the field testing, testing was performed at Battelle's metrology laboratory where flows indicated by the DryCal® were compared to known standard flows delivered using calibrated mass flow controllers. Results from this comparison demonstrated that the accuracy of the DryCal® met the acceptance criterion of ±10% difference. The rationale for this substitution is described more fully in Deviation 2 and in Section 3.3.

4.3 Audits

Two types of audits were performed during the verification test. TSAs of the verification test procedures and field QC measures were conducted, one at each of the two buildings, and one ADQ following completion of all field testing activities and analysis of all field samples. A

second ADQ of the results presented in this verification report was also conducted. Audit procedures are described further below.

4.3.1 Technical Systems Audits

To ensure that the verification test was performed in accordance with the AMS Center QMP[11] and with the QAPP the NAVFAC Atlantic Quality Assurance Officer (QAO) for this verification test performed two different TSAs, one at each of the buildings where the pressure control technique was implemented. The QAO was onsite at each of the buildings for the entire duration of each verification test. While onsite the QAO compared actual test procedures to those specified and referenced in the QAPP, and reviewed all pertinent project documentation and data acquisition and handling procedures. Moreover, the QAO observed all aspects of performing the field work, including collecting air samples, operating (and in one instance, troubleshooting) the real-time differential pressure and radon monitors, pre- and post-sampling canister/PVF bag integrity checks, and all field QC measures listed in Table 5.

The first TSA at the ASU House resulted in three findings and four observations. The first finding regarded maintenance of project records. The QAPP describes recordkeeping practices, and states that all documents and records will be maintained by the VTC during the test and transferred to secure storage at the conclusion of the test. However, technology vendor staff were conducting the field work and were required ready access to the project records during testing. Thus it was decided to allow the vendor to maintain the field data record sheets and logs throughout the duration of the field work. The VTC, QAO, and technology vendor staff discussed this procedural change and GSI Environmental agreed to provide the VTC photocopies of all records – specifically, the project's data collection forms – at the end of each test day. This solution was similar to the document maintenance and control procedures described in the QAPP for future testing at Moffett Field (where the VTC knew in advance that he would be absent); that is, GSI Environmental agreed to send electronic copies of all applicable project records to the VTC at the end of each test day.

The second finding regarded the observed discrepancy in tracer gas flow rates as measured by the DryCal® as compared to the rotameter, i.e. that they did not agree within ±10%. This finding was ultimately addressed by substitution of the DryCal® flow rates for those indicated by the rotameter, as discussed in QAPP Deviation 2 and in Sections 3.3 and 4.2 of this report.

The third finding was that the I/O pressure differential was not measured under BL conditions at the ASU House because only one differential pressure monitor was available at the start of testing. This finding was addressed in QAPP Deviation 1 and is discussed in Section 3.3.

Four observations also resulted from the first TSA. Observations were related to project records and recordkeeping practices. In response to these observations, the following actions were taken.

- The certificate of analysis for the SF_6 tracer gas was obtained for onsite review by the QAO and added to the project records.
- The calibration record for the DryCal was similarly obtained for onsite review by the QAO and added to the project records.

- Data recording practices of field staff were improved so as to avoid future issues with prompt recording of field-generated data onto data collection forms.
- Pre-printed sample labels were not used during testing at Moffett Field.

The NAVFAC Atlantic QAO also performed a TSA during testing at Moffett Field. This TSA resulted in one finding and one observation. The finding further documented the discrepancy in the tracer gas flow rates as indicated by the DryCal and the rotameter. This finding was ultimately addressed as described in the summary of the first TSA above. The observation regarded maintenance of the integrity of project records given that the VTC was absent from the test site. This observation was addressed in advance of the test by requiring that the onsite test team forward copies of project records to the VTC on a daily basis.

All of the findings and observations for both TSAs were determined to have either no or only minimal impact on test outcomes. TSA reports were prepared and copies were distributed to the EPA.

4.3.2 Audits of Data Quality

A Battelle technical staff member involved in this verification test reviewed all test records before such were used to calculate, evaluate, or report verification results. The person performing the review added his/her initials and the date to a hard copy of the record being reviewed. The VTC reviewed 100% of the verification test data for quality. The data were traced from the initial acquisition, through reduction and statistical analysis, to final reporting to ensure the integrity of the reported results. Statistical manipulations were performed using commercially available software (Stata and R) executing custom-written code; where applicable, the VTC cross-checked statistical outputs against outputs derived from independent calculations of results shown in the Appendix A.

In addition, the NAVFAC Atlantic QAO performed an ADQ where at least 10% of the data acquired during the verification test and 100% of the calibration and QC data were audited and compared against QAPP specifications. This first ADQ included a comprehensive audit of all data generated by the laboratories that analyzed the canisters (for CoCs and SF_6) and PVF bags (for radon).

This ADQ resulted in 4 findings and six observations, and each of the four findings ultimately resulted in a deviation from QAPP specifications. The first finding concerned the change in canister pressure during the time that elapsed between sample shipment and sample receipt. More details are provided in QAPP Deviation 3. Briefly, a total of 36 out of the 47 canisters collected at both field sites failed the QAPP-specified pressure difference criterion of < 1 inch Hg pressure change between sample shipment and receipt at the laboratory. Canister pressures did change, but they all decreased (i.e., the measurements indicated greater vacuum upon receipt at the laboratory). This is a physically impossible spontaneous phenomenon, and bias between the pressure gauges used for the measurements was suspected. However, it is clear that pressures in three of the SS canisters from the ASU Research House – BL-SS-VOC-1, NP-SS-VOC-1, and PP-SS-VOC-3 – increased (i.e., their vacuum decreased) over the time interval between laboratory receipt and analysis. These canisters fail the alternative acceptance criteria

pressure, i.e. that canister pressure cannot increase (i.e., that vacuum cannot decrease) during the time between completion of sample collection and analysis. For these three canisters, the results that are affected are shown in red text in Table A4. For the three canisters, the change in pressure ranged from 2.4 to 5.2 inch Hg; as a result, if the change in pressure was due to canister leakage, this resulted in a 10% to 20% dilution of the sample. However, in no instance did any of the final canister pressures reach 0 inch Hg gauge. Thus the impact on test outcomes is expected to be minimal since results from these three SS canister samples are not included in the calculation of any quantitative verification metrics, only in the verification of assumptions for the Mosley Model.

The second finding regarded analysis of continuing calibration verification (CCV) standards after completion of the analysis of all samples in a given batch. As detailed in Deviation 4, this QAPP requirement was in error. Final CCV analysis is not required by U.S. EPA Compendium Method TO-15,[15] nor is such required by the laboratory's standard operating procedure. As such, no impact on test outcomes is expected as a result of this deviation.

The third finding, written up as Deviation 5, was that not every batch of canisters analyzed for CoCs in IA, AA and SS gas included a replicate analysis. Subsequent to the completion of the first ADQ, additional replicate data were delivered to the QAO who determined that in fact a replicate had been analyzed with every batch and that all replicates met the appropriate acceptance criteria. Thus Deviation 5 no longer applied and was vacated.

The fourth finding covered the analysis of radon in PVF bags specifically that a matrix spike and method blank were not analyzed with every sample batch. This finding resulted in deviation 6. This deviation did not impact test outcomes given that the laboratory employed a wide variety of appropriate and applicable alternative QC techniques, generally in accordance with guidance provided by the EPA.[17] This guidance document specifies that the calibration of the radon measurement system be verified every 12 months, and states that the measurement system background be checked, but does not explicitly specify a frequency for such background checks. For convenience, the details of the actual radon analytical laboratory's QC measures are summarized below.

Radon analysis for the ETV test samples was performed on 10/6/2010-10/13/2010 for the ASU House batch and 11/3/2010-11/5/2010 for the Moffett Field samples. Leading up to the analysis of these samples, three different quality control checks were performed at different times. The first check was a channel confirmation using a cell containing ^{241}Am. Since December 2009, three ^{241}Am cell checks have been performed; in December 2009, in May 2010, and on October 14th, 2010. Variances in the counts per minute for all channels were less than 1%. The second QC check performed was the measurement of NIST-traceable ^{226}Ra standards to calibrate the efficiency of the cell/channel combinations. The efficiency test was performed September 23rd and 24th, 2010, immediately before analysis of samples from the ASU House. The results showed that the channels and cells were still within their calibrated efficiency range by comparing concentrations to the calculated mean for all channels and cells. The calculated results varied only ~ ± 5 % from the mean. The third check was a check of cell backgrounds; cells were checked a variety of different times from June through October 2010. Cells are segregated on the basis of background, with high background cells used to measure radon in SS

samples, and low background cells for IA and AA. Background values are subtracted from measured values to generate the reported disintegrations per minute and subsequently to radon concentrations in pCi L^{-1}. Background values are also used in the determination of MDLs.

The ADQ also revealed six observations, one related to data completeness and the remainder regarding QC exceedances for replicate (1 observation) and duplicate (3 observations) analyses, and the radon field blank. In response to these observations, the following actions were taken.

- The NAVFAC Atlantic QAO requested and received additional information from the analytical laboratory, thereby completing the data package in question.
- The impact of excessive variability in the various replicate and duplicate analyses was assessed. QC results are not specifically included in the quantitative verification metrics for this test, thus direct impacts on test outcomes is minimal. However, these QC exceedances demonstrate that, for the samples affected, there exists the chance for high variability in all of the measurements performed during this verification test. Affected samples are highlighted in orange text in Tables A2, A3, and A4.
- The concentration of radon in the field blank at the ASU House, 0.26 pCi L^{-1}, while exceeding the QAPP specification of 0.2 pCi L^{-1}, was found to be less than the corresponding MDL (0.36 pCi L^{-1}) for the subject analysis.

The NAVFAC QAO also performed a final ADQ that assessed overall data quality, including accuracy and completeness of this technical report. To ensure the integrity of the reported results, the QAO traced data from initial acquisition, through reduction and statistical analysis, to final reporting. The QAO confirmed that all audit findings and observations had been addressed, verified the integrity of all hand entered and manually calculated results, and confirmed that all formulae were accurate and consistent. The second ADQ revealed no findings or observations.

All of the findings and observations for the first ADQ were determined to have either no or only minimal impact on test outcomes. Audit reports covering both ADQs were prepared and distributed to the EPA.

Chapter 5
Statistical Methods

The statistical methods used to evaluate the quantitative performance factors listed in Section 3.3 are presented in this chapter. Qualitative observations were also used to evaluate verification test data.

5.1 Decision-making Support

5.1.1 Building Pressure Differential

The Omniguard 4® pressure differential instrument measured the minimum and maximum I/O ΔP every five minutes. This generated a time series of approximately 288 observations over 24 hours for each pressure condition at each building. Pressure differentials were corrected to account for the reference ports on each of the ΔP instruments being open to the indoor atmosphere so that a positive ΔP indicates the potential for downward flow of air from the building through the foundation and a negative ΔP indicates the potential for upward flow of soil gas through the foundation into the building. The arithmetic mean of the minimum and maximum ΔP for each observation in the time series was calculated, as was the overall mean of the entire time series of observations, its standard deviation, and the standard deviation of the mean. One-sided t-tests were performed to determine if the ΔP^- at each building was statistically significantly less than -1 Pa and if each ΔP^+ was statistically significantly greater than 1 Pa. The null (H_0) and alternative (H_1) hypotheses were formulated as follows.

Under NP:

H_0: $\Delta P^- = -1$ Pa
H_1: $\Delta P^- < -1$ Pa

Under PP:

H_0: $\Delta P^+ = 1$ Pa
H_1: $\Delta P^+ > 1$ Pa

In addition, the percentage of the individual observations either less than -1 Pa (under NP) or greater than 1 Pa (under PP) was calculated.

5.1.2 Vapor Intrusion Enhancement And Reduction

The degree that VI was enhanced under induced NP conditions was determined by comparison of $Q_i^- \cdot (R_i^- - R_a^-)$ to $Q_i \cdot (R_i - R_a)$. If $Q_i^- \cdot (R_i^- - R_a^-) > Q_i \cdot (R_i - R_a)$, then under induced NP conditions some degree of enhancement of VI has been verified. The degree that VI was reduced under induced PP conditions was similarly determined comparison of $Q_i^+ \cdot (R_i^+ - R_a^+)$ to $Q_i \cdot (R_i - R_a)$. If $Q_i^+ \cdot (R_i^+ - R_a^+) < Q_i \cdot (R_i - R_a)$, then under induced PP conditions some degree of reduction of VI has been verified. $Q_i \cdot (R_i - R_a)$, $Q_i^- \cdot (R_i^- - R_a^-)$, and $Q_i^+ \cdot (R_i^+ - R_a^+)$ for each building were calculated as described in Section 3.3.1.2. The errors in the R_i, R_i^-, and R_i^+ were taken to be the standard deviation of the three spatially distributed measurements; relative errors in R_a, R_a^-, and R_a^+ were assumed to be equal to relative errors in corresponding triplicate R_i, R_i^-, and R_i^+ measurements, respectively. The error in Q_i, Q_i^-, and Q_i^+, the quantities $(R_i - R_a)$, $(R_i^- - R_a^-)$, and $(R_i^+ - R_a^+)$, and the quantities $Q_i \cdot (R_i - R_a)$, $Q_i^- \cdot (R_i^- - R_a^-)$, and $Q_i^+ \cdot (R_i^+ - R_a^+)$ were estimated by propagation of errors.[xv] Results of these propagation of error calculations are given in Table A2. Two-sample one-sided paired t-tests were conducted to determine if the above inequalities could be verified statistically. Under NP, the following hypotheses were tested.

H_0: $Q_i \cdot (R_i - R_a) = Q_i^- \cdot (R_i^- - R_a^-)$
H_1: $Q_i \cdot (R_i - R_a) < Q_i^- \cdot (R_i^- - R_a^-)$

Under PP, the following hypotheses were tested.

H_0: $Q_i \cdot (R_i - R_a) = Q_i^+ \cdot (R_i^+ - R_a^+)$
H_1: $Q_i \cdot (R_i - R_a) < Q_i^+ \cdot (R_i^+ - R_a^+)$

Additional statistical tests were performed to investigate whether $R_i^+ = R_a^+$. The original data were transformed onto the natural log scale. Two-sample 2-sided t-tests assuming unequal variances were conducted. The null and alternative hypotheses were formulated as follows.

H_0: $R_i^+ = R_a^+$
H_1: $R_i^+ \neq R_a^+$

Estimated detection limits were substituted where concentrations were reported as either zero or not detectable.

[xv] Details are provided in Appendix C of QAPP[10] and results of this propagation of error are shown in Table A2 of this report. The estimated error in Q_i was based on percent error estimates of C_T (0.2%), acceptance limit of the % error in Q_T (±10%), and the standard deviation of the three IA measurements for SF_6 under BL conditions; see QAPP Equation C-8. Errors in Q_i^- and Q_i^+ were estimated similarly using the standard deviation of the three IA measurements of SF_6 under NP and PP, respectively. The estimated error for $(R_i - R_a)$ was determined by adding the estimated errors for R_i and R_a in quadrature; errors in the quantities $(R_i^- - R_a^-)$, and $(R_i^+ - R_a^+)$ were calculated similarly – see QAPP Equation C-2. The error in the quantity $Q_i \cdot (R_i - R_a)$ was estimated by adding the errors in Q_i and $(R_i - R_a)$ in quadrature; errors in the quantities $Q_i^- \cdot (R_i^- - R_a^-)$ and $Q_i^+ \cdot (R_i^+ - R_a^+)$ were similarly estimated – see QAPP Equation C-6.

In instances where statistically significant differences were not detected, the feasibility of performing a post-hoc calculation was investigated. Such a calculation would estimate the minimum detectable difference, with 80% power and a 5% false positive rate, given the observed sample size and variability. However, to perform such retrospective calculations, a number of prerequisites had to have been met, including that a sufficient number of observations were present (at least 3) for both samples in the comparison, the p-value was not significant, all measurements were greater than corresponding MDLs, and in the case of paired t-tests, the correlation between paired observations was positive. One or more of these prerequisites were not met for the comparisons in this section; as such, no post-hoc power calculations were performed.

5.1.3 Fractional Contribution of Vapor Intrusion to indoor CoC concentrations

The 16 F_{VI} were calculated as described in Section 3.3.1.3. The error in each F_{VI}, ΔF_{VI}, was estimated using a Monte Carlo technique instead of propagation of errors. The propagation of errors error estimation technique given in the QAPP ignores more than one covariance and these correlations cannot be assumed to be conservative. Furthermore, this experiment did not furnish sufficient data to estimate the correlations.

A number of variables were transformed onto the natural log scale ahead of the Monte Carlo analysis; these include C_i, C_i^-, C_i^+, R_i, R_i^-, R_a, and R_a^-.[xvi] Those variables that were not transformed included C_a, C_a^-, C_a^+, Q_i, Q_i^-, and Q_i^+. On the appropriate scale, errors in C_i, C_i^-, C_i^+, R_i, and R_i^- were taken to be the standard deviation of the three spatially distributed measurements; relative errors in R_a, and R_a^- were assumed to be equal to relative errors in corresponding triplicate R_i and R_i^- measurements, respectively. Errors in C_a, C_a^-, C_a^+ were assumed to be equal to the accuracy limit for the TO-15 volatiles analysis, ±30%. Errors in Q_i, Q_i^-, and Q_i^+ were estimated by propagation of error technique as described in Section 5.1.2.

Each Monte Carlo simulation generated random draws from the distributions of the quantities in equations 4 and 5 (for F_{VI}^-) and 6 and 5 (for F_{VI}^+) (see Section 3.3.1.3). Calculating both F_{VI}^- and F_{VI}^+ required univariate and bivariate normal sampling of random variables. For those random variables assumed to have correlations equal to zero, joint distributions were calculated as the product of the corresponding marginal distributions (i.e., a univariate normal distribution that was characterized by a mean and standard deviation). For those random variables known to have nonzero correlations, the joint distribution was a bivariate normal characterized by two means, two standard deviations, and the applicable correlation coefficient ρXY (where X and Y are the two variables in question). The formula for calculating F_{VI}^- required sampling from four univariate normal distributions (Q_iR_a, Q_iC_a, $Q_i^-R_a^-$, and $Q_i^-C_a^-$) and four bivariate normal distributions (Q_iC_i, $Q_i^-C_i^-$, Q_iR_i, and $Q_i^-R_i^-$); the Monte Carlo analysis for F_{VI}^+ required sampling from two univariate normal (Q_iC_a and $Q_i^+C_a^+$) and two bivariate normal distributions (Q_iC_i and $Q_i^+C_i^+$).[xvii]

[xvi] All log-transformed values were exponentiated before final results were reported.

[xvii] Inspection of applicable physical phenomena revealed that building flow rates and ambient levels of CoC and radon should be uncorrelated given that, to the first approximation, indoor air concentrations do not contribute substantially to outdoor levels; thus $\rho Q_iR_a = \rho Q_iC_a = \rho Q_i^-R_a^- = \rho Q_i^-C_a^- = \rho Q_i^+C_a^+ = 0$. Furthermore, all of the remaining applicable nonzero covariances (Q_iC_i, $Q_i^-C_i^-$, $Q_i^+C_i^+$, Q_iR_i, and $Q_i^-R_i^-$) should be negative under the

For each building/CoC combination, eleven sets of correlation coefficients were constructed that obeyed the appropriate ordering assumptions.[xviii] Confidence intervals were estimated for each set of coefficients to determine whether the results would be sensitive to the choice of those coefficients. For each combination of building, CoC, and correlation coefficients, N = 100,000 samples were generated from each sampling distribution required to calculate F_{VI}^{+} and F_{VI}^{-}. Results were combined using the appropriate formulae, and the 2.5 and 97.5 percentiles were calculated to obtain a 95% confidence interval for the various F_{VI}^{+} and F_{VI}^{-} estimates.

As explained in Chapter 6, post hoc power calculations were not performed for the F_{VI} values.

5.2 Comparability

Comparability of the observed I/O differential pressures is assessed by calculation of the relative percent difference (RPD) of the mean differential pressure under NP and PP conditions (RPD, ΔP^{-} and RPD, ΔP^{+}, respectively) using equations 4 and 5.

$$RPD, \Delta P^{-} = -\frac{\left|\Delta P_1^{-} - \Delta P_2^{-}\right|}{0.5 \cdot \left(\Delta P_1^{-} + \Delta P_2^{-}\right)} \cdot 100 \qquad (4)$$

$$RPD, \Delta P^{+} = \frac{\left|\Delta P_1^{+} - \Delta P_2^{+}\right|}{0.5 \cdot \left(\Delta P_1^{+} + \Delta P_2^{+}\right)} \cdot 100 \qquad (5)$$

5.3 Verification of Model Assumptions

A total of eight assumptions were tested at each building and are organized into three groups. The first group includes two assumptions to determine if inducing a NP in the building had a significant effect on CoC and radon concentrations in SS soil gas below the building foundation.

1. $C_s = C_s^{-}$
2. $R_s = R_s^{-}$

C_s and C_s^{-} for each CoC and R_s and R_s^{-} were calculated as the mean of the three SS concentration measurements under BL and NP conditions, respectively. Errors in these quantities were estimated as the standard deviations. All data were first transformed onto the natural log scale before means and standard deviations were calculated. Two-sample 2-sided paired t-tests were executed to investigate the following null and alternative hypotheses.

assumption that ambient levels of CoCs and radon are typically less than indoor levels.

[xviii] For instance, given that $C_a < C_i$, increasing Q_i will lead to a decrease in C_i; thus $\rho Q_i C_i < 0$. Reasoning along the same lines, for chemicals expected to have VI sources, i.e., TCE, 1,1-DCE, and PCE, $\rho(Q_i^{-}, C_i^{-}) < \rho(Q_i, C_i) < \rho(Q_i^{+}, C_i^{+})$ [i.e., $\rho(Q_i^{-}, C_i^{-})$ is more strongly correlated than $\rho(Q_i^{+}, C_i^{+})$] and similarly, $\rho(Q_i^{-}, R_i^{-}) < \rho(Q_i, R_i)$; for chemicals not expected to have VI sources, benzene and toluene, $\rho(Q_i^{-}, C_i^{-}) \sim \rho(Q_i, C_i) \sim \rho(Q_i^{+}, C_i^{+})$.

Assumption 1:

H_0: $C_s = C_s^-$
H_1: $C_s \neq C_s^-$

Assumption 2:

H_0: $R_s = R_s^-$
H_1: $R_s \neq R_s^-$

As described in more detail in Chapter 6, the assumptions above were tested both including and excluding the results from SS-1 at ASU House, and post hoc power calculations of minimum detectable differences were performed only for TCE, PCE, benzene and radon at Moffett Field.

The second group of assumptions whose validity were verified related to if radon concentrations in AA were in fact much lower than those in SS soil gas below the building foundation.

3. $R_a << R_s$
4. $R_a^- << R_s^-$
5. $R_a^+ << R_s^+$

Values of R_s and R_s^- were calculated as the mean of the three SS concentration measurements under BL and NP conditions, respectively; R_s^+ was calculated similarly as the mean under PP conditions. The values of R_a, R_a^-, and R_a^+ were taken as the results of a single grab sample of AA; the estimated relative error in their concentrations will be assumed to be equal to the relative error in the corresponding triplicate R_i, R_i^-, and R_i^+ measurements, respectively.[xix] All data were transformed to the natural log scale before conducting a 2-sample 1-sided (unpaired) t-test with unequal variances. Hypotheses were formulated as follows.

Assumption 3:

H_0: $R_a - R_s = 0$
H_1: $R_a - R_s < 0$

Assumption 4:

H_0: $R_a^- - R_s^- = 0$
H_1: $R_a^- - R_s^- < 0$

[xix] The error in R_a^- at ASU House was assumed equal to the standard deviation of R_i^-; that is, relative errors were not used. Assuming a relative error unreasonably inflated the error estimate for R_a^- given the high absolute values of R_i^- in comparison to R_a^-.

Assumption 5:

H_0: $R_a^+ - R_s^+ = 0$
H_1: $R_a^+ - R_s^+ < 0$

As described in more detail in Chapter 6, the assumptions above were tested both including and excluding the results from SS-1 at ASU House, and post hoc power calculations of minimum detectable differences were not performed.

The third and final group of assumptions tested included those to determine if, in IA, the loss of radon through building ventilation is much greater than the loss due to radioactive decay.

6. $Q_i >> \lambda V$
7. $Q_i^- >> \lambda V$
8. $Q_i^+ >> \lambda V$

Each of the two building's volumes was calculated using interior dimensions of each and the error in the building volume was conservatively estimated to be ± 30%.[xx] The decay rate of radon was found in the literature[13] and assumed to be known quite accurately (estimated error of ± 1%). The values of Q_i, Q_i^-, and Q_i^+ and estimates of their errors were calculated as described in section 5.1.3. Data were not log transformed. The number of standard deviations that the mean of λV was from the mean of Q_i was calculated and a one-sided p-value was generated assuming 2 degrees of freedom (Q_i was regarded as having a sample size of 3 and λV a sample size of 1). Minimum detectable differences were calculated if the null hypotheses were not rejected. The null and alternative hypotheses were formulated as follows.

Assumption 6:

H_0: $Q_i = \lambda V$
H_1: $Q_i > \lambda V$

Assumption 7:

H_0: $Q_i^- = \lambda V$
H_1: $Q_i^- > \lambda V$

Assumption 8:

H_0: $Q_i^+ = \lambda V$
H_1: $Q_i^+ > \lambda V$

[xx] This conservative estimate of error in building volume is insignificant compared to estimated errors in building ventilation rates. See Section 6.5.

Chapter 6
Test Results

The results of the verification test of the building pressure control technique are presented in this Chapter. Presented first in Section 6.1 are the results of the various field measurements, including differential pressures, calculations of building ventilation rates, presentation of the radon, SF_6, and CoC concentrations, and mass discharges of the various compounds. Where necessary for clarity, descriptions of the data manipulation methods are discussed. Presented in Sections 6.2 to 6.4 is the evaluation of the three different quantitative performance metrics: decision-making support, comparability, and operational factors. The IA concentration data in Section 6.1.4 and the mass discharges in Section 6.1.6 illustrate qualitative trends that aid in evaluating the performance of the pressure control technique in terms of decision-making support.

The data generated during the verification test, both used in the calculations presented in this Chapter and ancillary to the test, are presented in Appendix A.

6.1 Measurement Results From Both Buildings

6.1.1 Indoor/Outdoor and Cross-Foundation Pressure Differentials

During each verification test, both the I/O and cross foundation differential pressures were measured. Treatment of the ΔP data was described in detail in Section 5.1.1. The averages of the minimum and maximum ΔPs for each five-minute observation are plotted in Figure 9; also shown is the overall average ΔP for each of the three pressure conditions.

For the induced NP period, negative ΔPs were measured at both buildings, both I/O and across the foundation. Similarly, for the induced PP period, positive ΔPs were measured both I/O and across the foundation at both buildings. Such results indicate that the building pressure control technique was successful at manipulating building pressure.

The control of I/O ΔP is one of the quantitative performance metrics for this verification test; it and the cross-foundation differential pressures are discussed in more detail in Section 6.2.

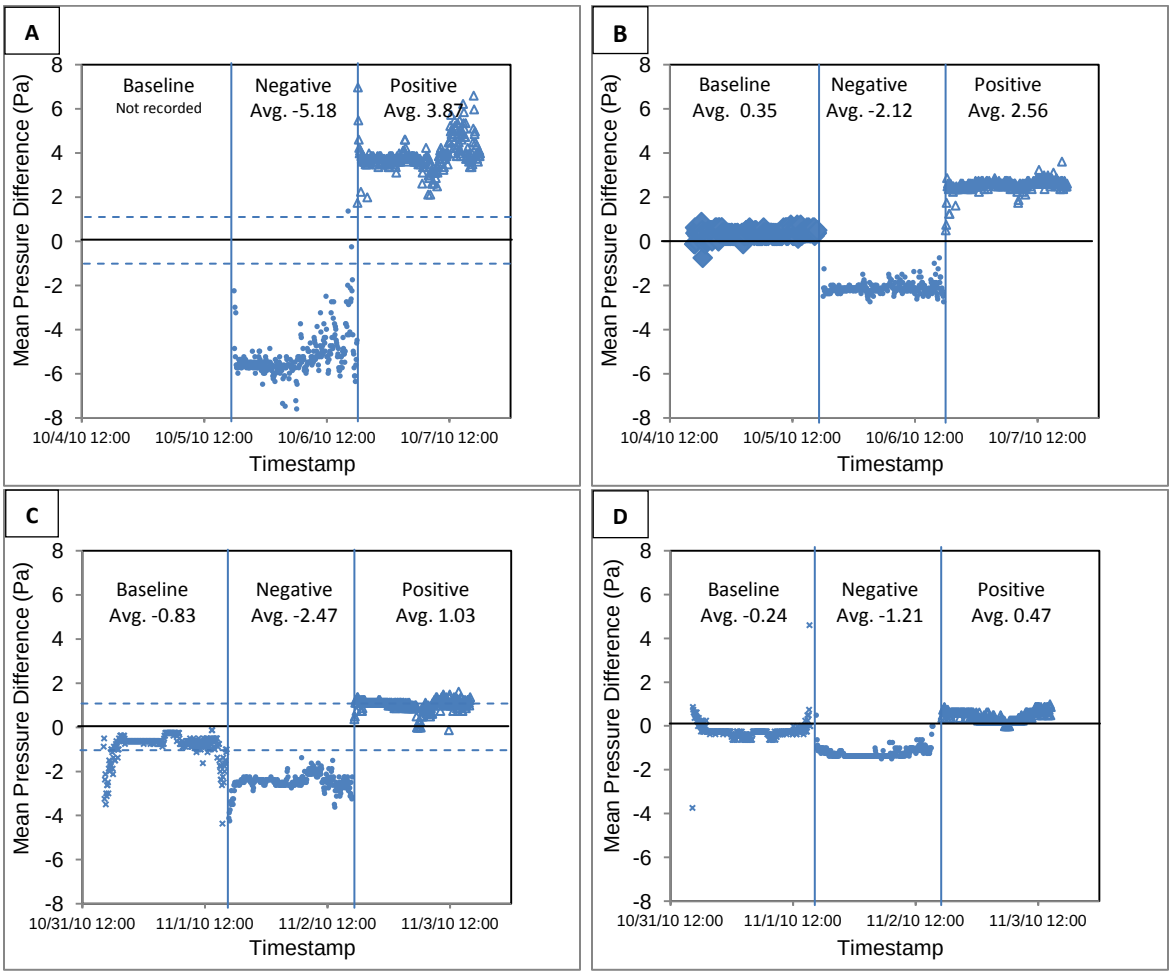

Figure 9. Indoor/Outdoor and Cross-Foundation Differential Pressure Measurements under Three Different Pressure Conditions. Shown are results for ASU House (I/O in Panel A and Cross-foundation in Panel B) and at Moffett Field Building 107 (I/O in Panel C and Cross-foundation in Panel D).

6.1.2 Building Ventilation Rates

Building ventilation rates (Q_i) were calculated for each pressure condition at each building as described in Section 3.3.1.2. They are shown graphically in Figure 10 along with their ± 1 standard deviation errors that were estimated as described in Section 5.1.2. The estimated errors in building ventilation rates are driven in large part by the variability in the spatially distributed IA SF_6 concentrations; the latter is likely the result of insufficient mixing of the tracer gas in the indoor atmosphere.

For both verification tests, building ventilation rates were higher under both induced NP and PP conditions compared to the BL. Building ventilation rates correspond to AERs of 0.2 h^{-1}, 1.4 h^{-1} and 1.3 h^{-1} for the ASU House, and 0.3 h^{-1}, 1.6 h^{-1}, and 1.7 h^{-1} for Moffett Field Building 107, under BL, induced NP, and induced PP conditions, respectively.

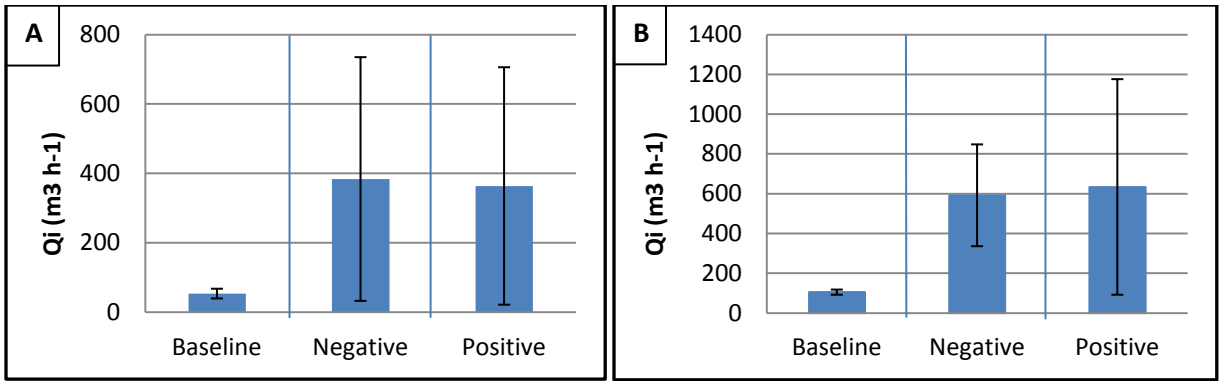

Figure 10. Building Ventilation Rates Measured under Three Different Pressure Conditions at ASU House (Panel A) and Moffett Field Building 107 (Panel B).

6.1.3 Concentrations of Compounds in Ambient Air

The ambient concentrations for the various compounds at each building are show in Figure 11. Plots in panels A and B in this Figure, and in Figures in subsequent sections, are divided to show three compounds that were expected to have predominately subsurface sources (radon, TCE, and 1,1-DCE for ASU House and radon, TCE, and PCE for Moffett Field Building 107) and the three compounds that were expected to have predominately indoor or ambient sources (SF_6, benzene, and toluene for both buildings).

For instances where compound concentrations were reported as not detectable, the MDL is shown and the data are flagged with "ND." In instances where reported radon concentrations were less than the MDL, the reported concentration is shown and the result is flagged with "<MDL." AA concentrations are based on single measurements, thus no error bars are shown.

The potential effect of ambient sources on compound concentrations measured in IA can be evaluated qualitatively by comparing the concentration measured in AA to the concentration measured in IA. IA concentrations are presented in the following section.

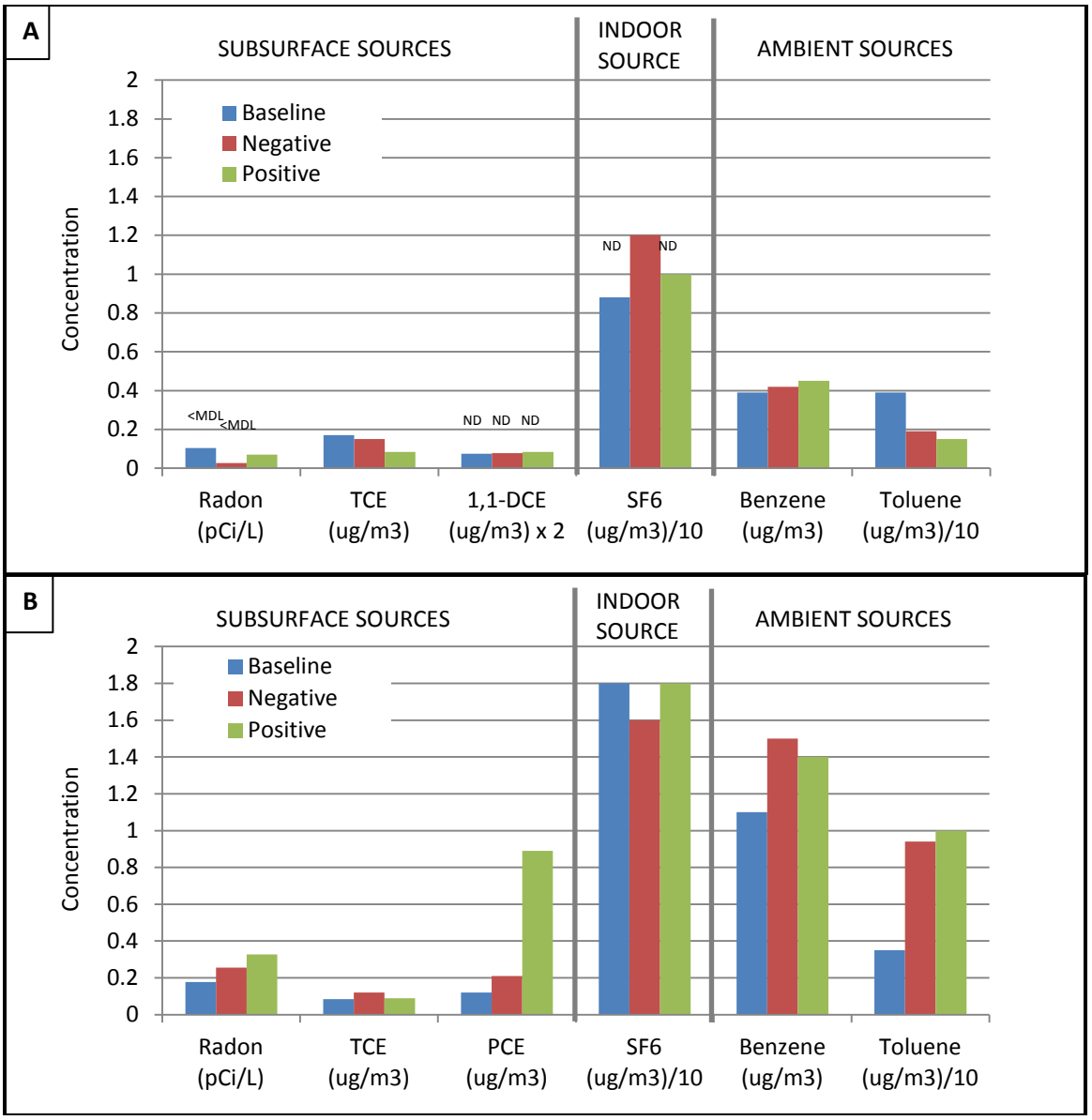

Figure 11. Concentrations of Compounds Measured in Ambient Air at ASU House (Panel A) and Moffett Field (Panel B).

6.1.4 Concentrations of Compounds in Indoor Air

Concentrations of the various compounds in IA were measured at three spatially separated locations in each test building. Figure 12 shows the average compound concentrations across the three measurement locations and error bars as ± 1 standard deviations. Where individual concentrations were reported as not detectable, the MDL was substituted into the average and standard deviation calculations. For these and future plots in this Section, asterisks (*) denote instances where at least one such MDL substitution was performed. No such substitutions were performed for radon, but plus signs (+) indicate instances where at least one reported radon value was less than its corresponding MDL.

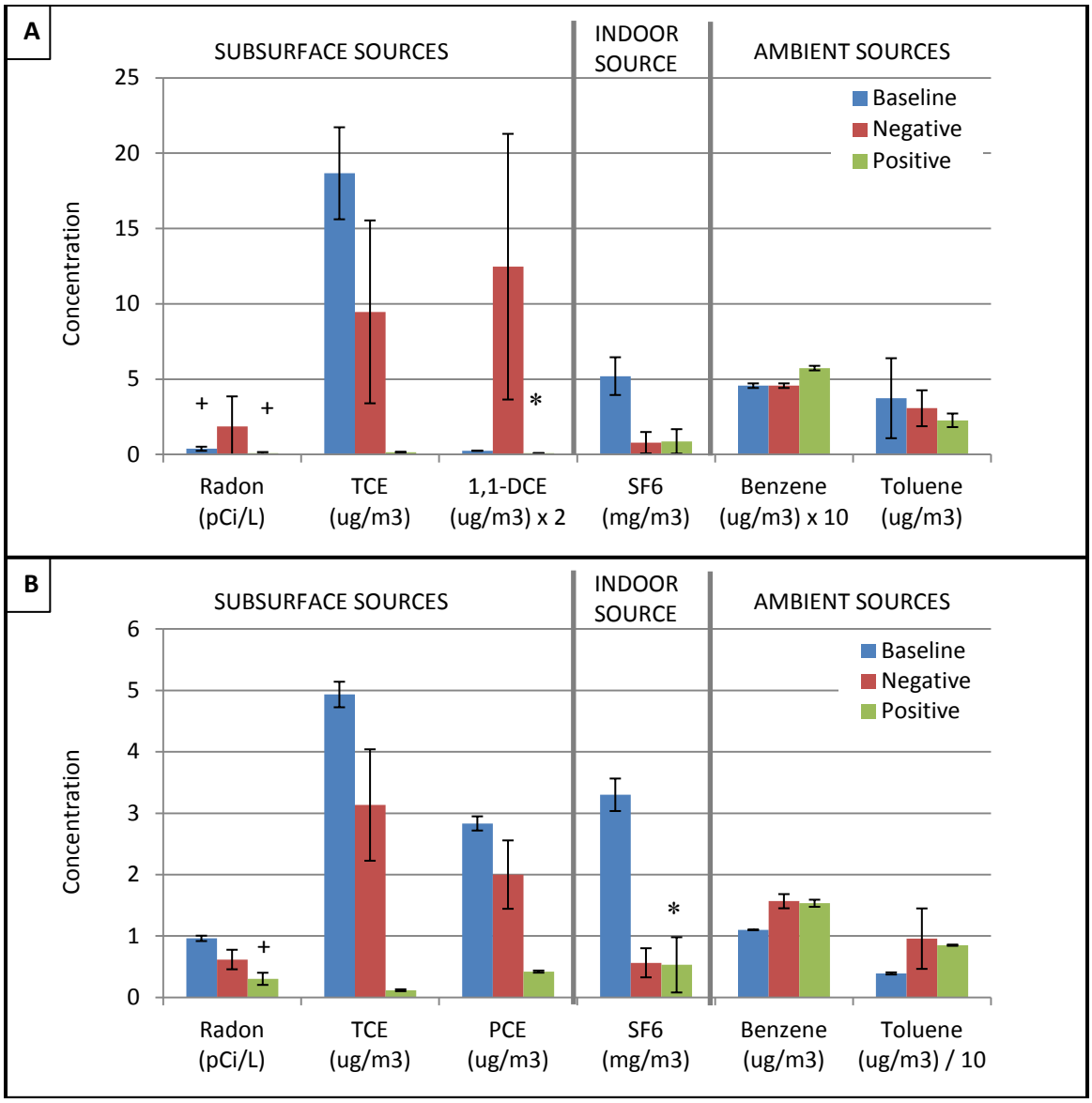

Figure 12. Concentrations of Compounds Measured in Indoor Air at ASU House (Panel A) and Moffett Field (Panel B).

For the ASU House, TCE was expected to have predominately a subsurface source. However, after the verification study was completed, it was discovered that a liquid TCE laboratory standard had been stored in a refrigerator in the garage throughout the duration of testing, thereby creating the potential for an unexpected TCE source at this location. This may explain the high IA TCE concentration under BL conditions at ASU House.[xxi] In the absence of such an indoor source, it was expected that its BL IA concentration would be lower than that under induced NP, similar to the trends observed for radon and 1,1-DEC, other compounds with

[xxi] The impact of the indoor TCE source may also be seen in the plot of the real-time TCE concentrations as measured by the HAPSITE GC/MS (Figure A3) in which TCE is quite high under BL despite the fact that the cross-foundation pressure differential was positive, indicating that VI should be suppressed under BL. In the absence of such a source, TCE concentrations in IA likely would have been lower than observed.

subsurface sources. This is in contrast to Moffett Field Building 107 where compounds with subsurface sources had higher IA concentrations under BL compared to NP since (a) VI was effectively turned on under BL conditions, as evidenced by the negative cross-foundation ΔP and (b) the combined effect of enhancing VI under NP was countered by the concomitant increase in ventilation rate. Nonetheless, in all cases for compounds with expected subsurface sources, concentrations in IA were lower under the induced PP condition compared to the induced NP condition.

For compounds with expected indoor or ambient sources, there was little change in concentrations between NP and PP. IA SF_6 concentrations did decrease under induced NP and PP compared to BL – due to dilution from the increased building ventilation rate, behavior consistent with having a dominant indoor source – but its concentration did not change between the two different induced pressure conditions given relatively constant building ventilation rates. Changes in the indoor concentrations of benzene and toluene between BL and NP/PP were similar to the changes in their AA concentrations, consistent with the expectation that AA was the major source of these compounds to IA.

Figure 13 shows the average compound concentrations measured in IA normalized by their concentrations in AA. Note that the graphs of normalized concentrations use a log scale. These figures show the relationship between the concentrations of the various compounds in IA compared to AA and demonstrate the differences and similarities in the sources of the compounds.

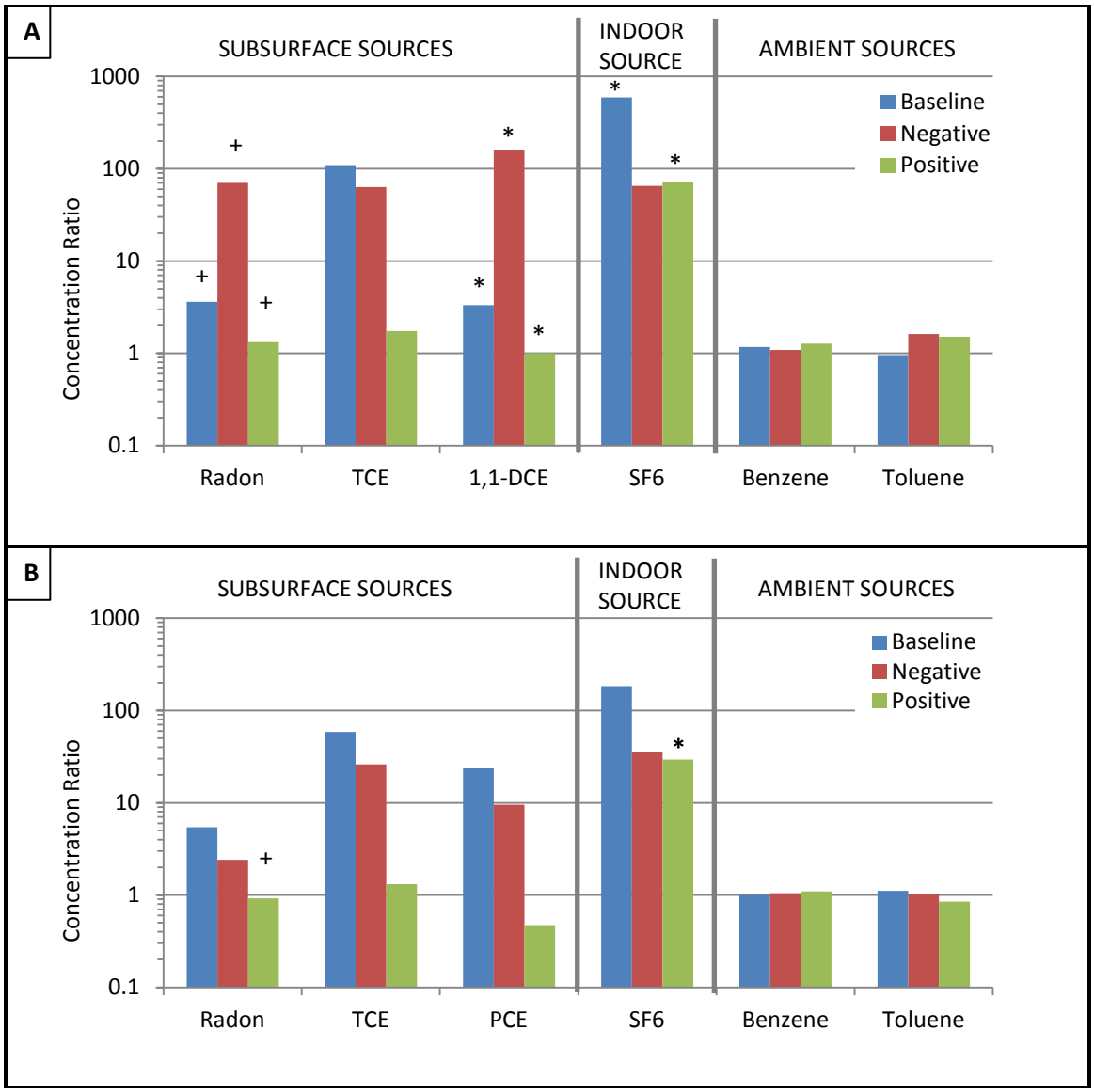

Figure 13. Average Indoor Air Concentrations Normalized by Ambient Concentrations at ASU House (Panel A) and Moffett Field Building 107 (Panel B).

For both buildings, compounds with expected subsurface sources (i.e., radon, TCE, 1,1-DCE, and PCE) had IA concentrations greater then AA (i.e., normalized concentrations > 1) under the induced NP condition but had IA concentrations similar to AA (i.e., normalized concentration close to 1) under the induced PP condition. For the compound with expected indoor source (i.e., SF_6), the IA concentration was greater than ambient for all pressure conditions. For the compounds with expected ambient sources (i.e., benzene and toluene), IA concentrations were similar to ambient for all pressure conditions. These plots demonstrate the ability of the building pressure technique to discern sources of various CoCs and judge the potential that certain CoCs may be present in IA due to VI. That is, compounds with expected subsurface sources – TCE, 1,1-DCE, and PCE – have patterns in their IA concentrations similar to radon, that has a known subsurface source. This indicates that these CoCs are likely present in IA under BL conditions due to VI. On the other hand, benzene and toluene have different concentration patterns

compared to radon, suggesting that VI is likely not a concern for these compounds. Decision-makers could use the qualitative information derived from such plots to evaluate compounds that are a VI concern at a specific building.

6.1.5 Concentrations of Compounds in Sub-Slab Soil Gas

SS soil gas samples were collected from three spatially distributed locations in each building. All three locations in each building were used to calculate the average SS compound concentrations (Figure 14). Error bars in the plots are the ± 1 standard deviation of the measured concentrations. Figure 15 presents the same data normalized by the indoor concentrations.

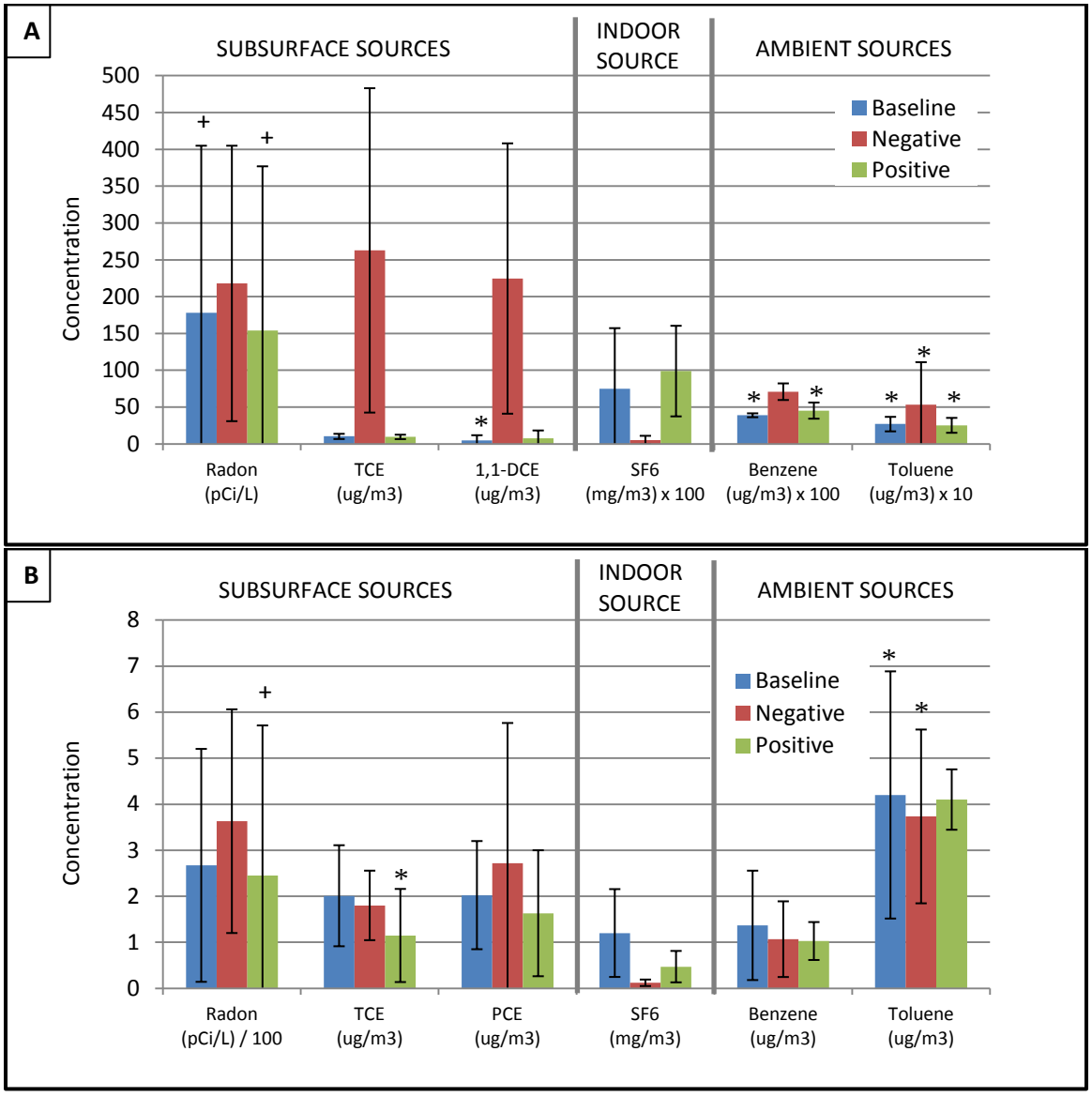

Figure 14. Concentrations of Compounds Measured in Sub Slab Soil Gas at ASU House (Panel A) and Moffett Field Building 107 (Panel B).

As shown in the normalized concentration graphs, at ASU House, the three compounds with nominally subsurface sources were present in SS gas at concentrations higher than measured in IA (except for TCE under BL conditions), consistent with a subsurface source for these compounds. For Moffett Field Building 107, radon, but not PCE or TCE, was present at a higher concentration below the building foundation. For both houses, concentrations of the indoor/ambient source compounds were similar in IA in SS soil gas. These plots further demonstrate the ability of the building pressure technique to discern sources of various CoCs.

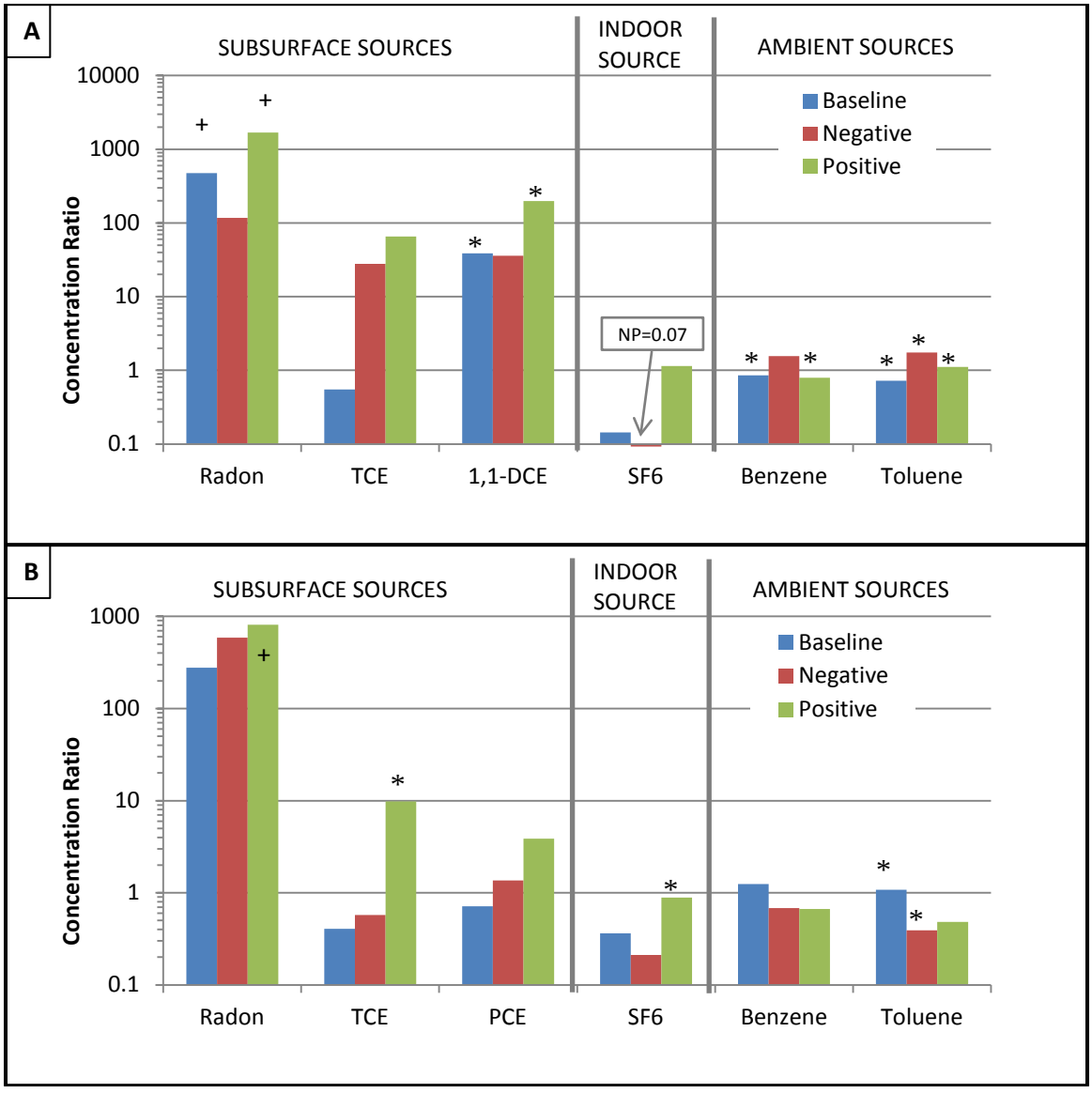

Figure 15. Average Sub-Slab Concentrations Normalized by Average Indoor Air Concentrations at ASU House (Panel A) and Moffett Field Building 107 (Panel B).

6.1.6 Mass Discharges

Mass discharge is the mass of a given compound that moves through the building per unit time. The mass discharge for each pressure condition is calculated by multiplying the building ventilation rate (Q_i) by the compound concentration. The total mass discharge is calculated as the product of Q_i and the compound's IA concentration (R_i, C_i, or T_i) and the mass discharge from ambient sources is calculated as the product of Q_i and the compound's AA (R_a, C_a, or T_a) concentration. The difference between the total mass discharge and the mass discharge from ambient sources provides the mass discharge from subsurface and indoor sources. As examples of these calculations, in Section 3.3.1.2 the total mass discharge, mass discharge from ambient sources, and mass discharge from subsurface and indoor sources were determined for radon using Equations 1, 2, and 3, respectively.[xxii]

The change in mass discharge between pressure conditions accounts for changes in both building ventilation rate and compound concentrations; thus, the change in mass discharge between pressure conditions provides a more comprehensive evaluation of the effect of the pressure condition on VI. Figures 16 and 17 provide the mass discharge for each compound under BL conditions, induced NP, and induced PP, normalized by the total mass discharge under the BL condition. In these Figures, normalized mass discharges are labeled in instances where the values are small relative to the chart scale. "S/I" and "A" refer to mass discharge from subsurface and indoor sources and from ambient sources, respectively. In a few cases, the mass discharge calculations yielded negative values. Although actual mass discharge cannot be negative, variability in measured compound concentrations can yield negative calculated values of mass discharges from indoor and subsurface sources, reflecting the uncertainty associated with small measured differences in compound concentrations in IA and AA.

In Figures 16 and 17, values greater than one indicate that the mass discharge was higher than under BL and values less than one indicate that mass discharge was lower than under BL. For example, for TCE in the ASU House, the normalized total mass discharge of 3.6 under induced NP and 0.05 under induced PP indicate that the total mass discharge increased over baseline (by 3.6 times) under the induced NP condition and decreased (by 95%) under induced PP. At both buildings, for compounds with expected subsurface sources, the total mass discharge was greater under induced NP than under induced PP. For benzene, toluene, and SF_6, (expected ambient and indoor sources), the total mass discharge was similar for both pressure conditions.

Furthermore, since the normalized BL mass discharge from ambient sources is equivalent to F_a, the fractional contribution of AA to the IA concentration of a given compound (see Section 3.3.1.3, Equation 7), much can be learned about the sources of the various compounds by inspection of these values.[xxiii] For instance, F_as are low and in many cases nearly 0 for radon,

[xxii] Note that, as explained in Section 3.3.1.2, indoor sources of radon are assumed to be negligible compared to subsurface sources, thus Equation 3 is the mass discharge of radon into IA from only subsurface sources.

[xxiii] Normalized mass discharges are also the basis of other Mosley Model calculations. For instance, under PP in which VI is 'turned off' ($R_i^+ = R_a^+$), $F_{VI}^+ = [Q_i \cdot (C_i - C_a) - Q_i^+ \cdot (C_i^+ - C_a^+)]/(Q_i \cdot C_i)$ = the normalized mass discharge from subsurface and indoor sources under BL – normalized mass discharge from subsurface and indoor sources under PP (Section 3.3.1.3, combination of Equations 5 and 7). In addition, $F_{in}^+ = Q_i^+ \cdot (C_i^+ - C_a^+)/(Q_i \cdot C_i)$ = normalized mass discharge from subsurface and indoor sources under PP (Equations 6 and 8). The calculation for F_{VI}^- and F_{in}^- are similar but somewhat more complicated since scaling factors are added based on radon.

TCE, 1,1-DCE, and PCE, indicating the predominance of subsurface/indoor sources (TCE and PCE have weak ambient sources). Moreover, an F_a of zero for SF_6 is consistent with it being the indoor tracer, and F_as of nearly 1 for benzene and toluene indicate strong ambient sources.

While the F_a information serves as indicator of a compound's source, the observed similarity of changes in mass discharges following building pressure perturbation is a more powerful, albeit still qualitative, CoC source attribution technique. That is, similar to the information gleaned from Figure 13 (Section 6.1.4), the mass discharges for compounds with expected subsurface sources – TCE, 1,1-DCE, and PCE – vary under application of the building pressure control technique similarly to radon (that has a known subsurface source) thereby indicating that these CoCs are likely present in IA under BL conditions due to VI. On the other hand, benzene and toluene have a different mass discharge pattern under pressure perturbation compared to radon, suggesting that VI is likely not a concern for these compounds. Such trends in mass discharges could aid decision-makers in evaluating compounds that are likely VI concerns at a specific building.

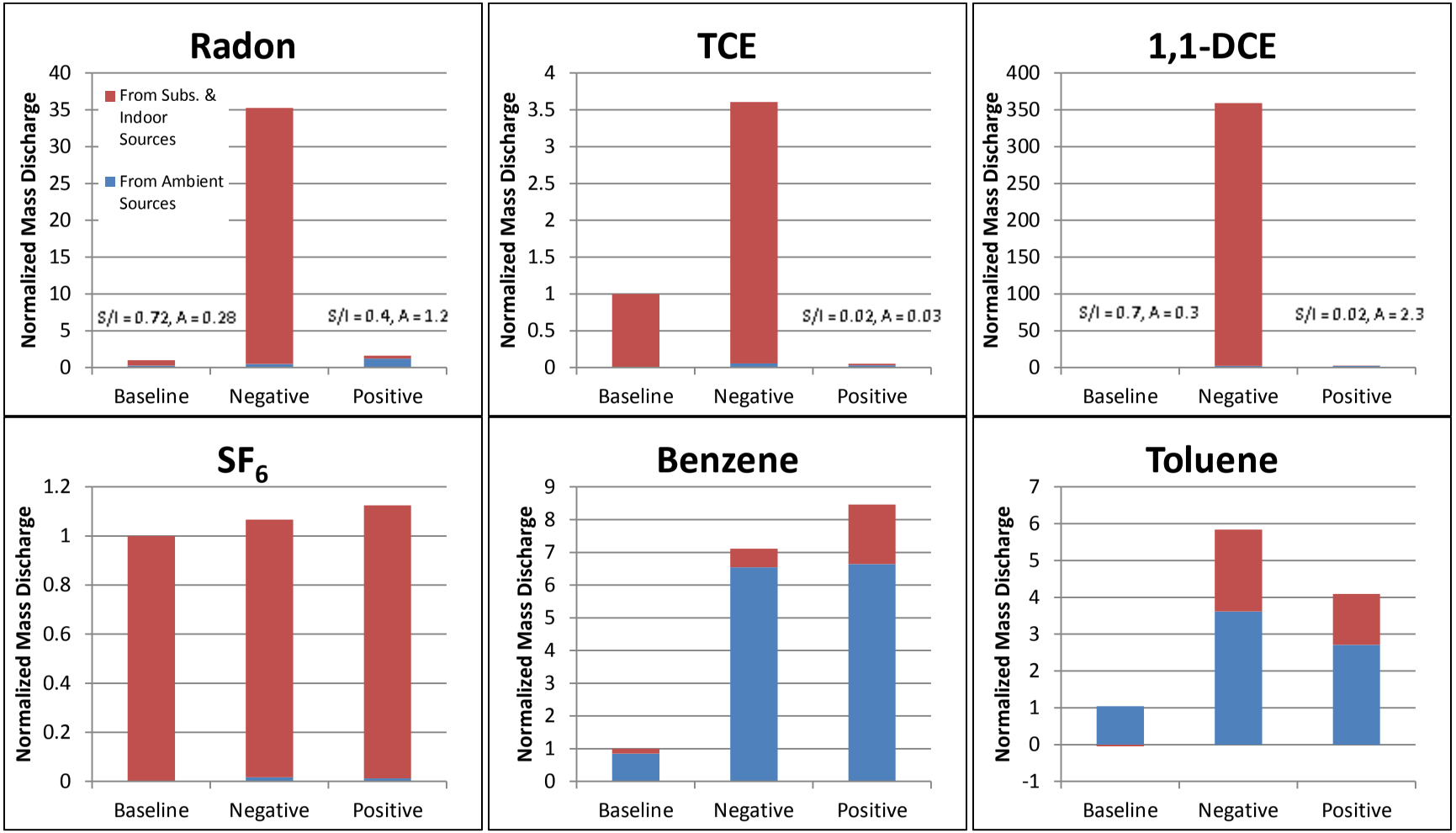

Figure 16. Normalized Mass Discharges at ASU House for Radon, TCE, and 1,1-DCE (Compounds With Primarily Subsurface Sources) and SF_6 (a Compound with a Dominant Indoor Source), and Benzene and Toluene (Compounds with Dominant Ambient Sources).

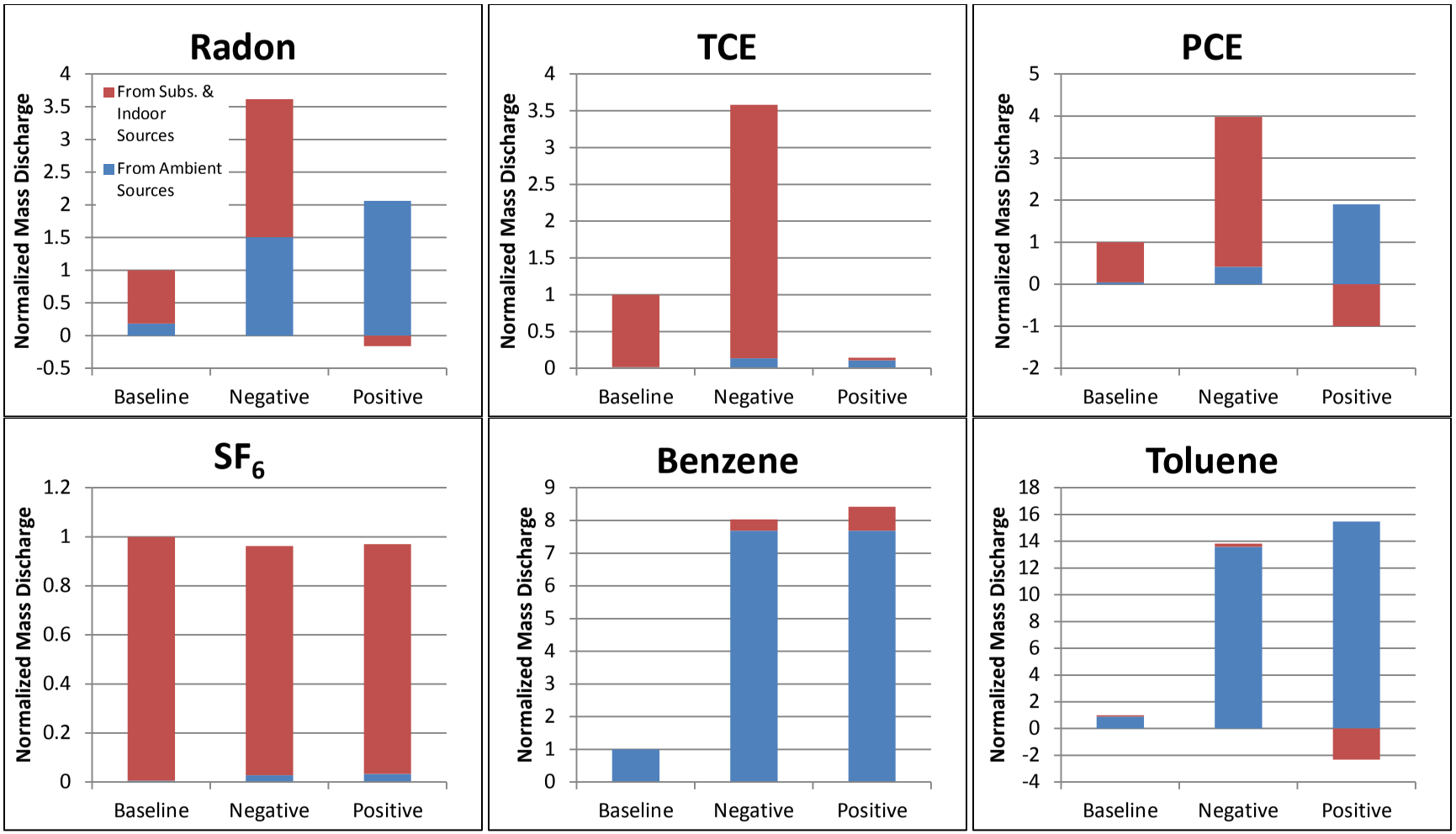

Figure 17. Normalized Mass Discharges at Moffett Field Building 107 for Radon, TCE, PCE (Compounds with Primarily Subsurface Sources) and SF_6 (a Compound with a Dominant Indoor Source), and Benzene and Toluene (Compounds with Dominant Ambient Sources).

6.2 Decision-making Support

6.2.1 Building Pressure Differential

The first verification metric for decision-making is the ability of the pressure control method to control building pressure. Building pressure control was verified by inspection of the mean I/O ΔP that was attained for the 24-hour periods of induced NP and PP at each of the two buildings. Statistical significance was tested to determine whether the observed mean ΔPs were less than -1 Pa under induced NP and greater than 1 Pa under induced PP. In each instance rejection of the null hypotheses – that the building pressure differentials were greater than or equal to -1 Pa (under NP) and less than or equal to 1 Pa (under PP) – at the 95% confidence level (5% false positive rate) indicates that building pressure control had been achieved. Results are shown in Table 7 below and were shown graphically in Figure 9, Panels A and C (Section 6.1.1).

Table 7. Indoor/outdoor pressure differentials at ASU House and Moffett Field Building 107.

ASU House

Test	ΔP	Mean ΔP, Pa	Std Dev, Pa	N[a]	Std dev/√N[b], Pa	$\Delta P^- < -1$ Pa?[c]	N below -1 Pa	$\Delta P^+ > 1$ Pa?[d]	N above 1 Pa
BL[e]	ΔP_1	N/A	N/A	N/A	N/A	N/A	N/A	N/A	N/A
NP	ΔP_1^-	-5.18	1.01	290	0.059	yes; $p < 0.0001$	288 (99%)	N/A	N/A
PP	ΔP_1^+	3.87	0.66	289	0.039	N/A	N/A	yes; $p < 0.0001$	289 (100%)

Moffett Field Building 107

Test	ΔP	Mean ΔP, Pa	Std Dev, Pa	N	Std dev/√N, Pa	$\Delta P^- < -1$ Pa?	N below -1 Pa	$\Delta P^+ > 1$ Pa?	N above 1 Pa
BL	ΔP_2	-0.83	0.60	290	0.035	N/A	N/A	N/A	N/A
NP	ΔP_2^-	-2.47	0.37	291	0.021	yes; $p < 0.0001$	291 (100%)	N/A	N/A
PP	ΔP_2^+	1.03	0.27	273	0.016	N/A	N/A	yes; $p = 0.044$	164 (60%)

[a]Number of observations

[b]Standard deviation of the mean

[c]H_0: mean = -1; H_1: mean < -1 Pa; H_0 rejected when $p < 0.05$

[d]H_0: mean = 1; H_1: mean > 1 Pa; H_0 rejected when $p < 0.05$

[e]Data are not available for BL conditions at ASU House; see Section 3.3

During each of the pressure perturbations at the two buildings, the mean building pressures were either below (under NP) or above (under PP) the target pressure of -1 Pa and 1 Pa, respectively, indicating that some degree of pressure building control was achieved under both pressure perturbation conditions at both buildings. In three of the four instances, mean building pressure differentials were either substantially less than the target pressure (under NP) or greater than the target pressure (under PP), as indicated by the low p values generated by the one-sided t-tests.

Indeed, not only were the target building pressures achieved (as evidenced by the overall mean), in these three instances the building pressures were maintained at the target ΔP over 99% of the time. Higher percentages indicate that the building pressure was maintained at the target pressure differential for a greater duration of time.

In one instance, under PP at Moffett Field Building 107, the observed ΔP was above 1 Pa ($p = 0.044$), but only 60% of the individual ΔP observations were greater than 1 Pa. While pressure control was achieved at Moffett Field Building 107 under PP, the attained ΔP was not as large as at ASU House and was only slightly above the target ΔP of 1 Pa. As can be seen in Figure 9 Panel C, Moffett Field Building 107 was under a slight negative pressure under BL conditions, ostensibly due to the action of the building's HVAC system; it appears that application of positive pressure to the building envelop using the window fan was just able to overcome this inherent negative pressure. This slight negative pressure under BL conditions was also observed in the cross-foundation ΔP measurements (Table A1).

6.2.2 Vapor Intrusion Enhancement and Reduction

The second verification metric for decision-making is the effect of the pressure control method on the enhancement and reduction of radon VI. This metric was evaluated using the mass discharge of radon from subsurface sources through the building foundation. Under induced NP, the mass discharge of chemicals with subsurface sources – including radon and CoCs – into the building may increase compared to BL. Similarly, under induced PP, the mass discharge from subsurface sources may either decrease compared to BL or be reduced to zero, where the latter condition indicates that VI has effectively been stopped.

As described in Sections 3.3.1.2 and 5.1.2, the radon mass discharge from subsurface sources was calculated under BL, induced NP, and induced PP for both buildings to determine if VI was enhanced under induced NP and reduced under induced PP. Results of these comparisons at both buildings are shown in Table 8. Mass discharges are in pCi h^{-1}.

Table 8. Comparison of Radon Mass Discharges from Subsurface Sources to Determine VI Enhancement and Reduction.

ASU House

Pressure	$Q_i \cdot (R_i - R_a)$	error in $Q_i \cdot (R_i - R_a)$	$Q_i^- \cdot (R_i^- - R_a^-) > Q_i \cdot (R_i - R_a)$?[a]	$Q_i^+ \cdot (R_i^+ - R_a^+) < Q_i \cdot (R_i - R_a)$?[b]
BL	14830	8704		
NP	706231	999852	No; p = 0.1769	No; p = 0.3794
PP	8143	32347		

Moffett Field Building 107

Pressure	$Q_i \cdot (R_i - R_a)$	error in $Q_i \cdot (R_i - R_a)$	$Q_i^- \cdot (R_i^- - R_a^-) > Q_i \cdot (R_i - R_a)$?[a]	$Q_i^+ \cdot (R_i^+ - R_a^+) < Q_i \cdot (R_i - R_a)$?[b]
BL	82556	11579		
NP	213492	137656	No; p = 0.1203	No; p = 0.1326
PP	-16153[c]	93610		

[a] H_0: $Q_i \cdot (R_i - R_a) = Q_i^- \cdot (R_i^- - R_a^-)$; H_1: $Q_i^- \cdot (R_i^- - R_a^-) > Q_i \cdot (R_i - R_a)$; H_0 rejected when $p < 0.05$

[b] H_0: $Q_i \cdot (R_i - R_a) = Q_i^+ \cdot (R_i^+ - R_a^+)$; H_1: $Q_i^+ \cdot (R_i^+ - R_a^+) < Q_i * (R_i - R_a)$; H_0 rejected when $p < 0.05$

[c] While mass discharges cannot be negative, this calculated value was < 0 due to the measurement variability at low radon concentrations. For the calculation of the p-value, $Q_i^+ \cdot (R_i^+ - R_a^+)$ was set equal to 0.

Qualitatively, VI was observed to have been enhanced under induced NP and reduced under induced PP at both buildings; this is apparent by comparison of the magnitudes of the mass discharges under NP vs. BL and PP vs. BL, respectively. Thus the building pressure manipulation method was shown to control VI to some extent. However, in none of the four cases was there sufficient statistical evidence to reject the null hypotheses and conclude that VI was enhanced under induced NP or reduced under induced PP. The failure to find statistically significant differences is due to the estimated errors in the various radon mass discharges. These estimated errors are driven by variability in the spatially distributed IA SF_6 concentrations (this led to large estimated errors in the calculated building ventilation rates – see the error bars on Q_is in Figure 10, Section 6.1.2) as well as variability in the spatially distributed IA radon concentrations (see error bars on R_i data presented in Figure 12, Section 6.1.4). Another driver of the observed variability is that several IA and AA radon measurements were at or below estimated method detection limits where measurement uncertainty is magnified.

Given that VI was qualitatively determined to have been reduced under induced PP, whether VI had been 'turned off' was investigated by comparison of R_i^+ to R_a^+ at each building. Results of the comparisons are summarized in Table 9. At neither building was there evidence sufficient to conclude that R_i^+ was different from R_a^+; VI was thus concluded to have been stopped under PP and the more simplified version of the Mosley Model was used to calculate the F_{VI}^+ values for each of the CoCs at each building.

Table 9. Comparison of Indoor and Ambient Air Radon Concentrations under Positive Pressure.

Building[a]	R_i^+	std dev R_i^+	R_a^+	est error in R_a^+	$R_i^+ = R_a^+$?[b]
ASU House	-2.74	1.17	-2.67	1.15	Yes; p = 0.949
Moffett Field Building 107	-1.24	0.37	-1.11	0.33	Yes; p = 0.690

[a]Data were log transformed

[b]H_0: $R_i^+ = R_a^+$; H_1: $R_i^+ \neq R_a^+$; H_0 rejected when $p < 0.05$

6.2.3 Fractional Contribution of Vapor Intrusion to Indoor CoC Concentrations

The third verification metric under decision-making support is the ability of the pressure control method to provide an improved understanding of the contribution of VI to IA CoC concentrations. This metric was assessed by calculation of two independent estimates of F_{VI} under BL using (i) CoC measurements from BL and induced NP (F_{VI}^-) and (ii) CoC measurements from BL and induced PP (F_{VI}^+) for each of four CoCs at both buildings. Error estimates in each F_{VI} were also calculated. Prior to the field program, two of the CoCs selected were expected to have primarily subsurface sources, TCE and 1,1-DCE at ASU House and TCE and PCE at Moffett Field Building 107; whereas the other two CoCs were expected only to have indoor/ambient sources (and no appreciable subsurface sources), benzene and toluene at both buildings.[xxiv] F_{VI}^- and F_{VI}^+ for each CoC at each building, as well as corresponding 95% confidence intervals generated by the Monte Carlo error analysis, are provided in Table 10.[xxv] F_a, F_{in}^- and F_{in}^+ are also given in Table 10 to provide the comprehensive picture of CoC source attribution that results from application of the building pressure technique at these two buildings.

[xxiv] As noted in Section 6.1.4, after completion of the verification test, it was discovered that TCE was being stored in the ASU house garage creating an additional potential indoor source of TCE.

[xxv] The 95% confidence interval estimates presented in Table 10 are the result of averaging the bounds over the eleven combinations of correlation coefficients for the given building/CoC combination. The bounds of the confidence intervals were quite consistent across different combinations of correlation coefficients. This implies that under the assumptions used in this analysis, the choice of correlation between any two dependent random variables in these two formulae does not substantively affect the 95% confidence interval of F_{VI}^+ or F_{VI}^-.

Table 10. Fractional Contribution of Ambient Sources, Indoor Sources, and VI to Indoor CoC Concentrations Under Baseline Conditions.

ASU House

	Using NP and BL results					Using PP and BL results, $R_i^+ = R_a^+$				
Compound	F_a	F_{in}^-	F_{VI}^-	LB[a] ΔF_{VI}^-	UB[b] ΔF_{VI}^-	F_a	F_{in}^+	F_{VI}^+	LB ΔF_{VI}^+	UB ΔF_{VI}^+
TCE	0.01	0.94	0.05	-9.2	5.3	0.01	0.02	0.97	0.84	1.1
1,1-DCE	0.30	-6.87	7.57	-1077	529	0.30	0.02	0.68	-6.0	8.2
Benzene	0.85	0.14	0.01	-18	17	0.85	1.81	-1.66	-25	22
Toluene	1.04	-0.09	0.05	-23	14	1.04	1.37	-1.42	-18	14

Moffett Field Building 107

	Using NP and BL results					Using PP and BL results, $R_i^+ = R_a^+$				
Compound	F_a	F_{in}^-	F_{VI}^-	LB ΔF_{VI}^-	UB ΔF_{VI}^-	F_a	F_{in}^+	F_{VI}^+	LB ΔF_{VI}^+	UB ΔF_{VI}^+
TCE	0.02	-0.56	1.55	-5.8	2.5	0.02	0.03	0.95	0.65	1.3
PCE	0.04	-0.68	1.64	-6.2	2.7	0.04	-1.00	1.96	-1.6	6.3
Benzene	1.00	-0.21	0.21	-10	10	1.00	0.73	-0.73	-20	21
Toluene	0.90	0.02	0.09	-21	19	0.90	-2.32	2.42	-33	42

[a]Lower bound of 95% error interval

[b]Upper bound of 95% error interval

By definition, F_{VI} is expected to be between 0 and 1 (i.e., between 0% and 100% of the CoC concentration in IA is attributable to VI) and the sum of the fractional contributions from all possible sources (ambient, indoor, and subsurface) is defined to be 1 (i.e., $F_a + F_{in} + F_{VI} = 1$). F_{VI} values of less than zero or greater than one are indicative of either variability in the dataset used for the calculations or incorrect model assumptions. Of the 16 F_{VI} values, five were greater than one and three were less than zero. In addition, the Monte Carlo uncertainty analysis indicated that uncertainties in the F_{VI} values are likely larger than calculated values. The best bounded estimates of F_{VI} were for TCE calculated using the BL and PP data at both the ASU House and Moffett Field, where F_{VI}^+ was 0.97 and 0.95 with 95% confidence intervals of 0.84 to 1.1 and 0.65 to 1.3, respectively.

Although the results of the F_{VI} calculations provide only modest quantitative information regarding the fraction of each CoC in IA attributable to VI, the qualitative pattern was generally as predicted and is similar to the observed qualitative trends in mass discharges discussed in Section 6.1.6. For instance, the F_{VI} values for the two CoCs with expected subsurface sources were close to or greater than one in seven of eight cases. The exception ($F_{VI} = 0.05$) was for TCE at the ASU House. As noted previously, an indoor source of TCE was found in the building after completion of the study; in this instance, the model may have predicted the presence of the indoor source. The F_{VI} values for the two CoCs without expected subsurface sources were close to or less than zero in seven of eight cases. The exception (toluene at Moffett Field Building 107) is discussed further below. Moreover, as described in Section 6.1.6, the F_a values are low and in many cases nearly 0 for radon, TCE, 1,1-DCE, and PCE, indicating the

predominance of subsurface/indoor sources; whereas F_as are nearly one for benzene and toluene, pointing to predominant ambient sources.

It is helpful to consider limitations in the Mosley Model to better understand the quantitative F_{VI} calculations. One limitation is the assumption that, under NP, radon may be used a tracer gas for the movement of subsurface vapors into the overlying structure. In the model radon is applied as a scaling factor [in the form of the term $Q_i \cdot (R_i - R_a)/\{Q_i^- \cdot (R_i^- - R_a^-) - Q_i \cdot (R_i - R_a)\}$] to the observed difference of NP and BL mass discharges for each CoC [the term $Q_i^- \cdot (C_i^- - C_a^-) - Q_i \cdot (C_i - C_a)$]. That several of the mean F_{VI}^- values were outside the [0, 1] interval may be due to radon serving as an imperfect indicator for the movement of other subsurface gases. Specifically, F_{VI}^- values of greater than one suggest that the induction of NP had a greater effect on the mass discharge of CoCs through the building foundation compared to radon.

Another limitation of the Mosley Model is its sensitivity to short-term variability in concentrations of CoCs and radon.[12] This sensitivity is illustrated by the F_{VI}^+ results for toluene for Moffett Field Building 107. Here the AA and IA concentrations of toluene were similar under all three pressure conditions, suggesting that AA is the predominant source of toluene in IA (reflected in the calculated value of F_a of 0.9). Under BL conditions, $C_i > C_a$, but under induced PP, $C_i^+ < C_a^+$ (see Figures 11 and 12, Sections 6.1.3 and 6.1.4). Although these observed differences are likely attributable to measurement variability, the Mosley Model yields nonsensical F_{VI}^+ and F_{in}^+ values of 2.42 and -2.32, respectively, because the model attributes the measured "decrease" in the IA concentration of toluene relative to AA as a decrease in the contribution from VI.

Highlighted in red in Table A3 are other specific instances where modeled F_{VI} values were impacted by measurement uncertainty or failure of specific model assumptions.[xxvi] In general, F_{VI} estimates may benefit from improvements in the sensitivity of critical measurements such as radon and CoCs in ambient and IA[xxvii] and from more homogeneous distribution of the SF_6 tracer gas such that building ventilation rates are more accurately known. It may also be beneficial to perform sampling over longer time intervals to reduce short-term variability in CoC and radon concentrations and to have more than a single observation of AA concentrations of CoCs and radon at each pressure condition to better characterize the true distributions of these concentrations.

[xxvi] F_{VI}^- estimates were impacted by the following issues. For example, at ASU House, R_a and R_a^- were both nondetects; measurements at such low concentrations are subject to elevated uncertainty which likely decreased the fidelity of the F_{VI}^- estimates. Also, as explained in more detail in Section 6.4, the assumption that $C_s = C_s^-$ was not valid for benzene; and if SS-1 was excluded, the assumption was also not valid for TCE and 1,1-DCE. The failure of this assumption demonstrates that the F_{VI}^- values for these three CoCs may be subject to greater uncertainty. The F_{VI}^- for toluene may also be of limited value given that $C_i < C_a$ which is contradictory given that one of the model assumptions is that a CoC's concentration in AA is less than in IA. Other examples of problems observed for F_{VI}^+ estimates include, for instance: 1,1-DCE at ASU House, where a number of ND results impacted the calculation; PCE at Moffett Field Building 107, where $C_a^+ > C_i^+$; benzene at both buildings, where $Q_i \cdot (C_i - C_a) < Q_i^+ \cdot (C_i^+ - C_a^+)$; toluene at ASU House in which $C_a > C_i$. Substitution of nondetects degrades the fidelity of model outputs; in all of the other F_{VI}^+ calculations, a model assumption was violated which most likely led to F_{VI}^+ results outside of the interval of 0 and 1.

[xxvii] Monte Carlo error estimates may have been artificially elevated given that several IA/AA radon and CoC measurements were at or below estimated method detection limits where measurement uncertainty is magnified.

Post hoc power analysis was not performed to the F_{VI} calculations. The 95% confidence intervals for F_{VI} that were calculated via Monte Carlo simulation extended well below zero and well above one, meaning that these data do not meaningfully narrow down the portion of the interval [0,1] likely to contain the true value of F_{VI}. A retrospective calculation to estimate minimum detectable differences is not useful in this context because the magnitude of ΔF_{VI} is so large that F_{VI} would have to be nonsensically large to outweigh ΔF_{VI} in a statistically significant manner.

6.3 Comparability

The comparability of the building pressure control technique as implemented at two different buildings is shown in Table 11. In general lower RPDs indicate better comparability. Given that each building's characteristics were different (ASU House is a single family home compared to Moffett Field Building 107 - a commercial building) and especially that the HVAC system at Moffett Field Building 107 caused a slight negative pressure differential under BL, it is not surprising that high RPDs were observed.

Table 11. Comparability of Building Pressure Control Results.

ΔP	Value, Pa	RPD
ΔP_1^-	-5.18	71
ΔP_2^-	-2.47	
ΔP_1^+	3.87	116
ΔP_2^+	1.03	

Moreover, the ability to evaluate comparability was limited because testing was conducted at only two buildings.

6.4 Operational Factors

The technology vendor executed all aspects of the building pressure control test at both buildings. Battelle oversaw testing at both sites; the VTC was onsite at the ASU House and conducted daily briefings with the team during testing at Moffett Field Building 107. A minimum of two people were required to execute the field work, and one staff person had to have the experience and specialized knowledge in indoor and outdoor air sampling and use of analytical instrumentation required for implementation of a typical VI sampling program. Also required for the field team was the ability to install SS sampling points. GSI Environmental is currently preparing an instruction manual with detailed guidance on how to execute the building pressure control technique. However, at the time of the verification test, no detailed instruction manual or written guidance was available, beyond the project QAPP, the vendor's ESTCP report[5], and instruction manuals for the Omniguard 4® and RAD7®. Examples of test procedures that should be included in such an instruction manual include: selection of appropriate locations for IA, AA, and SS sampling and tracer gas release; installation of SS sampling points; delivery

of tracer gas; receipt, pre- and post-sampling sample media integrity checks; and guidance on such issues as sample collection, shipment of canisters, flow control devices, and PVF bags.

It was determined that the Omniguard 4®, set up to measure I/O ΔP at ASU House, was not logging data during BL conditions. (Note that the lack of BL ASU House I/O ΔP data is the subject of QAPP Deviation 1.) Troubleshooting was performed by the vendor, the instrument was reconfigured in about 10 minutes, and datalogging was re-enabled coincident with the beginning of the NP condition. The instrument had not malfunctioned; rather, its default settings were inappropriate for the intended use. Inspection of the instrument's instruction manual helped to resolve the problem. No issues were encountered with the RAD7®. No canisters (out of 47) were rejected during pre-sampling integrity checks (based on pressures as received). The pressures in three canisters (out of 47; 6%) did increase after sampling and before analysis (subject of QAPP Deviation 3), indicating that these samples had been slightly diluted with gas of unknown composition. Two PVF bags (out of a total 48; 4%) failed pre-sampling checks and were not used; these failures did not impact study outcomes. One bag (out of 48; 2%) arrived at the analytical laboratory at a lower volume than the others, potentially indicating a leak.

The vendor required approximately one day to set up the equipment to conduct the field work, followed by three days for project execution. Labor, travel, and expenses for testing at both sites totaled approximately $23,000. Each Omniguard 4® was $1,500 and requires annual recalibration. Similarly, the RAD7® was $6,000 and requires annual recalibration. The total cost for the rental of canisters and flow control devices, purchase of PVF bags, and for the various analyses described in Section 3.3 was approximately $21,000. Moreover, miscellaneous gas sampling equipment and accessories were required. Thus, the total cost for implementing this technology for this verification test at two sites over 3.5 days at each site, excluding any data reduction, interpretation, and reporting, was approximately $50,000.

For the routine implementation of the technology at a given site, the field work is expected to require approximately 80 person-hours (2 staff · 4 days · 9 hours/day). Additional costs would include travel and expenses, as well as time for data evaluation and reporting after the field work is completed. One differential pressure instrument ($1,500) is required to perform the I/O monitoring. The cost for laboratory analysis of the basic set of canisters (VOCs and SF_6) and PVF bags (radon) samples is approximately $6,000, including media and shipping. This cost covers analysis of 9 IA samples, 3 AA samples, and two field duplicates. Routine implementation would not require SS sampling, either for gas-phase species or cross-foundation differential pressures.

6.5 Validation of Model Assumptions

The results of the validation of the various model assumptions, specifically those that can be explicitly tested, are presented in this section. Inspection of the verification of these assumptions helps to explain the outcomes of the F_{VI} calculations.

A total of eight assumptions were tested at each building and are organized into three groups. The first group includes two assumptions to determine if inducing a NP in the building had a significant effect on CoC and radon concentrations in SS soil gas below the building foundation.

Shown in Tables 12 and 13 are the results of testing if $C_s = C_s^-$ (model assumption 1) for the various CoCs and for $R_s = R_s^-$ (radon; model assumption 2), respectively, at both buildings. For F_{VI}^- to be most meaningful, the SS concentration of CoCs and radon should not change when NP is applied to the building; that is, source strengths and distributions of the CoCs and radon should not change under induced NP, given that such are required assumptions of the Mosley Model. As can be seen by inspection of the individual SS data points for the various CoCs and radon (see Tables A4 and A5 for the non-log transformed data), concentrations of CoCs and radon at SS-1 at the ASU House were quite different than those at the other two SS sampling points. Also, SS-1 was located in the garage, and the door connecting the garage to the remainder of the usable space (see Figure A1) was mainly kept closed during pressure testing. Thus additional statistical tests were conducted by excluding SS-1 to test the assumptions that $C_s = C_s^-$ and $R_s = R_s^-$.

As can be seen in Table 12, $C_s = C_s^-$ did not hold for benzene at ASU House and was also not valid for TCE and 1,1-DCE (if SS-1 was excluded). The failure of this assumption demonstrates that F_{VI}^- for these three CoCs may be subject to greater uncertainty since the strength of the subsurface source changed under induced NP. Applied building pressures were effectively smaller at Moffett Field Building 107, likely explaining the lower observed perturbation in soil gas CoC concentrations. SS radon concentrations at both buildings remained relatively constant under induced NP compared to BL (Table 13; see also Table A5 for individual data points and non-log transformed data).

Table 12. Validation of Model Assumption 1.

ASU House					
Compound[a]	C_s	std dev C_s	C_s^-	std dev C_s^-	$C_s = C_s^-$?[b]
TCE	2.29	0.35	4.69	2.2	Yes; p = 0.2390
1,1-DCE	0.52	1.83	4.74	1.82	Yes; p = 0.1804
Benzene	-0.94	0.07	-0.35	0.15	No; p = 0.0075
Toluene	0.95	0.35	1.29	1.03	Yes; p = 0.4952
ASU House (excluding SS-1)					
Compound	C_s	std dev C_s	C_s^-	std dev C_s^-	$C_s = C_s^-$?
TCE	2.12	0.25	5.97	0	No; p = 0.0287
1,1-DCE	-0.51	0.65	5.8	0.09	No; p = 0.0401
Benzene	-0.98	0.02	-0.44	0.01	No; p = 0.0247
Toluene	0.76	0.17	0.69	0	Yes; p = 0.6746
Moffett Field Building 107					
Compound	C_s	std dev C_s	C_s^-	std dev C_s^-	$C_s = C_s^-$?
TCE	0.57	0.67	0.52	0.47	Yes; p = 0.8384
PCE	0.55	0.73	0.52	1.22	Yes; p = 0.9384
Benzene	0.04	0.93	-0.13	0.76	Yes; p = 0.2943
Toluene	1.29	0.69	1.23	0.51	Yes; p = 0.6635

[a]Data were log transformed

[b]H_0: $C_s = C_s^-$; H_1: $C_s \neq C_s^-$; H_0 rejected when $p < 0.05$

Table 13. Validation of Model Assumption 2.

Building[a]	R_s	std dev R_s	R_s^-	std dev R_s^-	$R_s = R_s^-$?[b]
ASU House	4.42	1.65	5.15	0.80	Yes; p = 0.3502
ASU House (excluding SS-1)	3.59	1.13	4.70	0.05	Yes; p = 0.4109
Moffett Field	5.28	0.97	5.75	0.63	Yes; p = 0.2884

[a]Data were log transformed
[b]H_0: $R_s = R_s^-$; H_1: $R_s \neq R_s^-$; H_0 rejected when $p < 0.05$

The second group of assumptions whose validity were verified related to if radon concentrations in AA were in fact much lower than those in SS soil gas below the building foundation. The results of the validation of model assumptions 3, 4, and 5, that is, that $R_a << R_s$, $R_a^- << R_s^-$, and $R_a^+ << R_s^+$, are shown in Table 14. (In addition, see Table A5 for individual data points and non-log transformed data.) In all cases, including those where SS-1 was excluded at ASU House, all assumptions were statistically validated. That these assumptions were validated supports the use of the Mosley Model and the veracity of the F_{VI} calculations.

Table 14. Validation of Model Assumptions 3, 4, and 5.

Baseline					
Building[a]	R_a	std dev R_i[b]	R_s	std dev R_s	$R_a < R_s$?[c]
ASU House	-2.26	0.78	4.42	1.65	Yes; p = 0.0046
ASU House (excluding SS-1)	-2.26	0.78	3.59	1.13	Yes; p = 0.0187
Moffett Field Building 107	-1.73	1.96	5.28	0.97	Yes; p = 0.0062
Negative Pressure					
Building	R_a^-	std dev R_i^-	R_s^-	std dev R_s^-	$R_a^- < R_s^-$?[d]
ASU House[e]	-3.65	1.20	5.15	0.80	Yes; p = 0.0005
ASU House (excluding SS-1)[e]	-3.65	1.20	4.70	0.05	Yes; p = 0.0034
Moffett Field Building 107	-1.36	0.66	5.75	0.63	Yes; p < 0.0001
Positive Pressure					
Building	R_a^+	std dev R_i^+	R_s^+	std dev R_s^+	$R_a^+ < R_s^+$?[f]
ASU House	-2.67	1.15	3.88	2.11	Yes; p = 0.0084
ASU House (excluding SS-1)	-2.67	1.15	2.81	1.43	Yes; p = 0.0256
Moffett Field Building 107	-1.11	0.33	4.64	1.76	Yes; p = 0.0131

[a]Data were log transformed
[b]Standard deviation of AA radon based standard deviation of IA radon; see text Chapter 5
[c]H_0: $R_a - R_s = 0$; H_1: $R_a - R_s < 0$; H_0 rejected when $p < 0.05$
[d]H_0: $R_a^- - R_s^- = 0$; H_1: $R_a^- - R_s^- < 0$; H_0 rejected when $p < 0.05$
[e]Standard deviation of AA radon assumed equal to standard deviation of IA radon; see text Chapter 5
[d]H_0: $R_a^+ - R_s^+ = 0$; H_1: $R_a^+ - R_s^+ < 0$; H_0 rejected when $p < 0.05$

With respect to the validation of model assumptions 1 through 5, it is important to recognize that a number of the C_s and R_s observations were at or below estimated detection limits. In such

cases measurement uncertainty is magnified, and statistical difference testing is likely adversely impacted.

The third and final group of assumptions tested included those to determine if, in IA, the loss of radon through building ventilation is much greater than the loss due to radioactive decay. Shown in Table 15 are the results of validating model assumptions 6, 7, and 8, that is, $Q_i >> \lambda V$, $Q_i^- >> \lambda V$, and $Q_i^+ >> \lambda V$. These results are also shown graphically in Figures A4 through A9. Under all three pressure conditions at both buildings, building ventilation rates were indeed larger than λV (by at least a factor of 26 in all cases), but only under BL conditions was there sufficient statistical evidence to conclude that $Q_i > \lambda V$. Failure to reject the null hypotheses under induced NP and induced PP was due to the large variability in Q_i, that is due in large part to the observed spatial heterogeneity in the IA SF_6 concentrations that determine Q_i (see error bars in Figure 10, Section 6.1.2). That these assumptions were either statistically validated, or shown to be verified at least qualitatively, supports the simplification performed in the Mosley Model, that is, that λV is negligible compared to Q_i, Q_i^-, and Q_i^+.

Table 15. Validation of Model Assumptions 6, 7, and 8.

ASU House

Pressure	Q_i	est error Q_i	λV	est error λV	$Q_i > \lambda V$?[a,b,c]	#SD that $\lambda V < Q_i$	Minimum detectable difference
BL	54.5	14.2	2.07	0.62	Yes; p = 0.0332	3.69	N/A
NP	384	351	2.07	0.62	No; p = 0.1955	1.09	1614
PP	364	342	2.07	0.62	No; p = 0.2004	1.06	1571

Moffett Field Building 107

Pressure	Q_i	est error Q_i	λV	est error λV	$Q_i > \lambda V$?	#SD that $\lambda V < Q_i$	Minimum detectable difference
BL	105	13.5	2.76	0.83	Yes; p = 0.0084	7.6	N/A
NP	592	256	2.76	0.83	No; p = 0.0740	2.3	1178
PP	634	542	2.76	0.83	No; p = 0.1823	1.16	2492

[a]BL: H_0: $Q_i = \lambda V$; H_1: $Q_i > \lambda V$; H_0 rejected when $p < 0.05$

[b]NP: H_0: $Q_i^- = \lambda V$; H_1: $Q_i^- > \lambda V$; H_0 rejected when $p < 0.05$

[b]PP: H_0: $Q_i^+ = \lambda V$; H_1: $Q_i^+ > \lambda V$; H_0 rejected when $p < 0.05$

As shown in Table 16, post-hoc power analyses (assuming 80 % power and 5% false positive rate) were performed to determine the minimum detectable differences between Q_i and λV under induced NP and induced PP at both buildings. Such post-hoc analyses were performed only in those instances where the prerequisites were met, including that a sufficient number of observations were present (at least 3) for both samples in the comparison, the p-value was not significant, and all concentrations were greater than MDLs.

Minimum detectable differences between Q_i^- and λV and Q_i^+ and λV indicate that, assuming the measured variability in building ventilation rates remain constant, ventilation rates would need to

be on the order of 1200 to 2500 $m^3 h^{-1}$, or roughly 3.3 to 6.8 air changes h^{-1} to detect a statistically significant difference between the ventilation rates and the radon radioactive decay constant. One important conclusion from these calculations of minimum detectable differences is that the variability in the building flow rates are quite high under induced NP and induced PP, given that ventilation rates must exceed λV by a factor of 1000 before it can be concluded with statistical confidence that the former is greater than the latter. An alternative, and potentially superior, method to better ensure a statistically significant difference in future testing would be to improve the spatial homogeneity of the concentration of the indoor atmosphere, as the error in the building ventilation rates is driven in large part by the observed spatial heterogeneity of the SF_6 IA concentrations.

In a similar way, minimum detectable differences were calculated for C_s and C_s^- for TCE, PCE, and benzene (assumption 1) and for radon (R_s and R_s^-) at Moffett Field Building 107 (Table 16). These differences may be interpreted as how much larger the concentrations measured under NP conditions would have to be in order for the difference to be observed as statistically significant. Essentially differences in SS TCE and PCE would have to be fairly large (relative to observed mean concentrations of ~ 2 $\mu g\ m^{-3}$) in order to detect differences. R_s^- would have to be even larger than R_s (by nearly 15,000 $pCi\ L^{-1}$). The calculated minimum detectable difference for benzene reveals a limitation in the post-hoc power calculation itself, since only a nonsensically large difference between BL and NP SS benzene concentrations is predicted to be statistically observable.

Table 16. Minimum Detectable Differences for Model Assumptions 1 and 2 at Moffett Field Building 107.

Compound	Minimum Detectable Difference[a]
TCE	27
PCE	1,620
Benzene	92,107,564
Radon	14,933

[a]Concentrations expressed in $\mu g\ m^{-3}$ for CoCs, and $pCi\ L^{-1}$ for radon

The benzene result notwithstanding, the outcomes of the various minimum detectable difference estimates suggest that the observed variability in these SS concentrations are quite large; consequently, the ability to assess the accuracy of assumptions 1 and 2 – and thereby confirm the utility of the Mosley Model – is negatively impacted. Essentially, the large observed variability in concentrations combined with the relatively few spatially distributed measurements increase the likelihood of false negatives (incorrectly retaining the null hypotheses formulated for assumptions 1 and 2 , that $C_s = C_s^-$ and $R_s = R_s^-$), thereby leading to the conclusion that the F_{VI}^- estimates are of a higher fidelity than they otherwise may be.

Chapter 7
Performance Summary

The objective of this verification test was to generate performance data on the use of the building pressure control technique, as conducted by GSI Environmental, as a method to understand the impact of VI on the concentrations of CoCs in IA. The data generated from this verification test are intended to provide organizations and users with information on the utility of such a methodology.

The pressure control technique was evaluated at two different buildings where VI was a known concern using the following types of performance parameters.

- Decision-making support
- Comparability
- Operational factors

In general, the goal of implementing the building pressure control method is to obtain a better understanding of VI in a building. If the control of building pressure results in clear changes in building conditions, such as I/O differential pressures and concentrations of radon and CoCs, then the pressure control method may yield results that are useful for decision-making (i.e., is VI a concern for this building?). The effectiveness of the building pressure control method to support decision-making was evaluated via three metrics.

1. Building pressure differential: Did the pressure control method control building pressure?

2. Vapor intrusion enhancement and reduction: Did the pressure control method increase the mass discharge of radon from subsurface sources through the building foundation under induced NP conditions and/or decrease the mass discharge of radon from subsurface sources through the building foundation under induced PP conditions?

3. Fractional contribution of vapor intrusion to indoor CoC concentrations: Did the pressure control method provide an improved understanding of the contribution of VI to the concentration of individual CoCs detected in IA?

Additional support to decision-makers was also provided by qualitative trends, with respect to changes in building pressure, in concentrations of compounds in IA, as well as trends in the changes of compound mass discharges.

Beyond the three metrics comprising decision-making support, the performance metric of comparability was assessed for the pressure control technique as the similarity of the I/O differential pressures achieved under induced NP and PP conditions at each of two buildings. The final performance metric was comprised of an assessment of operational factors such as ease of implementation of the pressure control technology, the expertise required to carry out the field work and interpret the results were also determined, and costs to perform the testing. The results of the verification are summarized below.

Building Pressure Differential

For both buildings, the building pressure control method achieved a measureable negative pressure gradient both across the building envelope (the I/O differential pressure) and the building foundation under induced NP, as well as a measureable positive pressure gradient across the building envelope and building foundation under induced PP. Furthermore, during each of the pressure perturbations at the two buildings, the mean I/O differential pressures were either below (under NP) or above (under PP) the target pressure of -1 Pa and 1 Pa, respectively. These results indicate that some degree of building pressure control was achieved under both pressure perturbation conditions at both buildings.

Vapor Intrusion Enhancement and Reduction

At both buildings, the building pressure control method had the expected qualitative effect on the mass discharge of radon from subsurface sources through the building foundation. That is, under induced NP, the mass discharge of radon from subsurface sources through the building foundation increased compared to BL, indicating that radon vapor intrusion had been enhanced; and under induced PP, the mass discharge of radon from subsurface sources through the building foundation decreased compared to BL, indicating that radon vapor intrusion had been reduced. However, in none of these four cases (NP and PP comparisons to BL at two buildings) was the difference in mass discharges found to be statistically significant – due to the large estimated errors in the measured mass discharges. Radon concentrations in IA and AA under induced PP were also compared to ascertain if radon vapor intrusion had been stopped under induced PP. For both buildings IA and AA radon concentrations were not found to be statistically different, thus indicating an absence of radon vapor intrusion under induced PP.

Fractional Contribution of Vapor Intrusion to Indoor CoC Concentrations

The pressure control method had the expected qualitative effect on CoC concentrations in IA. For both radon (that has a known subsurface source) and the CoCs with expected subsurface sources (TCE, 1,1-DCE, and PCE), concentrations in IA were greater than in AA under induced NP, but similar to concentrations in AA under induced PP. For the CoCs without expected subsurface sources (benzene and toluene), concentrations in IA were similar to concentrations in AA for all pressure conditions. Similar trends were seen in mass discharges. Mass discharges of the CoCs with expected subsurface sources varied under application of the building pressure control technique similarly to radon, but compounds without expected subsurface sources had a pattern different than radon under pressure perturbation.

The building pressure control technique generated less definitive quantitative results. F_{VI} is the fraction of the measured IA concentration of a given CoC (under BL conditions) that is due to VI. By definition, F_{VI} is expected to be between 0 and 1 (i.e., between 0% and 100% of the CoC concentration in IA is attributable to VI). Under each induced pressure condition, and at both buildings, a total of 16 F_{VI}s were calculated. For the two CoCs expected to have subsurface sources – TCE and 1,1-DCE at ASU House and TCE and PCE at Moffett Field Building 107 – and for two CoCs expected only to have indoor/ambient sources – benzene and toluene at both buildings (2 buildings · 2 pressure conditions · 4 CoCs). F_{VI} values of less than zero or greater than one are indicative of either variability in the dataset used for the calculations or incorrect model assumptions. Of the 16 F_{VI} values, five were greater than one and three were less than zero. In addition, the uncertainty analysis indicated that uncertainties in the F_{VI} values are likely larger than calculated values. Nonetheless, the F_{VI} values for the two CoCs with expected subsurface sources were close to or greater than one in seven of eight cases, and the F_{VI} values for the two CoCs without expected subsurface sources were close to or less than zero in seven of eight cases. In general, the variability in measured concentrations limited the quantitative interpretation of the F_{VI} values.

Comparability

The comparability of the building pressure differential achieved at two buildings was assessed as the RPD between the mean pressure differentials measured under both induced NP and induced PP. RPDs were 71% and 116% under NP and PP, respectively. In general lower RPDs indicate better comparability. Thus, while pressure control was achieved at both buildings, the magnitude of the induced pressure gradients varied, most likely due to differences in building characteristics such as HVAC systems. Moreover, implementation of the pressure control method in only two buildings provided a limited dataset for evaluation of comparability.

Operational Factors

A minimum of two people were required to execute the field work, and at least one of these personnel must have the experience and specialized knowledge in indoor and outdoor air sampling, the use of analytical instrumentation required for a typical VI field investigation, and the ability to install SS sampling points. No detailed instruction manual or written guidance was available that provided guidance on how to execute various test procedures; however, such guidance is expected to be available in the future. Settings on one pressure differential measurement instrument had to be reconfigured during the test; no issues were encountered with the real-time radon instruments. No canisters (out of 47) were rejected during pre-sampling integrity checks (based on pressures as received). The pressures did increase (i.e., the vacuum decreased) in three canisters (out of 47; 6%) after sampling and before analysis, indicating that these samples had been slightly diluted with gas of unknown composition. Two PVF bags (out of a total 48; 4%) failed pre-sampling checks and were not used; these failures did not impact study outcomes. One bag (out of 48; 2%) arrived at the analytical laboratory at a lower volume than the others, potentially indicating a leak.

For the routine implementation of the technology at a given site, the field work is expected to require approximately 80 person-hours (2 staff · 4 days · 9 hours/day). Additional costs would

include travel and expenses, as well as time for data evaluation and reporting after the field work is completed. One differential pressure instrument ($1,500) is required to perform the I/O monitoring. The cost for laboratory analysis of the basic set of canisters (VOCs and SF_6) and PVF bags (radon) samples is approximately $6,000, including media and shipping. This cost covers analysis of 9 IA samples, 3 AA samples, and two field duplicates. Note that SS sampling is not required for routine implementation of this technology.

Chapter 8
References

1. U.S. EPA (2002). OSWER Draft Guidance for Evaluating the Vapor Intrusion to Indoor Air Pathway from Groundwater and Soils (Subsurface Vapor Intrusion Guidance). November 2002 EPA 530-D-02-004.

2. U.S. Navy (2004). Memorandum entitled "Navy Policy on the Use of Background Chemical Levels." January 30, 2004. Available at http://web.ead.anl.gov/ecorisk/policy/pdf/Final_Navy_Background_Policy.pdf, accessed December 11, 2011.

3. U.S. Navy (2008). Memorandum entitled "Navy/Marine Corps Policy on Vapor Intrusion." April 29, 2008. Available at https://portal.navfac.navy.mil/portal/page/portal/navfac/navfac_ww_pp/navfac_nfesc_pp/environmental/erb/resourceerb/don%20vi%20policy-final.pdf, accessed December 11, 2011.

4. Interstate Technology and Regulatory Council (ITRC) 2007. "Vapor Intrusion Pathway: A Practical Guideline." Washington, DC, January 2007. Available at http://www.itrcweb.org/Documents/VI-1.pdf, accessed December 11, 2011.

5. GSI Environmental, Inc. (2009). "Results and Lessons Learned Interim Report; Proposed Tier 2 Screening Criteria and Tier 3 Field Procedures for Evaluation of Vapor Intrusion." ESTCP Project ER-0707, October 30, 2009.

6. McAlary T., R. Ettinger, P. Johnson, B. Eklund, H. Hayes, D.B. Chadwick, I. Rivera-Duarte (2009). Review of Best Practices, Knowledge and Data Gaps, and Research Opportunities of the U.S. Department of Navy Vapor Intrusion Focus Areas. Technical Report 1982, SPAWAR Systems Center Pacific, May 2009. Available at http://www.spawar.navy.mil/sti/publications/pubs/tr/1982/tr1982cond.pdf, accessed December 11, 2011.

7. McAlary, T.A., R. Ettinger and P. Johnson, 2005, "Reference Handbook for Site-Specific Assessment of Subsurface Vapor Intrusion to Indoor Air," EPRI, Palo Alto, CA, 2005, EPRI Document #1008492.

8. McHugh, T.E., D.E. Hammond, T. Nickels, and B. Hartman (2008). "Use of radon measurements for evaluation of volatile organic compound (VOC) vapor intrusion." *Environmental Forensics* 9: 107-114.

9. U.S. EPA (1993). A Physician's Guide to Radon. U.S. EPA Office of Air and Radiation, EPA-402-K-93-008, Washington, DC, September 1993. Available at http://www.epa.gov/radon/pubs/physic.html, accessed December 11, 2011.

10. Battelle, Quality Assurance Project Plan for Verification of Building Pressure Control for the Assessment of Vapor Intrusion. Prepared by Battelle, Columbus, Ohio, October 1, 2010. Available at http://www.epa.gov/nrmrl/pubs/600r10157/600r10157.pdf, accessed December 11, 2011.

11. Battelle, Quality Management Plan for the ETV Advanced Monitoring Systems Center, Version 7.0, U.S. EPA Environmental Technology Verification Program. Prepared by Battelle, Columbus, Ohio, November 2008.

12. Mosley, R.B., D. Greenwell, and C. Lutes (2010). "Use of Integrated Indoor Concentrations of Tracer Gases and Volatile Organic Compounds to Distinguish Soil Sources from Above-Ground Sources." Poster #968, Presented at *Seventh International Conference, Remediation of Chlorinated and Recalcitrant Compounds*, Monterey, CA, May 24-27. Record ID: 220117.

13. CRC Handbook of Chemistry and Physics, 85th ed., David R. Lide, editor. Boca Raton: CRC Press, 2004.

14. Brenner, D. (2010). "Results of a Long-Term Study of Vapor Intrusion at Four Large Buildings at the NASA Ames Research Center." *Journal of the Air & Waste Management Association* 60: 747-758.

15. U.S. EPA Compendium Method TO-15, "Determination of Volatile Organic Compounds (VOCs) In Air Collected In Specially-Prepared Canisters and Analyzed By Gas Chromatography/Mass Spectrometry (GC/MS)." Second edition. Available at http://www.epa.gov/ttnamti1/files/ambient/airtox/to-15r.pdf, accessed December 11, 2011.

16. NIOSH Method 6602, "Sulfur hexafluoride by portable GC." Available at http://www.cdc.gov/niosh/docs/2003-154/pdfs/6602.pdf, accessed December 11, 2011.

17. U.S. EPA (1992). Indoor Radon and Radon Decay Product Measurement Device Protocols. Washington, DC: U.S. EPA Office of Air and Radiation, 402-R-92-004, July 1992. Available at http://www.epa.gov/radon/pubs/devprot1.html, accessed December 11, 2011.

18. ITRC (Interstate Technology & Regulatory Council) (2010). *Use and Measurement of Mass Flux and Mass Discharge*. MASSFLUX-1. Washington, D.C.: Interstate Technology & Regulatory Council, Integrated DNAPL Site Strategy Team. http://www.itrcweb.org/Documents/MASSFLUX1.pdf, accessed December 11, 2011.

19. Nazaroff, W.W., H. Feustel, A.V. Nero, K.L. Revzan, D.T. Grimsrud, M.A. Essling, R.E. Toohey (1985). "Radon transport into a detached one-story house with a basement." *Atmospheric Environment* 19: 31-46.

20. U.S. EPA (1997). National Radon Proficiency Program Guidance on Quality Assurance. Montgomery, AL: National Air and Radiation Environmental Laboratory, 401-R-95-012, October 1997. http://www.nrsb.org/images/file/QualityAssurranceProgram.pdf, accessed December 11, 2011.

Appendix A
Supplemental Information

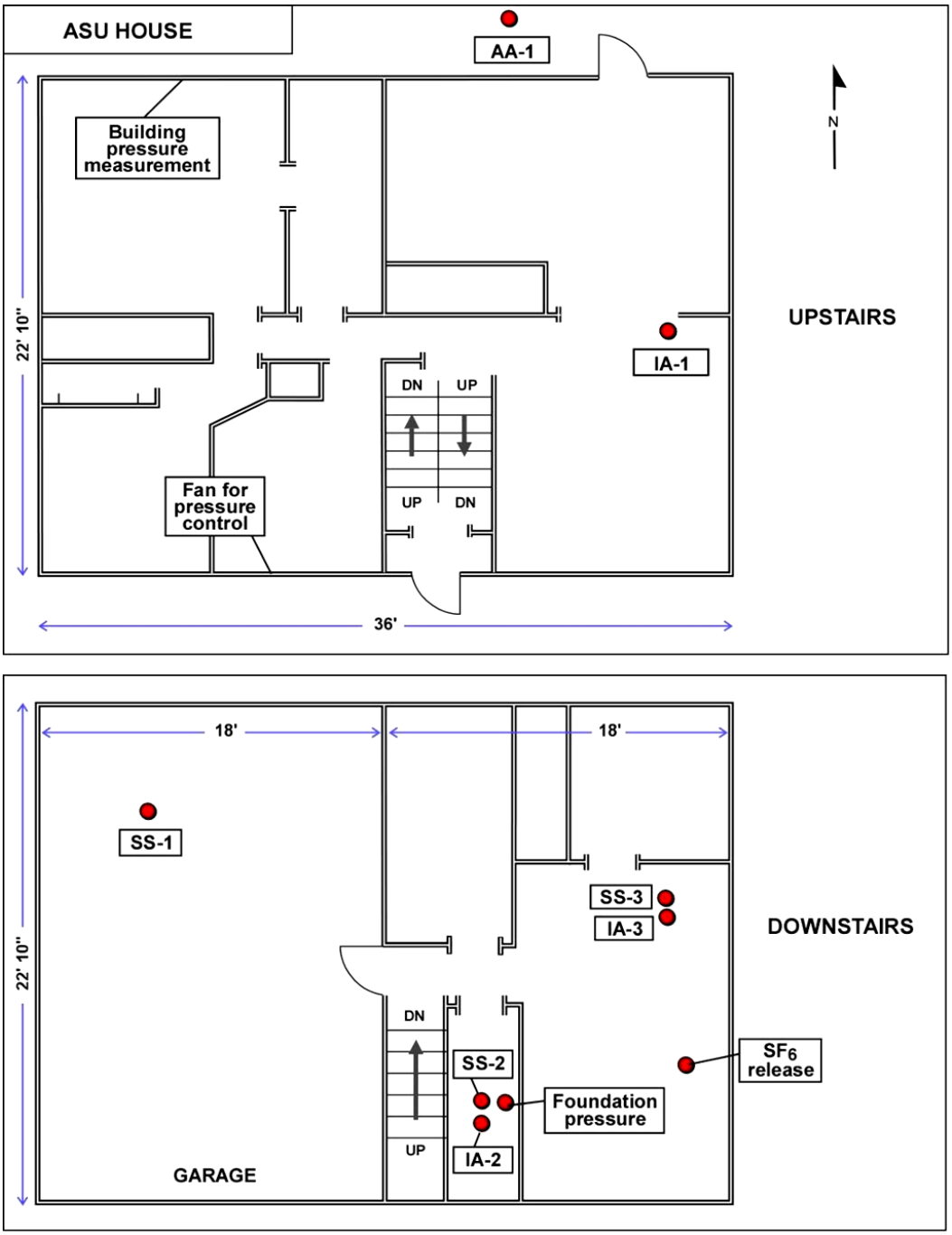

Figure A1. Floorplan for ASU VI Research House. Shown are the locations for IA, AA, and SS sampling, cross-foundation and building (I/O) differential pressure measurements, the release point for the SF_6 tracer gas, and placement of the fan for pressure control. Dimension are of the building interior and are in feet (') and inches ("). Ceiling height upstairs is 8', downstairs is 7'6". Figures courtesy of GSI.

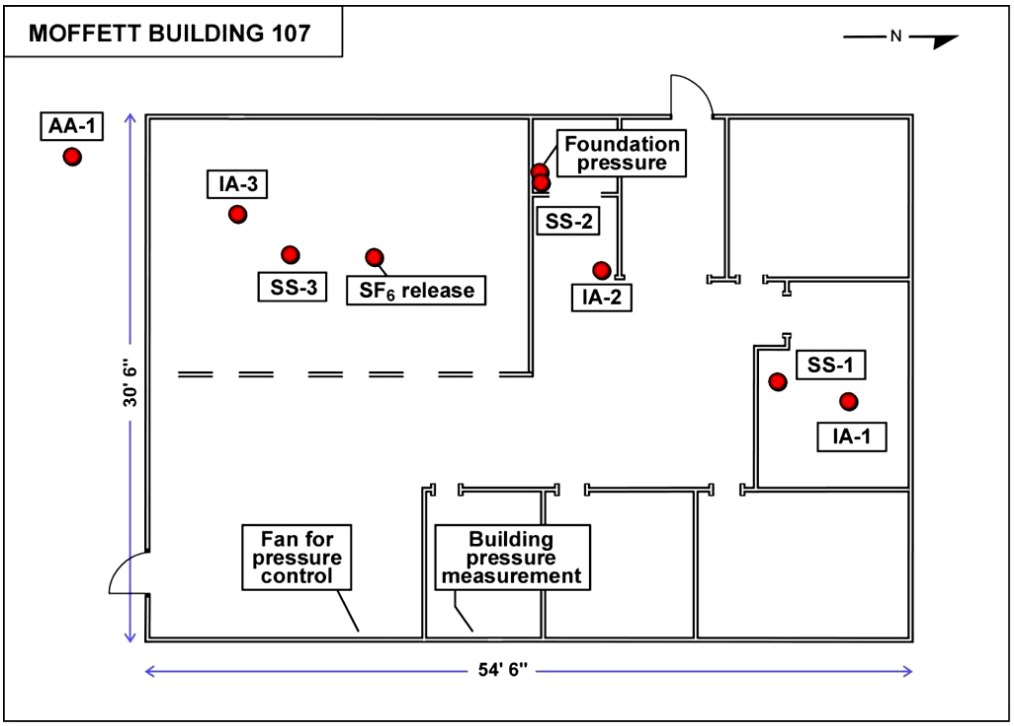

Figure A2. Floorplan for Moffett Field Building 107. Shown are the locations for IA, AA and SS sampling, cross-foundation and building (indoor/ourdoor) differential pressure measurements, the release point for the SF_6 tracer gas, and placement of the fan for pressure control. Dimension are of the building interior and are in feet (') and inches ("). Ceiling height 7'9". Figure courtesy of GSI.

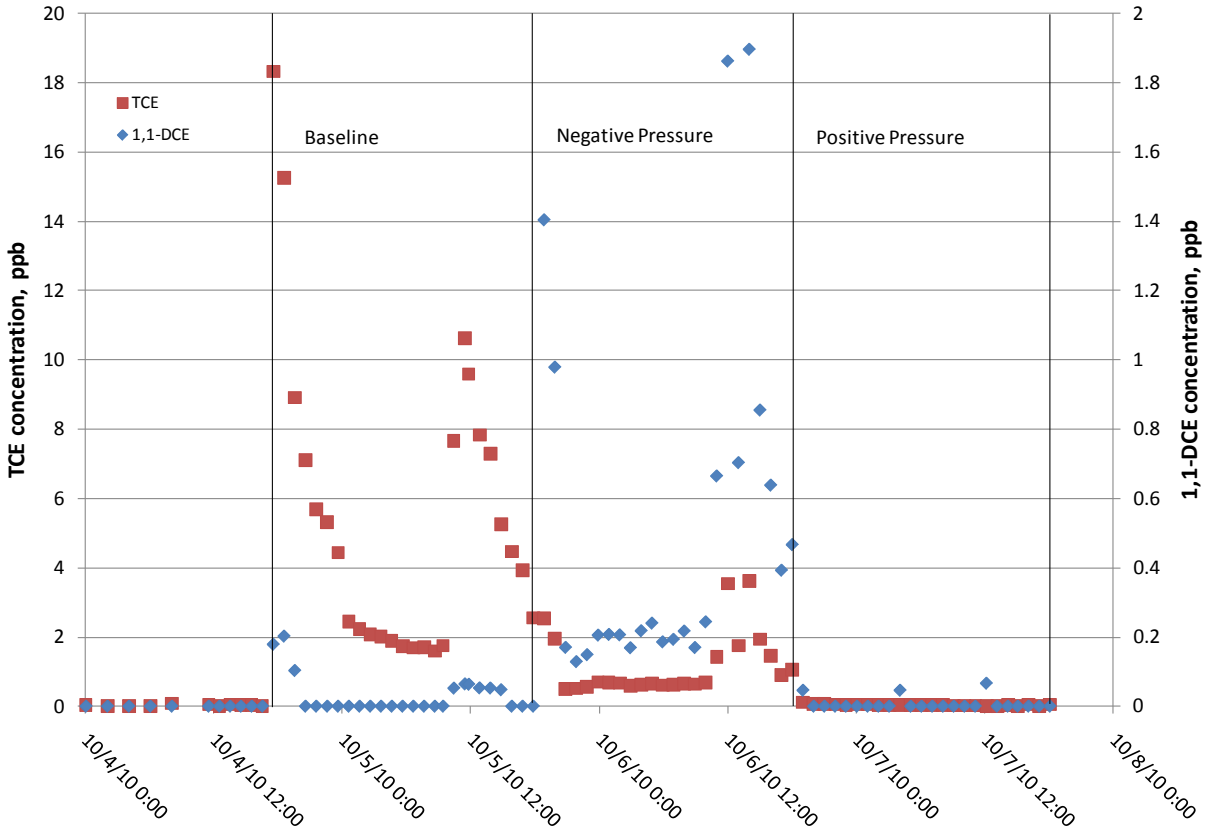

Figure A3. Real-time indoor air data from the HAPSITE at ASU House.

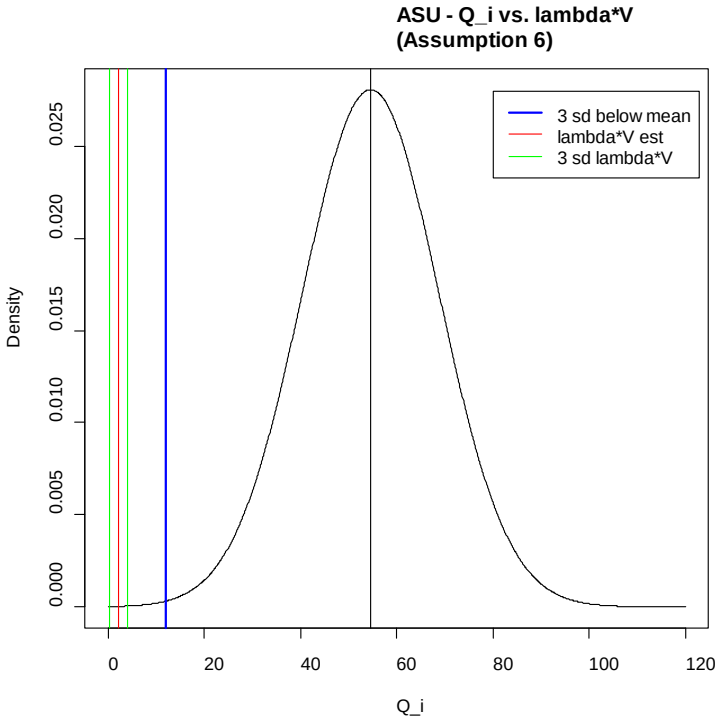

Figure A4. Graphical presentation of validation of Mosley Model assumptions: Q_i compared to λV at ASU House.

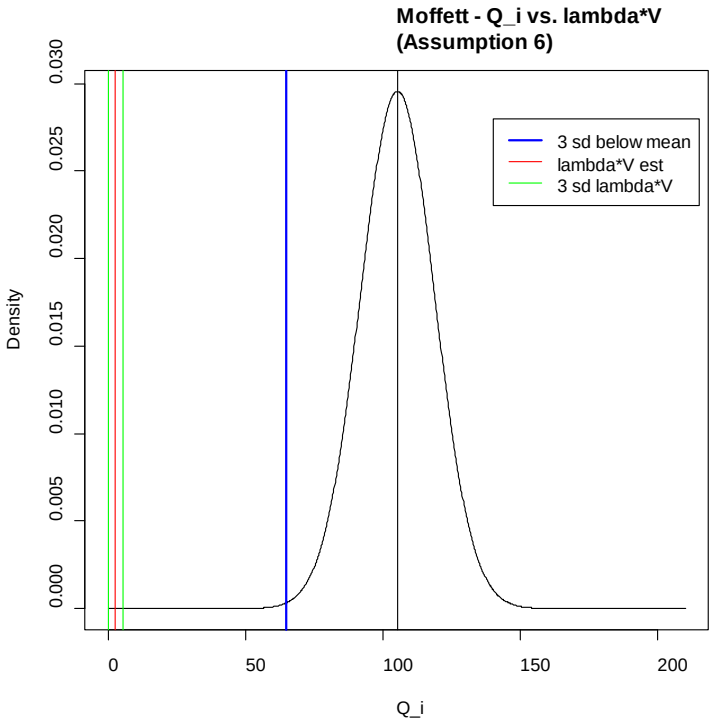

Figure A5. Graphical presentation of validation of Mosley Model assumptions: Q_i compared to λV at Moffett Field.

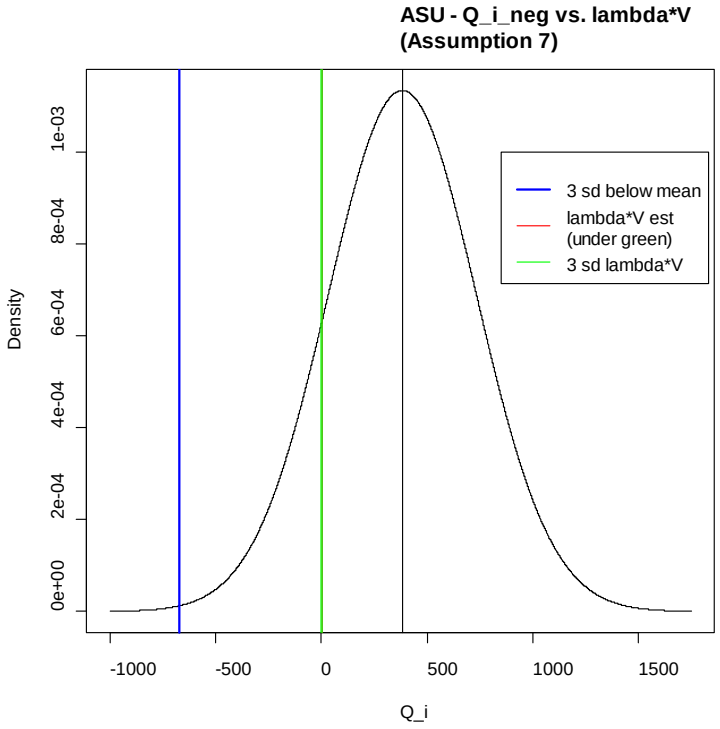

Figure A6. Graphical presentation of validation of Mosley Model assumptions: Q_i^- compared to λV at ASU House.

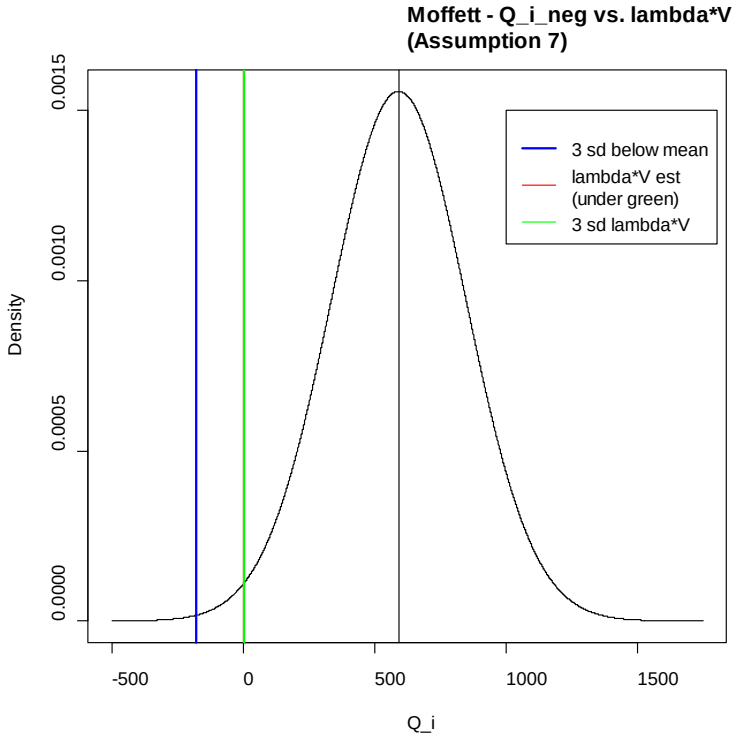

Figure A7. Graphical presentation of validation of Mosley Model assumptions: Q_i^- compared to λV at Moffett Field.

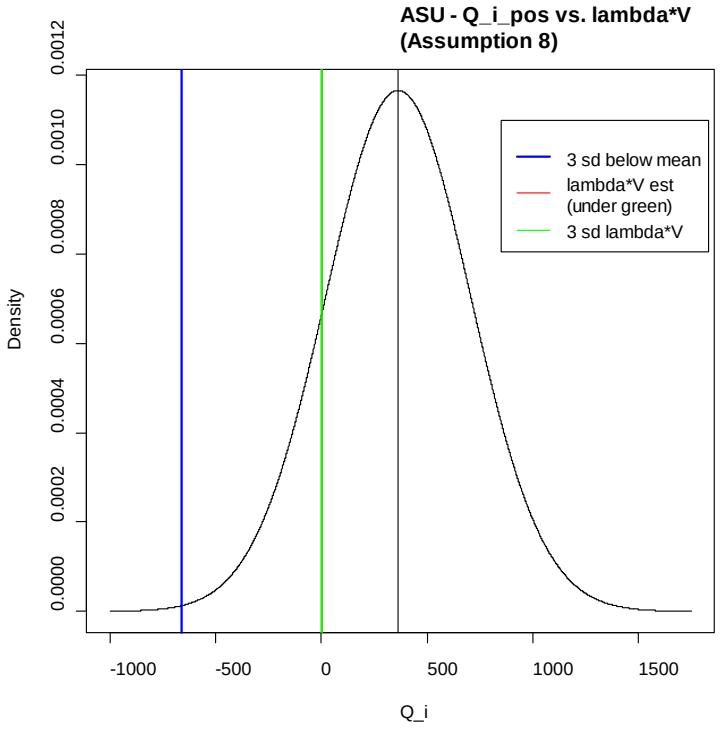

Figure A8. Graphical presentation of validation of Mosley Model assumptions: Q_i^+ compared to λV at ASU House.

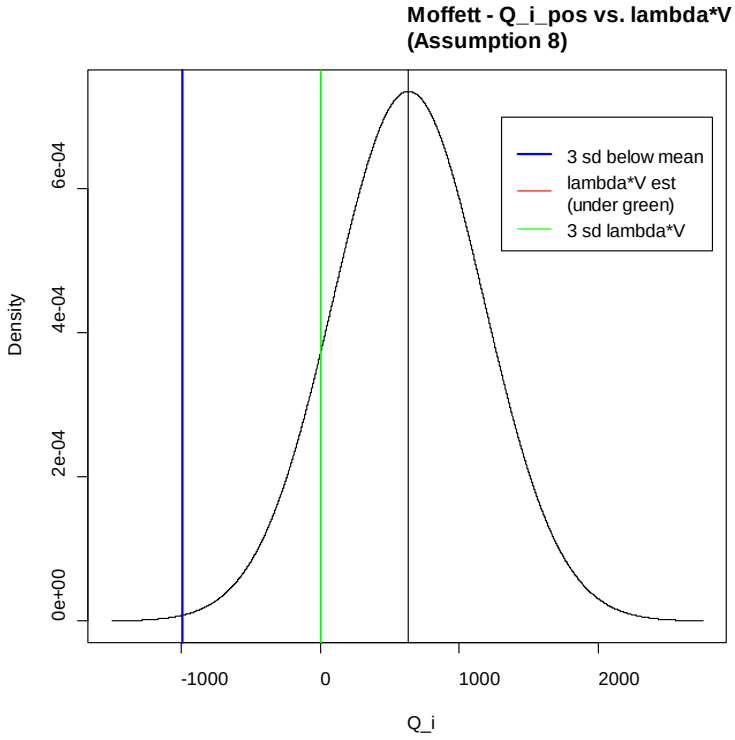

Figure A9. Graphical presentation of validation of Mosley Model assumptions: Q_i^+ compared to λV at Moffett Field.

Table A1. Mean subslab pressure differentials (in Pa) at ASU House and Moffett Field. Also presented are standard deviations, number of observations (N), and standard deviation of the mean. Pressures have been corrected to account for the reference port being open to the indoor atmosphere.

	ASU House			
Test	Mean	Std Dev	N	Std dev/√N
BL	0.35	0.16	290	0.009
NP	-2.12	0.25	290	0.015
PP	2.56	0.27	289	0.016

	Moffett Field			
Test	Mean	Std Dev	N	Std dev/√N
BL	-0.24	0.45	278	0.027
NP	-1.21	0.24	275	0.015
PP	0.47	0.22	256	0.014

Tables A2 through A8, presented on the following pages, provide the raw IA, AA, and SS data generated during the testing at both buildings, as well as quantities calculated using and derived from these raw data. Data are organized and presented in tabular format according to which verification parameter or assumption required the use of which raw data. Names of specific field samples are in the nomenclature described in the Data Collection Forms in Appendix D of the QAPP, such as 1-PP-IA-VOC-1 to indicate the positive pressure IA sample for VOCs and SF_6 collected at IA-1, either at ASU House or Moffett Field. The system of nomenclature in the table headers generally follows that presented in Table 1 of Chapter 3, with the exception that subscripts have been replaced by underscores followed by normal text, and superscripts have simply become normal text: for instance T_i^+ is now T_i+. Note that quantities presented using nomenclature from Table 1 are generally derived from several other data; for instance, T_i+ is the arithmetic mean of three SF_6 measurements: 1-PP-IA-VOC-1, 1-PP-IA-VOC-2, and 1-PP-IA-VOC-3. Moreover, tags such as std_dev_, delta_, _MDL, _AVG, _SF_6, _Rn, _TCE, _DCE, _PCE, _Ben, _Tol. These tag names stand for, respectively, standard deviation, estimated error (according to principles in Appendix C of the QAPP), estimated method detection limit, arithmetic mean, SF_6, radon, trichloroethylene, 1,1-dichloroethylene, tetrachloroethylene, benzene, and toluene, have been appended to names, as appropriate, to clarify the identity of the quantify presented. Additional information is also provided under the tables, including a roadmap of variable names, units for all results, references to concentration data that were less than MDLs, and to data impacted by various quality control issues. Finally, for calculation of the statistics and results of hypothesis testing presented in Chapter 6 of the present report, much of the raw data were first transformed onto the log scale; as such, derived quantities such as standard deviations and error estimates will not match those presented in Tables A2 through A8.

Table A2. Data used in the calculation of VI enhancement and reduction

Pressure	Building	Q_T	delta_Q_T	IA-1_SF_6	IA-1_SF_6 _MDL	IA-2_SF_6	IA-2_SF_6 MDL
BL	ASU	4.755E-05	10%	*4,000*	120	*5,100*	96
NP	ASU	5.022E-05	10%	*360*	21	*380*	19
PP	ASU	5.301E-05	10%	*82*	9.9	*820*	11

Pressure	Building	Q_T	delta_Q_T	IA-1_SF_6	IA-1_SF_6 _MDL	IA-2_SF_6	IA-2_SF_6 MDL
BL	Moffett	5.83E-05	10%	***3,000***	91	***3,400***	88
NP	Moffett	5.60E-05	10%	***310***	8.8	***600***	9.8
PP	Moffett	5.64E-05	10%	***790***	11	***790***	9.6

Variable names							
Baseline	Building	Q_T	delta_Q_T	**1-BL-IA-VOC-1**	1-BL-IA-VOC-1_MDL	**1-BL-IA-VOC-2**	1-BL-IA-VOC-2_MDL
Negative Pressure	Building	Q_T-	delta_Q_T-	**1-NP-IA-VOC-1**	1-NP-IA-VOC-1_MDL	**1-NP-IA-VOC-2**	1-NP-IA-VOC-2_MDL
Positive Pressure	Building	Q_T+	delta_Q_T+	**1-PP-IA-VOC-1**	1-PP-IA-VOC-1_MDL	**1-PP-IA-VOC-2**	1-PP-IA-VOC-2_MDL
Units							
pCi/h	none	m3/h	%	µg/m3	µg/m3	µg/m3	µg/m3

reported value < MDL

italics: data used in calcs

orange text: ADQ observations

bold text: deviation 5

Table A2. Data used in the calculation of VI enhancement and reduction (Continued)

Pressure	Building	IA-3_SF_6	IA-3_SF_6 MDL	T_i	std_dev_T_i	C_T	delta_C_T	V
BL	ASU	*6,500*	910	5,200	1,253	5.96E+09	0.2%	273.5
NP	ASU	*1,600*	22	780	710	5.96E+09	0.2%	273.5
PP	ASU	*1,700*	93	867	810	5.96E+09	0.2%	273.5

Pressure	Building	IA-3_SF_6	IA-3_SF_6 MDL	T_i	std_dev_T_i	C_T	delta_C_T	V
BL	Moffett	***3,500***	90	3,300	265	5.96E+09	0.2%	364.8
NP	Moffett	***780***	8.8	563	237	5.96E+09	0.2%	364.8
PP	Moffett	**0**	*10*	530	450	5.96E+09	0.2%	364.8

Variable names								
Baseline	Building	**1-BL-IA-VOC-3**	1-BL-IA-VOC-3_MDL	T_i	std_dev_T_i	C_T	delta_C_T	V
Negative Pressure	Building	**1-NP-IA-VOC-3**	1-NP-IA-VOC-3_MDL	T_i-	std_dev_T_i-	C_T-	delta_C_T-	V
Positive Pressure	Building	**1-PP-IA-VOC-3**	1-PP-IA-VOC-3_MDL	T_i+	std_dev_T_i+	C_T+	delta_C_T+	V
Units								
pCi/h	none	µg/m3	µg/m3	µg/m3	µg/m3	µg/m3	%	m3

reported value < MDL

italics: data used in calcs

orange text: ADQ observations

bold text: deviation 5

Table A2. Data used in the calculation of VI enhancement and reduction (Continued)

Pressure	Building	delta_V	Q_i	delta_Q_i	IA-1_Rn	IA-1_Rn_MDL	IA-2_Rn	IA-2_Rn_MDL
BL	ASU	30%	54	14	*0.271*	0.244	*0.326*	0.438
NP	ASU	30%	384	351	*1.103*	0.478	*4.124*	0.863
PP	ASU	30%	364	342	*0.017*	0.095	*0.153*	0.057

Pressure	Building	delta_V	Q_i	delta_Q_i	IA-1_Rn	IA-1_Rn_MDL	IA-2_Rn	IA-2_Rn_MDL
BL	Moffett	30%	105	13	*1.008*	0.284	*0.921*	0.327
NP	Moffett	30%	592	256	*0.520*	0.211	*0.530*	0.334
PP	Moffett	30%	634	542	*0.346*	0.247	*0.372*	0.206

Variable names								
Baseline	Building	delta_V	Q_i	delta_Q_i	1-BL-IA-Rn-1	1-BL-IA-Rn-1_MDL	1-BL-IA-Rn-2	1-BL-IA-Rn-2_MDL
Negative Pressure	Building	delta_V	Q_i-	delta_Q_i-	1-NP-IA-Rn-1	1-NP-IA-Rn-1_MDL	1-NP-IA-Rn-2	1-NP-IA-Rn-2_MDL
Positive Pressure	Building	delta_V	Q_i+	delta_Q_i+	1-PP-IA-Rn-1	1-PP-IA-Rn-1_MDL	1-PP-IA-Rn-2	1-PP-IA-Rn-2_MDL
Units								
pCi/h	none	%	m3/h	m3/h	pCi/L	pCi/L	pCi/L	pCi/L

reported value < MDL

italics: data used in calcs

orange text: ADQ observations

bold text: deviation 5

Table A2. Data used in the calculation of VI enhancement and reduction (Continued)

Pressure	Building	IA-3_Rn	IA-3_Rn_MDL	R_i	std_dev_R_i	R_a	R_a_MDL	delta_R_a
BL	ASU	*0.533*	0.295	377	138	*104*	289	38
NP	ASU	*0.376*	0.189	1868	1987	*26*	220	28
PP	ASU	*0.104*	0.072	91	69	*69*	55	52

Pressure	Building	IA-3_Rn	IA-3_Rn_MDL	R_i	std_dev_R_i	R_a	R_a_MDL	delta_R_a
BL	Moffett	*0.955*	0.228	961	44	*177*	175	8
NP	Moffett	*0.800*	0.336	617	159	*256*	237	66
PP	Moffett	*0.189*	0.196	302	99	*328*	165	107

Variable names								
Baseline	Building	1-BL-IA-Rn-3	1-BL-IA-Rn-3_MDL	R_i	std_dev_R_i	R_a	R_a_MDL	delta_R_a
Negative Pressure	Building	1-NP-IA-Rn-3	1-NP-IA-Rn-3_MDL	R_i-	std_dev_R_i-	R_a-	R_a-_MDL	delta_R_a-
Positive Pressure	Building	1-PP-IA-Rn-3	1-PP-IA-Rn-3_MDL	R_i+	std_dev_R_i+	R_a+	R_a+_MDL	delta_R_a+
Units								
pCi/h	none	pCi/L	pCi/L	pCi/m3	pCi/m3	pCi/m3	pCi/m3	pCi/m3

reported value < MDL

italics: data used in calcs

orange text: ADQ observations

bold text: deviation 5

Table A2. Data used in the calculation of VI enhancement and reduction (Continued)

Pressure	Building	R_i-R_a	delta_(R_i-R_a)	Q*(R_i-R_a)	delta_(Q_i*(R_i-R_a)]
BL	ASU	272	143	14830	8704
NP	ASU	1841	1987	706231	999852
PP	ASU	22	86	8143	32347

Pressure	Building	R_i-R_a	delta_(R_i-R_a)	Q*(R_i-R_a)	delta_[Q_i*(R_i-R_a)]
BL	Moffett	784	45	82556	11579
NP	Moffett	360	172	213492	137656
PP	Moffett	-25	146	-16153	93610

Variable names					
Baseline	Building	R_i-R_a	delta_(R_i*R_i)	Q_i*R_i	delta_[Q_i*(R_i-R_a)]
Negative Pressure	Building	R_i--R_a-	delta_(R_i-*R_i-)	Q_i-*R_i-	delta_[Q_i-*(R_i--R_a-)]
Positive Pressure	Building	R_i+-R_a+	delta_(R_i+*R_i+)	Q_i+*R_i+	delta_[Q_i+*(R_i+-R_a+)]
Units					
pCi/h	none	pCi/m3	pCi/m3	pCi/h	pCi/h

reported value < MDL

italics: data used in calcs

orange text: ADQ observations

bold text: deviation 5

Table A3. Data used for F_{VI} calculations

Calculation	Building	Q_i	delta_Q_i	R_i	std_dev_R_i	R_a	R_a_MDL	delta_R_a	R_i/R_a
F_vi-	ASU	54	14	377	138	*104*	289	38	3.6
F_vi+	ASU	384	351	1868	1987	*26*	220	28	70.5
F_vi+_(R_i+=R_a+)	ASU	364	342	91	69	*69*	55	52	1.3

Calculation	Building	Q_i	delta_Q_i	R_i	std_dev_R_i	R_a	R_a_MDL	delta_R_a	R_i/R_a
F_vi-	Moffett	105	13	961	44	*177*	175	8	5.4
F_vi+	Moffett	592	256	617	159	*256*	237	66	2.4
F_vi+_(R_i+=R_a+)	Moffett	634	542	302	99	*328*	165	107	0.9

Roadmap of variable names

F_vi-	Building	Q_i	delta_Q_i	R_i	std_dev_R_i	R_a	R_a_MDL	delta_R_a	R_i/R_a
F_vi+	Building	Q_i-	delta_Q_i-	R_i-	std_dev_R_i-	R_a-	R_a-_MDL	delta_R_a-	R_i-/R_a-
F_vi+_(R_i+=R_a+)	Building	Q_i+	delta_Q_i+	R_i+	std_dev_R_i+	R_a+	R_a+_MDL	delta_R_a+	R_i+/R_a+
Units									
none	none	m3/h	m3/h	pCi/m3	pCi/m3	pCi/m3	pCi/m3	pCi/m3	unitless

reported value < MDL

italicized text: data used in calcs

Problem with model calculation

bold text: deviation 5

Table A3. Data used for F_{VI} calculations (Continued)

TCE=trichloroethene

Calculation	Building	IA-1_TCE	IA-1_TCE_MDL	IA-2_TCE	IA-2_TCE_MDL	IA-3_TCE
F_vi-	ASU	*18*	0.05	*22*	0.04	*16*
F_vi+	ASU	*4*	0.044	*16*	0.04	*8.4*
F_vi+_(R_i+=R_a+)	ASU	*0.11*	0.041	*0.15*	0.047	*0.18*

Calculation	Building	IA-1_TCE	IA-1_TCE_MDL	IA-2_TCE	IA-2_TCE_MDL	IA-3_TCE
F_vi-	Moffett	***4.7***	0.038	***5***	0.037	***5.1***
F_vi+	Moffett	***2.3***	0.037	***3***	0.041	***4.1***
F_vi+_(R_i+=R_a+)	Moffett	***0.12***	0.045	***0.1***	0.040	***0.13***

Roadmap of variable names

F_vi-	Building	**1-BL-IA-VOC-1**	1-BL-IA-VOC-1_MDL	**1-BL-IA-VOC-2**	1-BL-IA-VOC-2_MDL	**1-BL-IA-VOC-3**
F_vi+	Building	**1-NP-IA-VOC-1**	1-NP-IA-VOC-1_MDL	**1-NP-IA-VOC-2**	1-NP-IA-VOC-2_MDL	**1-NP-IA-VOC-3**
F_vi+_(R_i+=R_a+)	Building	**1-PP-IA-VOC-1**	1-PP-IA-VOC-1_MDL	**1-PP-IA-VOC-2**	1-PP-IA-VOC-2_MDL	**1-PP-IA-VOC-3**

Units						
none	none	µg/m3	µg/m3	µg/m3	µg/m3	µg/m3

reported value < MDL

italicized text: data used in calcs

Problem with model calculation

bold text: deviation 5

Table A3. Data used for F_{VI} calculations (Continued)

Calculation	Building	IA-3_TCE_MDL	C_i_TCE	std_dev_C_i_TCE	C_a_TCE	C_a_TCE_MDL	delta_C_a_TCE
F_vi-	ASU	0.038	18.7	3.1	*0.17*	0.037	30%
F_vi+	ASU	0.047	9.5	6.1	*0.15*	0.039	30%
F_vi+_(R_i+=R_a+)	ASU	0.039	0.15	0.04	*0.084*	0.042	30%

Calculation	Building	IA-3_TCE_MDL	C_i_TCE	std_dev_C_i_TCE	C_a_TCE	C_a_TCE_MDL	delta_C_a_TCE
F_vi-	Moffett	0.038	4.9	0.2	***0.084***	0.037	30%
F_vi+	Moffett	0.037	3.1	0.9	***0.12***	0.033	30%
F_vi+_(R_i+=R_a+)	Moffett	0.043	0.12	0.02	***0.089***	0.038	30%

Roadmap of variable names

F_vi-	Building	1-BL-IA-VOC-3_MDL	C_i	std_dev_C_i	**C_a**	C_a_MDL	delta_C_a
F_vi+	Building	1-NP-IA-VOC-3_MDL	C_i-	std_dev_C_i-	**C_a-**	C_a-_MDL	delta_C_a-
F_vi+_(R_i+=R_a+)	Building	1-PP-IA-VOC-3_MDL	C_i+	std_dev_C_i+	**C_a+**	C_a+_MDL	delta_C_a+
Units							
none	none	µg/m3	µg/m3	µg/m3	µg/m3	µg/m3	%

reported value < MDL

italicized text: data used in calcs

Problem with model calculation

bold text: deviation 5

Table A3. Data used for F_{VI} calculations (Continued)

Calculation	Building	C_i/C_a_TCE	Q_i-*(C_i--C_a-)_TCE	Q_i*(C_i-C_a)_TCE	Q_i+*(C_i+-C_a+)_TCE	Q_i-*(C_i--C_a-)-Q_i*(C_i-C_a)_TCE
F_vi-	ASU	110	3574	1008	23	2566
F_vi+	ASU	63	none	none	none	none
F_vi+_(R_i+=R_a+)	ASU	1.7	none	none	none	none

Calculation	Building	C_i/C_a_TCE	Q_i-*(C_i--C_a-)_TCE	Q_i*(C_i-C_a)_TCE	Q_i+*(C_i+-C_a+)_TCE	Q_i-*(C_i--C_a-)-Q_i*(C_i-C_a)_TCE
F_vi-	Moffett	59	1785	511	18	1274
F_vi+	Moffett	26	none	none	none	none
F_vi+_(R_i+=R_a+)	Moffett	1.3	none	none	none	none

Roadmap of variable names

F_vi-	Building	C_i/C_a	none	Q_i*(C_i-C_a)	Q_i+*(C_i+-C_a+)	Q_i-*(C_i--C_a-)-Q_i*(C_i-C_a)
F_vi+	Building	C_i-/C_a-	Q_i-*(C_i--C_a-)	none	none	none
F_vi+_(R_i+=R_a+)	Building	C_i+/C_a+	none	none	none	none
Units						
none	none	Unitless	µg/h	µg/h	µg/h	µg/h

reported value < MDL

italicized text: data used in calcs

Problem with model calculation

bold text: deviation 5

Table A3. Data used for F_{VI} calculations (Continued)

Calculation	Building	Q_i*(C_i-C_a)-Q_i+*(C_i+-C_a+)_TCE	Q_i*(R_i-R_a)	Q_i-*(R_i--R_a-)	Q_i+*(R_i+-R_a+)	Q_i*(R_i-R_a)/[Q_i-*(R_i--R_a-)-Q_i*(R_i-R_a)]
F_vi-	ASU	985	14830	706231	8143	0.021
F_vi+	ASU	None	none	none	none	none
F_vi+_(R_i+=R_a+)	ASU	None	none	none	none	none

Calculation	Building	Q_i*(C_i-C_a)-Q_i+*(C_i+-C_a+)_TCE	Q_i*(R_i-R_a)	Q_i-*(R_i--R_a-)	Q_i+*(R_i+-R_a+)	Q_i*(R_i-R_a)/[Q_i-*(R_i--R_a-)-Q_i*(R_i-R_a)]
F_vi-	Moffett	493	82556	213492	-16153	0.631
F_vi+	Moffett	None	none	none	none	none
F_vi+_(R_i+=R_a+)	Moffett	None	none	none	none	none

Roadmap of variable names

F_vi-	Building	Q_i*(C_i-C_a)-Q_i+*(C_i+-C_a+)	Q_i*(R_i-R_a)	Q_i-*(R_i--R_a-)	Q_i+*(R_i+-R_a+)	Q_i*(R_i-R_a)/[Q_i-*(R_i--R_a-)-Q_i*(R_i-R_a)]
F_vi+	Building	None	none	none	none	none
F_vi+_(R_i+=R_a+)	Building	None	none	none	none	none
Units						
none	none	µg/h	pCi/h	pCi/h	pCi/h	none

reported value < MDL

italicized text: data used in calcs

Problem with model calculation

bold text: deviation 5

Table A3. Data used for F_{VI} calculations (Continued)

Calculation	Building	Q_i*(R_i-R_a)/[Q_i*(R_i-R_a)-Q_i+*(R_i+-R_a+)]	Q_i*C_i_TCE	E_C_TCE	F_a_TCE	F_in_TCE	F_vi_TCE
F_vi-	ASU	2.22	1017	55	0.01	0.94	0.05
F_vi+	ASU	None	none	2184	0.01	-1.16	2.15
F_vi+_(R_i+=R_a+)	ASU	None	none	985	0.01	0.02	0.97

Calculation	Building	Q_i*(R_i-R_a)/[Q_i*(R_i-R_a)-Q_i+*(R_i+-R_a+)]	Q_i*C_i_TCE	E_C_TCE	F_a_TCE	F_in_TCE	F_vi_TCE
F_vi-	Moffett	0.84	519	804	0.02	-0.56	1.55
F_vi+	Moffett	None	none	412	0.02	0.19	0.79
F_vi+_(R_i+=R_a+)	Moffett	None	none	493	0.02	0.03	0.95

Roadmap of variable names

F_vi-	Building	Q_i*(R_i-R_a)/[Q_i*(R_i-R_a)-Q_i+*(R_i+-R_a+)]	Q_i*C_i	E_C-	F_a	F_in-	F_vi-
F_vi+	Building	None	none	E_C+	none	F_in+	F_vi+
F_vi+_(R_i+=R_a+)	Building	None	none	E_C_(R_i+=R_a+)	none	F_in_(R_i+=R_a+)	F_vi+_(R_i+=R_a+)
Units							
none	none	None	µg/h	µg/h	none	none	none

reported value < MDL

italicized text: data used in calcs

Problem with model calculation

bold text: deviation 5

Table A3. Data used for F_{VI} calculations (Continued)

DCE=1,1-dichloroethene

Calculation	Building	IA-1_DCE	IA-1_DCE_MDL	IA-2_DCE	IA-2_DCE_MDL	IA-3_DCE
F_vi-	ASU	*0.12*	0.05	*0.13*	0.04	*0.12*
F_vi+	ASU	*2.3*	0.044	*11*	0.04	*5.4*
F_vi+_(R_i+=R_a+)	ASU	0	*0.041*	0	*0.047*	0

Calculation	Building	IA-1_DCE	IA-1_DCE_MDL	IA-2_DCE	IA-2_DCE_MDL	IA-3_DCE
F_vi-	Moffett	N/A	N/A	N/A	N/A	N/A
F_vi+	Moffett	N/A	N/A	N/A	N/A	N/A
F_vi+_(R_i+=R_a+)	Moffett	N/A	N/A	N/A	N/A	N/A

Roadmap of variable names

F_vi-	Building	1-BL-IA-VOC-1	1-BL-IA-VOC-1_MDL	1-BL-IA-VOC-2	1-BL-IA-VOC-2_MDL	1-BL-IA-VOC-3
F_vi+	Building	1-NP-IA-VOC-1	1-NP-IA-VOC-1_MDL	1-NP-IA-VOC-2	1-NP-IA-VOC-2_MDL	1-NP-IA-VOC-3
F_vi+_(R_i+=R_a+)	Building	1-PP-IA-VOC-1	1-PP-IA-VOC-1_MDL	1-PP-IA-VOC-2	1-PP-IA-VOC-2_MDL	1-PP-IA-VOC-3

Units						
none	none	µg/m3	µg/m3	µg/m3	µg/m3	µg/m3

reported value < MDL

italicized text: data used in calcs

Problem with model calculation

bold text: deviation 5

Table A3. Data used for F_{VI} calculations (Continued)

Calculation	Building	IA-3_DCE_MDL	C_i_DCE	std_dev_C_i_DCE	C_a_DCE	C_a_DCE_MDL	delta_C_a_DCE
F_vi-	ASU	0.038	0.12	0.006	0	*0.037*	30%
F_vi+	ASU	0.047	6.2	4.4	0	*0.039*	30%
F_vi+_(R_i+=R_a+)	ASU	*0.039*	0.0423	0.004	0	*0.042*	30%

Calculation	Building	IA-3_DCE_MDL	C_i_DCE	std_dev_C_i_DCE	C_a_DCE	C_a_DCE_MDL	delta_C_a_DCE
F_vi-	Moffett	N/A	N/A	N/A	N/A	N/A	N/A
F_vi+	Moffett	N/A	N/A	N/A	N/A	N/A	N/A
F_vi+_(R_i+=R_a+)	Moffett	N/A	N/A	N/A	N/A	N/A	N/A

Roadmap of variable names

F_vi-	Building	1-BL-IA-VOC-3_MDL	C_i	std_dev_C_i	C_a	C_a_MDL	delta_C_a
F_vi+	Building	1-NP-IA-VOC-3_MDL	C_i-	std_dev_C_i-	C_a-	C_a-_MDL	delta_C_a-
F_vi+_(R_i+=R_a+)	Building	1-PP-IA-VOC-3_MDL	C_i+	std_dev_C_i+	C_a+	C_a+_MDL	delta_C_a+
Units							
none	none	µg/m3	µg/m3	µg/m3	µg/m3	µg/m3	%

reported value < MDL

italicized text: data used in calcs

Problem with model calculation

bold text: deviation 5

Table A3. Data used for F_{VI} calculations (Continued)

Calculation	Building	C_i/C_a_DCE	Q_i-*(C_i--C_a-)_DCE	Q_i*(C_i-C_a)_DCE	Q_i+*(C_i+-C_a+)_DCE	Q_i-*(C_i--C_a-)-Q_i*(C_i-C_a)_DCE
F_vi-	ASU	3.3	2376	4.7	0.1	2371
F_vi+	ASU	160	none	none	none	none
F_vi+_(R_i+=R_a+)	ASU	1.0	none	none	none	none

Calculation	Building	C_i/C_a_DCE	Q_i-*(C_i--C_a-)_DCE	Q_i*(C_i-C_a)_DCE	Q_i+*(C_i+-C_a+)_DCE	Q_i-*(C_i--C_a-)-Q_i*(C_i-C_a)_DCE
F_vi-	Moffett	N/A	N/A	N/A	N/A	N/A
F_vi+	Moffett	N/A	N/A	N/A	N/A	N/A
F_vi+_(R_i+=R_a+)	Moffett	N/A	N/A	N/A	N/A	N/A

Roadmap of variable names

F_vi-	Building	C_i/C_a	none	Q_i*(C_i-C_a)	Q_i+*(C_i+-C_a+)	Q_i-*(C_i--C_a-)-Q_i*(C_i-C_a)
F_vi+	Building	C_i-/C_a-	Q_i-*(C_i--C_a-)	none	none	none
F_vi+_(R_i+=R_a+)	Building	C_i+/C_a+	none	none	none	none

Units						
none	none	Unitless	µg/h	µg/h	µg/h	µg/h

reported value < MDL

italicized text: data used in calcs

Problem with model calculation

bold text: deviation 5

Table A3. Data used for F_{VI} calculations (Continued)

Calculation	Building	Q_i*(C_i-C_a)-Q_i+*(C_i+-C_a+)_DCE	Q_i*(R_i-R_a)	Q_i-*(R_i--R_a-)	Q_i+*(R_i+-R_a+)	Q_i*(R_i-R_a)/[Q_i-*(R_i--R_a-)-Q_i*(R_i-R_a)]
F_vi-	ASU	4.6	14830	706231	8143	0.021
F_vi+	ASU	None	none	none	none	none
F_vi+_(R_i+=R_a+)	ASU	None	none	none	none	none

Calculation	Building	Q_i*(C_i-C_a)-Q_i+*(C_i+-C_a+)_DCE	Q_i*(R_i-R_a)	Q_i-*(R_i--R_a-)	Q_i+*(R_i+-R_a+)	Q_i*(R_i-R_a)/[Q_i-*(R_i--R_a-)-Q_i*(R_i-R_a)]
F_vi-	Moffett	N/A	N/A	N/A	N/A	N/A
F_vi+	Moffett	N/A	N/A	N/A	N/A	N/A
F_vi+_(R_i+=R_a+)	Moffett	N/A	N/A	N/A	N/A	N/A

Roadmap of variable names

F_vi-	Building	Q_i*(C_i-C_a)-Q_i+*(C_i+-C_a+)	Q_i*(R_i-R_a)	Q_i-*(R_i--R_a-)	Q_i+*(R_i+-R_a+)	Q_i*(R_i-R_a)/[Q_i-*(R_i--R_a-)-Q_i*(R_i-R_a)]
F_vi+	Building	None	none	none	none	none
F_vi+_(R_i+=R_a+)	Building	None	none	none	none	none

Units

none	none	µg/h	pCi/h	pCi/h	pCi/h	none

reported value < MDL

italicized text: data used in calcs

Problem with model calculation

bold text: deviation 5

Table A3. Data used for F_{VI} calculations (Continued)

Calculation	Building	Q_i*(R_i-R_a)/[Q_i*(R_i-R_a)-Q_i+*(R_i+-R_a+)]	Q_i*C_i_DCE	E_C_DCE	F_a_DCE	F_in_DCE
F_vi-	ASU	2.22	6.7	51	0.30	-6.87
F_vi+	ASU	none	none	10	0.30	-0.81
F_vi+_(R_i+=R_a+)	ASU	none	none	5	0.30	0.02

Calculation	Building	Q_i*(R_i-R_a)/[Q_i*(R_i-R_a)-Q_i+*(R_i+-R_a+)]	Q_i*C_i_DCE	E_C_DCE	F_a_DCE	F_in_DCE
F_vi-	Moffett	N/A	N/A	N/A	N/A	N/A
F_vi+	Moffett	N/A	N/A	N/A	N/A	N/A
F_vi+_(R_i+=R_a+)	Moffett	N/A	N/A	N/A	N/A	N/A

Roadmap of variable names

F_vi-	Building	Q_i*(R_i-R_a)/[Q_i*(R_i-R_a)-Q_i+*(R_i+-R_a+)]	Q_i*C_i	E_C-	F_a	F_in-
F_vi+	Building	none	none	E_C+	none	F_in+
F_vi+_(R_i+=R_a+)	Building	none	none	E_C_(R_i+=R_a+)	none	F_in_(R_i+=R_a+)
Units						
none	none	none	µg/h	µg/h	none	none

reported value < MDL

italicized text: data used in calcs

Problem with model calculation

bold text: deviation 5

Table A3. Data used for F_{VI} calculations (Continued)

PCE=tetrachloroethene

Calculation	Building	F_vi_DCE	IA-1_PCE	IA-1_PCE_MDL	IA-2_PCE	IA-2_PCE_MDL
F_vi-	ASU	7.57	N/A	N/A	N/A	N/A
F_vi+	ASU	1.51	N/A	N/A	N/A	N/A
F_vi+_(R_i+=R_a+)	ASU	0.68	N/A	N/A	N/A	N/A

Calculation	Building	F_vi_DCE	IA-1_PCE	IA-1_PCE_MDL	IA-2_PCE	IA-2_PCE_MDL
F_vi-	Moffett	N/A	***2.7***	0.038	***2.9***	0.037
F_vi+	Moffett	N/A	***1.5***	0.037	***1.9***	0.041
F_vi+_(R_i+=R_a+)	Moffett	N/A	***0.44***	0.045	***0.41***	0.040

Roadmap of variable names

F_vi-	Building	F_vi-	**1-BL-IA-VOC-1**	1-BL-IA-VOC-1_MDL	**1-BL-IA-VOC-2**	1-BL-IA-VOC-2_MDL
F_vi+	Building	F_vi+	**1-NP-IA-VOC-1**	1-NP-IA-VOC-1_MDL	**1-NP-IA-VOC-2**	1-NP-IA-VOC-2_MDL
F_vi+_(R_i+=R_a+)	Building	F_vi+_(R_i+=R_a+)	**1-PP-IA-VOC-1**	1-PP-IA-VOC-1_MDL	**1-PP-IA-VOC-2**	1-PP-IA-VOC-2_MDL
Units						
none	none	none	µg/m3	µg/m3	µg/m3	µg/m3

reported value < MDL

italicized text: data used in calcs

Problem with model calculation

bold text: deviation 5

Table A3. Data used for F_{VI} calculations (Continued)

Calculation	Building	IA-3_PCE	IA-3_PCE_MDL	C_i_PCE	std_dev_C_i_PCE	C_a_PCE	C_a_PCE_MDL
F_vi-	ASU	N/A	N/A	N/A	N/A	N/A	N/A
F_vi+	ASU	N/A	N/A	N/A	N/A	N/A	N/A
F_vi+_(R_i+=R_a+)	ASU	N/A	N/A	N/A	N/A	N/A	N/A

Calculation	Building	IA-3_PCE	IA-3_PCE_MDL	C_i_PCE	std_dev_C_i_PCE	C_a_PCE	C_a_PCE_MDL
F_vi-	Moffett	***2.9***	0.038	2.8	0.12	***0.12***	0.037
F_vi+	Moffett	***2.6***	0.037	2.0	0.56	***0.21***	0.033
F_vi+_(R_i+=R_a+)	Moffett	***0.41***	0.043	0.42	0.02	***0.89***	0.038

Roadmap of variable names

F_vi-	Building	**1-BL-IA-VOC-3**	1-BL-IA-VOC-3_MDL	C_i	std_dev_C_i	**C_a**	C_a_MDL
F_vi+	Building	**1-NP-IA-VOC-3**	1-NP-IA-VOC-3_MDL	C_i-	std_dev_C_i-	**C_a-**	C_a-_MDL
F_vi+_(R_i+=R_a+)	Building	**1-PP-IA-VOC-3**	1-PP-IA-VOC-3_MDL	C_i+	std_dev_C_i+	**C_a+**	C_a+_MDL
Units							
none	none	µg/m3	µg/m3	µg/m3	µg/m3	µg/m3	µg/m3

reported value < MDL

italicized text: data used in calcs

Problem with model calculation

bold text: deviation 5

Table A3. Data used for F_{VI} calculations (Continued)

Calculation	Building	delta_C_a_PCE	C_i/C_a_PCE	Q_i-*(C_i--C_a-)_PCE	Q_i*(C_i-C_a)_PCE	Q_i+*(C_i+-C_a+)_PCE
F_vi-	ASU	N/A	N/A	N/A	N/A	N/A
F_vi+	ASU	N/A	N/A	N/A	N/A	N/A
F_vi+_(R_i+=R_a+)	ASU	N/A	N/A	N/A	N/A	N/A

Calculation	Building	delta_C_a_PCE	C_i/C_a_PCE	Q_i-*(C_i--C_a-)_PCE	Q_i*(C_i-C_a)_PCE	Q_i+*(C_i+-C_a+)_PCE
F_vi-	Moffett	30%	24	1060	286	-298
F_vi+	Moffett	30%	10	none	none	none
F_vi+_(R_i+=R_a+)	Moffett	30%	0.47	none	none	none

Roadmap of variable names

F_vi-	Building	delta_C_a	C_i/C_a	none	Q_i*(C_i-C_a)	Q_i+*(C_i+-C_a+)
F_vi+	Building	delta_C_a-	C_i-/C_a-	Q_i-*(C_i--C_a-)	none	none
F_vi+_(R_i+=R_a+)	Building	delta_C_a+	C_i+/C_a+	none	none	none
Units						
none	none	%	unitless	µg/h	µg/h	µg/h

reported value < MDL

italicized text: data used in calcs

Problem with model calculation

bold text: deviation 5

Table A3. Data used for F_{VI} calculations (Continued)

Calculation	Building	Q_i-*(C_i--C_a-)-Q_i*(C_i-C_a)_PCE	Q_i*(C_i-C_a)-Q_i+*(C_i+-C_a+)_PCE	Q_i*(R_i-R_a)	Q_i-*(R_i--R_a-)	Q_i+*(R_i+-R_a+)
F_vi-	ASU	N/A	N/A	N/A	N/A	N/A
F_vi+	ASU	N/A	N/A	N/A	N/A	N/A
F_vi+_(R_i+=R_a+)	ASU	N/A	N/A	N/A	N/A	N/A

Calculation	Building	Q_i-*(C_i--C_a-)-Q_i*(C_i-C_a)_PCE	Q_i*(C_i-C_a)-Q_i+*(C_i+-C_a+)_PCE	Q_i*(R_i-R_a)	Q_i-*(R_i--R_a-)	Q_i+*(R_i+-R_a+)
F_vi-	Moffett	775	584	82556	213492	-16153
F_vi+	Moffett	none	none	none	none	none
F_vi+_(R_i+=R_a+)	Moffett	none	none	none	none	none

Roadmap of variable names

F_vi-	Building	Q_i-*(C_i--C_a-)-Q_i*(C_i-C_a)	Q_i*(C_i-C_a)-Q_i+*(C_i+-C_a+)	Q_i*(R_i-R_a)	Q_i-*(R_i--R_a-)	Q_i+*(R_i+-R_a+)
F_vi+	Building	none	none	none	none	none
F_vi+_(R_i+=R_a+)	Building	none	none	none	none	none

Units

none	none	µg/h	µg/h	pCi/h	pCi/h	pCi/h

reported value < MDL

italicized text: data used in calcs

Problem with model calculation

bold text: deviation 5

Table A3. Data used for F_{VI} calculations (Continued)

Calculation	Building	Q_i*(R_i-R_a)/[Q_i-*(R_i--R_a-)-Q_i*(R_i-R_a)]	Q_i*(R_i-R_a)/[Q_i*(R_i-R_a)-Q_i+*(R_i+-R_a+)]	Q_i*C_i_PCE	E_C_PCE
F_vi-	ASU	N/A	N/A	N/A	N/A
F_vi+	ASU	N/A	N/A	N/A	N/A
F_vi+_(R_i+=R_a+)	ASU	N/A	N/A	N/A	N/A

Calculation	Building	Q_i*(R_i-R_a)/[Q_i-*(R_i--R_a-)-Q_i*(R_i-R_a)]	Q_i*(R_i-R_a)/[Q_i*(R_i-R_a)-Q_i+*(R_i+-R_a+)]	Q_i*C_i_PCE	E_C_PCE
F_vi-	Moffett	0.631	0.84	298	488
F_vi+	Moffett	none	none	none	488
F_vi+_(R_i+=R_a+)	Moffett	none	none	none	584

Roadmap of variable names

F_vi-	Building	Q_i*(R_i-R_a)/[Q_i-*(R_i--R_a-)-Q_i*(R_i-R_a)]	Q_i*(R_i-R_a)/[Q_i*(R_i-R_a)-Q_i+*(R_i+-R_a+)]	Q_i*C_i	E_C-
F_vi+	Building	None	none	none	E_C+
F_vi+_(R_i+=R_a+)	Building	none	none	none	E_C_(R_i+=R_a+)
Units					
none	none	none	none	µg/h	µg/h

reported value < MDL

italicized text: data used in calcs

Problem with model calculation

bold text: deviation 5

Table A3. Data used for F_{VI} calculations (Continued)

Ben=benzene

Calculation	Building	F_a_PCE	F_in_PCE	F_vi_PCE	IA-1_Ben	IA-1_Ben_MDL	IA-2_Ben
F_vi-	ASU	N/A	N/A	N/A	*0.47*	0.15	*0.46*
F_vi+	ASU	N/A	N/A	N/A	*0.44*	0.13	*0.47*
F_vi+_(R_i+=R_a+)	ASU	N/A	N/A	N/A	*0.56*	0.12	*0.57*

Calculation	Building	F_a_PCE	F_in_PCE	F_vi_PCE	IA-1_Ben	IA-1_Ben_MDL	IA-2_Ben
F_vi-	Moffett	0.04	-0.68	1.64	***1.1***	0.11	***1.1***
F_vi+	Moffett	0.04	-0.68	1.64	***1.5***	0.11	***1.7***
F_vi+_(R_i+=R_a+)	Moffett	0.04	-1.00	1.96	***1.5***	0.14	***1.6***

Roadmap of variable names

F_vi-	Building	F_a	F_in-	F_vi-	**1-BL-IA-VOC-1**	1-BL-IA-VOC-1_MDL	**1-BL-IA-VOC-2**
F_vi+	Building	none	F_in+	F_vi+	**1-NP-IA-VOC-1**	1-NP-IA-VOC-1_MDL	**1-NP-IA-VOC-2**
F_vi+_(R_i+=R_a+)	Building	none	F_in_(R_i+=R_a+)	F_vi+_(R_i+=R_a+)	**1-PP-IA-VOC-1**	1-PP-IA-VOC-1_MDL	**1-PP-IA-VOC-2**
Units							
none	none	none	none	none	µg/m3	µg/m3	µg/m3

reported value < MDL

italicized text: data used in calcs

Problem with model calculation

bold text: deviation 5

Table A3. Data used for F_{VI} calculations (Continued)

Calculation	Building	IA-2_Ben_MDL	IA-3_Ben	IA-3_Ben_MDL	C_i_Ben	std_dev_C_i_Ben
F_vi-	ASU	0.12	*0.44*	0.11	0.46	0.015
F_vi+	ASU	0.12	*0.46*	0.14	0.46	0.015
F_vi+_(R_i+=R_a+)	ASU	0.14	*0.59*	0.12	0.57	0.015

Calculation	Building	IA-2_Ben_MDL	IA-3_Ben	IA-3_Ben_MDL	C_i_Ben	std_dev_C_i_Ben
F_vi-	Moffett	0.11	***1.1***	0.11	1.1	0.00
F_vi+	Moffett	0.12	***1.5***	0.11	1.6	0.12
F_vi+_(R_i+=R_a+)	Moffett	0.12	***1.5***	0.13	1.5	0.06

Roadmap of variable names

F_vi-	Building	1-BL-IA-VOC-2_MDL	**1-BL-IA-VOC-3**	1-BL-IA-VOC-3_MDL	C_i	std_dev_C_i
F_vi+	Building	1-NP-IA-VOC-2_MDL	**1-NP-IA-VOC-3**	1-NP-IA-VOC-3_MDL	C_i-	std_dev_C_i-
F_vi+_(R_i+=R_a+)	Building	1-PP-IA-VOC-2_MDL	**1-PP-IA-VOC-3**	1-PP-IA-VOC-3_MDL	C_i+	std_dev_C_i+

Units						
none	none	µg/m3	µg/m3	µg/m3	µg/m3	µg/m3

reported value < MDL

italicized text: data used in calcs

Problem with model calculation

bold text: deviation 5

Table A3. Data used for F_{VI} calculations (Continued)

Calculation	Building	C_a_Ben	C_a_Ben_MDL	delta_C_a_Ben	C_i/C_a_Ben	Q_i-*(C_i--C_a-)_Ben
F_vi-	ASU	*0.39*	0.11	30%	1.2	14
F_vi+	ASU	*0.42*	0.12	30%	1.1	none
F_vi+_(R_i+=R_a+)	ASU	*0.45*	0.13	30%	1.3	none

Calculation	Building	C_a_Ben	C_a_Ben_MDL	delta_C_a_Ben	C_i/C_a_Ben	Q_i-*(C_i--C_a-)_Ben
F_vi-	Moffett	***1.1***	0.11	30%	1.0	39
F_vi+	Moffett	***1.5***	0.1	30%	1.0	none
F_vi+_(R_i+=R_a+)	Moffett	***1.4***	0.11	30%	1.1	none

Roadmap of variable names

F_vi-	Building	**C_a**	C_a_MDL	delta_C_a	C_i/C_a	none
F_vi+	Building	**C_a-**	C_a-_MDL	delta_C_a-	C_i-/C_a-	Q_i-*(C_i--C_a-)
F_vi+_(R_i+=R_a+)	Building	**C_a+**	C_a+_MDL	delta_C_a+	C_i+/C_a+	none
Units						
none	none	µg/m3	µg/m3	%	unitless	µg/h

reported value < MDL

italicized text: data used in calcs

Problem with model calculation

bold text: deviation 5

Table A3. Data used for F_{VI} calculations (Continued)

Calculation	Building	Q_i*(C_i-C_a)_Ben	Q_i+*(C_i+-C_a+)_Ben	Q_i-*(C_i--C_a-)-Q_i*(C_i-C_a)_Ben	Q_i*(C_i-C_a)-Q_i+*(C_i+-C_a+)_Ben	Q_i*(R_i-R_a)
F_vi-	ASU	4	45	10	-41	14830
F_vi+	ASU	None	none	none	none	none
F_vi+_(R_i+=R_a+)	ASU	None	none	none	none	none

Calculation	Building	Q_i*(C_i-C_a)_Ben	Q_i+*(C_i+-C_a+)_Ben	Q_i-*(C_i--C_a-)-Q_i*(C_i-C_a)_Ben	Q_i*(C_i-C_a)-Q_i+*(C_i+-C_a+)_Ben	Q_i*(R_i-R_a)
F_vi-	Moffett	0.0	85	39	-85	82556
F_vi+	Moffett	None	none	none	none	none
F_vi+_(R_i+=R_a+)	Moffett	None	none	none	none	none

Roadmap of variable names

F_vi-	Building	Q_i*(C_i-C_a)	Q_i+*(C_i+-C_a+)	Q_i-*(C_i--C_a-)-Q_i*(C_i-C_a)	Q_i*(C_i-C_a)-Q_i+*(C_i+-C_a+)	Q_i*(R_i-R_a)
F_vi+	Building	None	none	none	none	none
F_vi+_(R_i+=R_a+)	Building	None	none	none	none	none
Units						
none	none	µg/h	µg/h	µg/h	µg/h	pCi/h

reported value < MDL

italicized text: data used in calcs

Problem with model calculation

bold text: deviation 5

Table A3. Data used for F_{VI} calculations (Continued)

Calculation	Building	Q_i-*(R_i--R_a-)	Q_i+*(R_i+-R_a+)	Q_i*(R_i-R_a)/[Q_i-*(R_i--R_a-)-Q_i*(R_i-R_a)]	Q_i*(R_i-R_a)/[Q_i*(R_i-R_a)-Q_i+*(R_i+-R_a+)]
F_vi-	ASU	706231	8143	0.021	2.22
F_vi+	ASU	None	none	none	none
F_vi+_(R_i+=R_a+)	ASU	None	none	none	none

Calculation	Building	Q_i-*(R_i--R_a-)	Q_i+*(R_i+-R_a+)	Q_i*(R_i-R_a)/[Q_i-*(R_i--R_a-)-Q_i*(R_i-R_a)]	Q_i*(R_i-R_a)/[Q_i*(R_i-R_a)-Q_i+*(R_i+-R_a+)]
F_vi-	Moffett	213492	-16153	0.631	0.84
F_vi+	Moffett	None	none	none	none
F_vi+_(R_i+=R_a+)	Moffett	None	none	none	none

Roadmap of variable names

F_vi-	Building	Q_i-*(R_i--R_a-)	Q_i+*(R_i+-R_a+)	Q_i*(R_i-R_a)/[Q_i-*(R_i--R_a-)-Q_i*(R_i-R_a)]	Q_i*(R_i-R_a)/[Q_i*(R_i-R_a)-Q_i+*(R_i+-R_a+)]
F_vi+	Building	None	none	none	none
F_vi+_(R_i+=R_a+)	Building	None	none	none	none
Units					
none	none	pCi/h	pCi/h	none	none

reported value < MDL

italicized text: data used in calcs

Problem with model calculation

bold text: deviation 5

Table A3. Data used for F_{VI} calculations (Continued)

Tol=toluene

Calculation	Building	Q_i*C_i_Ben	E_C_Ben	F_a_Ben	F_in_Ben	F_vi_Ben	IA-1_Tol
F_vi-	ASU	25	0	0.85	0.14	0.01	*6.8*
F_vi+	ASU	None	-92	0.85	3.83	-3.68	*2.1*
F_vi+_(R_i+=R_a+)	ASU	None	-41	0.85	1.81	-1.66	*1.8*

Calculation	Building	Q_i*C_i_Ben	E_C_Ben	F_a_Ben	F_in_Ben	F_vi_Ben	IA-1_Tol
F_vi-	Moffett	116	25	1.00	-0.21	0.21	***3.7***
F_vi+	Moffett	None	-71	1.00	0.61	-0.61	***5.4***
F_vi+_(R_i+=R_a+)	Moffett	None	-85	1.00	0.73	-0.73	***8.6***

Roadmap of variable names

F_vi-	Building	Q_i*C_i	E_C-	F_a	F_in-	F_vi-	**1-BL-IA-VOC-1**
F_vi+	Building	None	E_C+	none	F_in+	F_vi+	**1-NP-IA-VOC-1**
F_vi+_(R_i+=R_a+)	Building	None	E_C_(R_i+=R_a+)	none	F_in_(R_i+=R_a+)	F_vi+_(R_i+=R_a+)	**1-PP-IA-VOC-1**
Units							
none	none	µg/h	µg/h	none	none	none	µg/m3

reported value < MDL

italicized text: data used in calcs

Problem with model calculation

bold text: deviation 5

Table A3. Data used for F_{VI} calculations (Continued)

Calculation	Building	IA-1_Tol_MDL	IA-2_Tol	IA-2_Tol_MDL	IA-3_Tol	IA-3_Tol_MDL
F_vi-	ASU	0.2	*2.2*	0.16	*2.2*	0.15
F_vi+	ASU	0.18	*4.4*	0.16	*2.7*	0.19
F_vi+_(R_i+=R_a+)	ASU	0.17	*2.3*	0.19	*2.7*	0.16

Calculation	Building	IA-1_Tol_MDL	IA-2_Tol	IA-2_Tol_MDL	IA-3_Tol	IA-3_Tol_MDL
F_vi-	Moffett	0.15	***4***	0.150	***4***	0.15
F_vi+	Moffett	0.15	***8.3***	0.160	***15***	0.15
F_vi+_(R_i+=R_a+)	Moffett	0.18	***8.4***	0.160	***8.5***	0.17

Roadmap of variable names

F_vi-	Building	1-BL-IA-VOC-1_MDL	**1-BL-IA-VOC-2**	1-BL-IA-VOC-2_MDL	**1-BL-IA-VOC-3**	1-BL-IA-VOC-3_MDL
F_vi+	Building	1-NP-IA-VOC-1_MDL	**1-NP-IA-VOC-2**	1-NP-IA-VOC-2_MDL	**1-NP-IA-VOC-3**	1-NP-IA-VOC-3_MDL
F_vi+_(R_i+=R_a+)	Building	1-PP-IA-VOC-1_MDL	**1-PP-IA-VOC-2**	1-PP-IA-VOC-2_MDL	**1-PP-IA-VOC-3**	1-PP-IA-VOC-3_MDL
Units						
none	none	µg/m3	µg/m3	µg/m3	µg/m3	µg/m3

reported value < MDL

italicized text: data used in calcs

Problem with model calculation

bold text: deviation 5

Table A3. Data used for F_{VI} calculations (Continued)

Calculation	Building	C_i_Tol	std_dev_C_i_Tol	C_a_Tol	C_a_Tol_MDL	delta_C_a_Tol	C_i/C_a_Tol
F_vi-	ASU	3.7	2.7	*3.9*	0.15	30%	1.0
F_vi+	ASU	3.1	1.2	*1.9*	0.16	30%	1.6
F_vi+_(R_i+=R_a+)	ASU	2.3	0.45	*1.5*	0.17	30%	1.5

Calculation	Building	C_i_Tol	std_dev_C_i_Tol	C_a_Tol	C_a_Tol_MDL	delta_C_a_Tol	C_i/C_a_Tol
F_vi-	Moffett	3.9	0.17	***3.5***	0.15	30%	1.1
F_vi+	Moffett	9.6	4.9	***9.4***	0.13	30%	1.0
F_vi+_(R_i+=R_a+)	Moffett	8.5	0.10	***10***	0.15	30%	0.9

Roadmap of variable names

F_vi-	Building	C_i	std_dev_C_i	**C_a**	C_a_MDL	delta_C_a	C_i/C_a
F_vi+	Building	C_i-	std_dev_C_i-	**C_a-**	C_a-_MDL	delta_C_a-	C_i-/C_a-
F_vi+_(R_i+=R_a+)	Building	C_i+	std_dev_C_i+	**C_a+**	C_a+_MDL	delta_C_a+	C_i+/C_a+
Units							
none	none	µg/m3	µg/m3	µg/m3	µg/m3	%	unitless

reported value < MDL

italicized text: data used in calcs

Problem with model calculation

bold text: deviation 5

Table A3. Data used for F_{VI} calculations (Continued)

Calculation	Building	Q_i-*(C_i--C_a-)_Tol	Q_i*(C_i-C_a)_Tol	Q_i+*(C_i+-C_a+)_Tol	Q_i-*(C_i--C_a-)-Q_i*(C_i-C_a)_Tol
F_vi-	ASU	448	-9	279	457
F_vi+	ASU	none	none	none	none
F_vi+_(R_i+=R_a+)	ASU	none	none	none	none

Calculation	Building	Q_i-*(C_i--C_a-)_Tol	Q_i*(C_i-C_a)_Tol	Q_i+*(C_i+-C_a+)_Tol	Q_i-*(C_i--C_a-)-Q_i*(C_i-C_a)_Tol
F_vi-	Moffett	99	42.1	-951	57
F_vi+	Moffett	none	none	none	none
F_vi+_(R_i+=R_a+)	Moffett	none	none	none	none

Roadmap of variable names

F_vi-	Building	none	Q_i*(C_i-C_a)	Q_i+*(C_i+-C_a+)	Q_i-*(C_i--C_a-)-Q_i*(C_i-C_a)
F_vi+	Building	Q_i-*(C_i--C_a-)	none	none	none
F_vi+_(R_i+=R_a+)	Building	none	none	none	none
Units					
none	none	µg/h	µg/h	µg/h	µg/h

reported value < MDL

italicized text: data used in calcs

Problem with model calculation

bold text: deviation 5

Table A3. Data used for F_{VI} calculations (Continued)

Calculation	Building	Q_i*(C_i-C_a)-Q_i+*(C_i+-C_a+)_Tol	Q_i*(R_i-R_a)	Q_i-*(R_i--R_a-)	Q_i+*(R_i+-R_a+)	Q_i*(R_i-R_a)/[Q_i-*(R_i--R_a-)-Q_i*(R_i-R_a)]
F_vi-	ASU	-288	14830	706231	8143	0.021
F_vi+	ASU	None	none	none	none	none
F_vi+_(R_i+=R_a+)	ASU	None	none	none	none	none

Calculation	Building	Q_i*(C_i-C_a)-Q_i+*(C_i+-C_a+)_Tol	Q_i*(R_i-R_a)	Q_i-*(R_i--R_a-)	Q_i+*(R_i+-R_a+)	Q_i*(R_i-R_a)/[Q_i-*(R_i--R_a-)-Q_i*(R_i-R_a)]
F_vi-	Moffett	993	82556	213492	-16153	0.631
F_vi+	Moffett	None	none	none	none	none
F_vi+_(R_i+=R_a+)	Moffett	None	none	none	none	none

Roadmap of variable names

F_vi-	Building	Q_i*(C_i-C_a)-Q_i+*(C_i+-C_a+)	Q_i*(R_i-R_a)	Q_i-*(R_i--R_a-)	Q_i+*(R_i+-R_a+)	Q_i*(R_i-R_a)/[Q_i-*(R_i--R_a-)-Q_i*(R_i-R_a)]
F_vi+	Building	None	none	none	none	none
F_vi+_(R_i+=R_a+)	Building	None	none	none	none	none
Units						
none	none	µg/h	pCi/h	pCi/h	pCi/h	none

reported value < MDL

italicized text: data used in calcs

Problem with model calculation

bold text: deviation 5

Table A3. Data used for F_{VI} calculations (Continued)

Calculation	Building	Q_i*(R_i-R_a)/[Q_i*(R_i-R_a)-Q_i+*(R_i+-R_a+)]	Q_i*C_i_Tol	E_C_Tol	F_a_Tol	F_in_Tol	F_vi_Tol
F_vi-	ASU	2.22	203	10	1.04	-0.09	0.05
F_vi+	ASU	none	none	-639	1.04	3.10	-3.14
F_vi+_(R_i+=R_a+)	ASU	none	none	-288	1.04	1.37	-1.42

Calculation	Building	Q_i*(R_i-R_a)/[Q_i*(R_i-R_a)-Q_i+*(R_i+-R_a+)]	Q_i*C_i_Tol	E_C_Tol	F_a_Tol	F_in_Tol	F_vi_Tol
F_vi-	Moffett	0.84	411	36	0.90	0.02	0.09
F_vi+	Moffett	none	none	831	0.90	-1.92	2.02
F_vi+_(R_i+=R_a+)	Moffett	none	none	993	0.90	-2.32	2.42

Roadmap of variable names

F_vi-	Building	Q_i*(R_i-R_a)/[Q_i*(R_i-R_a)-Q_i+*(R_i+-R_a+)]	Q_i*C_i	E_C-	F_a	F_in-	F_vi-
F_vi+	Building	none	none	E_C+	none	F_in+	F_vi+
F_vi+_(R_i+=R_a+)	Building	none	none	E_C_(R_i+=R_a+)	none	F_in_(R_i+=R_a+)	F_vi+_(R_i+=R_a+)
Units							
none	none	none	µg/h	µg/h	none	none	none

reported value < MDL

italicized text: data used in calcs

Problem with model calculation

bold text: deviation 5

Table A4. Data used to verify model assumption $C_s = C_s^-$

TCE=trichloroethene

Calculation	Building	SS-1_TCE	SS-1_TCE_ MDL	SS-2_TCE	SS-2_TCE_MDL	SS-3_TCE
C_s	ASU	***14***	0.35	***7***	0.38	***9.9***
C_s-	ASU	***8.6***	0.35	***390***	0.4	***390***
C_s+	ASU	***13***	0.39	***8.6***	0.39	***7.2***

Calculation	Building	SS-1_TCE	SS-1_TCE_ MDL	SS-2_TCE	SS-2_TCE_MDL	SS-3_TCE
C_s	Moffett	***3***	0.73	***0.83***	0.37	***2.2***
C_s-	Moffett	***1.9***	0.4	***1***	0.41	***2.5***
C_s+	Moffett	***0.73***	0.42	**0**	*0.41*	***2.3***

Roadmap of variable names

C_s	Building	**1-BL-SS-VOC-1**	1-BL-SS-VOC-1_MDL	**1-BL-SS-VOC-2**	1-BL-SS-VOC-2_MDL	**1-BL-SS-VOC-3**
C_s-	Building	**1-NP-SS-VOC-1**	1-NP-SS-VOC-1_MDL	**1-NP-SS-VOC-2**	1-NP-SS-VOC-2_MDL	**1-NP-SS-VOC-3**
C_s+	Building	**1-PP-SS-VOC-1**	1-PP-SS-VOC-1_MDL	**1-PP-SS-VOC-2**	1-PP-SS-VOC-2_MDL	**1-PP-SS-VOC-3**

Units						
µg/m3	none	µg/m3	µg/m3	µg/m3	µg/m3	µg/m3

reported value < MDL

italics: data used in calcs

Red text: can leak; deviation 3

bold text: deviation 5

orange text: ADQ observations

Table A4. Data used to verify model assumption $C_s = C_s^-$ (Continued)

						excluding SS-1	
Calculation	Building	SS-3_TCE_MDL	C_s_TCE	std_dev_C_s_TCE	C_s/C_i_TCE	C_s_TCE	std_dev_C_s_TCE
C_s	ASU	0.37	10.3	3.5	0.6	8.5	2.1
C_s-	ASU	2	263	220	28	390	0
C_s+	ASU	0.35	9.6	3.0	65	7.9	1.0

Calculation	Building	SS-3_TCE_MDL	C_s_TCE	std_dev_C_s_TCE	C_s/C_i_TCE	C_s_TCE	std_dev_C_s_TCE
C_s	Moffett	0.39	2.0	1.1	0.4	1.5	1.0
C_s-	Moffett	0.42	1.8	0.75	0.6	1.8	1.1
C_s+	Moffett	0.52	1.1	1.0	9.8	1.4	1.3

Roadmap of variable names

C_s	Building	1-BL-SS-VOC-3_MDL	C_s	std_dev_C_s	C_s/C_i	C_s	std_dev_C_s
C_s-	Building	1-NP-SS-VOC-3_MDL	C_s-	std_dev_C_s-	C_s-/C_i-	C_s-	std_dev_C_s-
C_s+	Building	1-PP-SS-VOC-3_MDL	C_s+	std_dev_C_s+	C_s+/C_i+	C_s+	std_dev_C_s+

Units							
µg/m3	none	µg/m3	µg/m3	µg/m3	unitless	µg/m3	µg/m3
reported value < MDL							omit SS-1

italics: data used in calcs

Red text: can leak; deviation 3

bold text: deviation 5

orange text: ADQ observations

Table A4. Data used to verify model assumption $C_s = C_s^-$ (Continued)

DCE=1,1-dichloroethene

Calculation	Building	SS-1_DCE	SS-1_DCE_MDL	SS-2_DCE	SS-2_DCE_MDL	SS-3_DCE
C_s	ASU	***13***	0.35	**0**	*0.38*	***0.95***
C_s-	ASU	***14***	0.35	***310***	0.4	***350***
C_s+	ASU	***20***	0.39	***0.43***	0.39	***2.2***

Calculation	Building	SS-1_DCE	SS-1_DCE_MDL	SS-2_DCE	SS-2_DCE_MDL	SS-3_DCE
C_s	Moffett	N/A	N/A	N/A	N/A	N/A
C_s-	Moffett	N/A	N/A	N/A	N/A	N/A
C_s+	Moffett	N/A	N/A	N/A	N/A	N/A

Roadmap of variable names

C_s	Building	**1-BL-SS-VOC-1**	1-BL-SS-VOC-1_MDL	**1-BL-SS-VOC-2**	1-BL-SS-VOC-2_MDL	**1-BL-SS-VOC-3**
C_s-	Building	**1-NP-SS-VOC-1**	1-NP-SS-VOC-1_MDL	**1-NP-SS-VOC-2**	1-NP-SS-VOC-2_MDL	**1-NP-SS-VOC-3**
C_s+	Building	**1-PP-SS-VOC-1**	1-PP-SS-VOC-1_MDL	**1-PP-SS-VOC-2**	1-PP-SS-VOC-2_MDL	**1-PP-SS-VOC-3**
Units						
µg/m3	none	µg/m3	µg/m3	µg/m3	µg/m3	µg/m3

reported value < MDL

italics: data used in calcs

Red text: can leak; deviation 3

bold text: deviation 5

orange text: ADQ observations

Table A4. Data used to verify model assumption $C_s = C_s^-$ (Continued)

						excluding SS-1	
Calculation	Building	SS-3_DCE_MDL	C_s_DCE	std_dev_C_s_DCE	C_s/C_i_DCE	C_s_DCE	std_dev_C_s_DCE
C_s	ASU	0.37	4.8	7.1	39	0.7	0.4
C_s-	ASU	0.39	225	184	36	330	28
C_s+	ASU	0.35	7.5	10.8	178	1.3	1.3

Calculation	Building	SS-3_DCE_MDL	C_s_DCE	std_dev_C_s_DCE	C_s/C_i_DCE	C_s_DCE	std_dev_C_s_DCE
C_s	Moffett	N/A	N/A	N/A	N/A	N/A	N/A
C_s-	Moffett	N/A	N/A	N/A	N/A	N/A	N/A
C_s+	Moffett	N/A	N/A	N/A	N/A	N/A	N/A

Roadmap of variable names							
C_s	Building	1-BL-SS-VOC-3_MDL	C_s	std_dev_C_s	C_s/C_i	C_s	std_dev_C_s
C_s-	Building	1-NP-SS-VOC-3_MDL	C_s-	std_dev_C_s-	C_s-/C_i-	C_s-	std_dev_C_s-
C_s+	Building	1-PP-SS-VOC-3_MDL	C_s+	std_dev_C_s+	C_s+/C_i+	C_s+	std_dev_C_s+
Units							
µg/m3	none	µg/m3	µg/m3	µg/m3	unitless	µg/m3	µg/m3

reported value < MDL

italics: data used in calcs

Red text: can leak; deviation 3

bold text: deviation 5

orange text: ADQ observations

Table A4. Data used to verify model assumption $C_s = C_s^-$ (Continued)

PCE=tetrachloroethene

Calculation	Building	SS-1_PCE	SS-1_PCE_MDL	SS-2_PCE	SS-2_PCE_MDL	SS-3_PCE
C_s	ASU	N/A	N/A	N/A	N/A	N/A
C_s-	ASU	N/A	N/A	N/A	N/A	N/A
C_s+	ASU	N/A	N/A	N/A	N/A	N/A

Calculation	Building	SS-1_PCE	SS-1_PCE_MDL	SS-2_PCE	SS-2_PCE_MDL	SS-3_PCE
C_s	Moffett	***2.2***	0.73	***0.77***	0.37	***3.1***
C_s-	Moffett	***1.4***	0.4	*0.55*	0.41	***6.2***
C_s+	Moffett	***0.69***	0.42	***1***	0.41	***3.2***

Roadmap of variable names

C_s	Building	**1-BL-SS-VOC-1**	1-BL-SS-VOC-1_MDL	**1-BL-SS-VOC-2**	1-BL-SS-VOC-2_MDL	**1-BL-SS-VOC-3**
C_s-	Building	**1-NP-SS-VOC-1**	1-NP-SS-VOC-1_MDL	**1-NP-SS-VOC-2**	1-NP-SS-VOC-2_MDL	**1-NP-SS-VOC-3**
C_s+	Building	**1-PP-SS-VOC-1**	1-PP-SS-VOC-1_MDL	**1-PP-SS-VOC-2**	1-PP-SS-VOC-2_MDL	**1-PP-SS-VOC-3**

Units						
µg/m3	none	µg/m3	µg/m3	µg/m3	µg/m3	µg/m3

reported value < MDL

italics: data used in calcs

Red text: can leak; deviation 3

bold text: deviation 5

orange text: ADQ observations

Table A4. Data used to verify model assumption $C_s = C_s^-$ (Continued)

						excluding SS-1	
Calculation	Building	SS-3_PCE_MDL	C_s_PCE	std_dev_C_s_PCE	C_s/C_i_PCE	C_s_PCE	std_dev_C_s_PCE
C_s	ASU	N/A	N/A	N/A	N/A	N/A	N/A
C_s-	ASU	N/A	N/A	N/A	N/A	N/A	N/A
C_s+	ASU	N/A	N/A	N/A	N/A	N/A	N/A

Calculation	Building	SS-3_PCE_MDL	C_s_PCE	std_dev_C_s_PCE	C_s/C_i_PCE	C_s_PCE	std_dev_C_s_PCE
C_s	Moffett	0.39	2.0	1.2	0.7	1.9	1.6
C_s-	Moffett	0.42	2.7	3.0	1.4	3.4	4.0
C_s+	Moffett	0.52	1.6	1.4	3.9	2.1	1.6

Roadmap of variable names							
C_s	Building	1-BL-SS-VOC-3_MDL	C_s	std_dev_C_s	C_s/C_i	C_s	std_dev_C_s
C_s-	Building	1-NP-SS-VOC-3_MDL	C_s-	std_dev_C_s-	C_s-/C_i-	C_s-	std_dev_C_s-
C_s+	Building	1-PP-SS-VOC-3_MDL	C_s+	std_dev_C_s+	C_s+/C_i+	C_s+	std_dev_C_s+
Units							
µg/m3	none	µg/m3	µg/m3	µg/m3	unitless	µg/m3	µg/m3
reported value < MDL						omit SS-1	

italics: data used in calcs

Red text: can leak; deviation 3

bold text: deviation 5

orange text: ADQ observations

Table A4. Data used to verify model assumption $C_s = C_s^-$ (Continued)

		Ben=benzene				
Calculation	Building	SS-1_Ben	SS-1_Ben_MDL	SS-2_Ben	SS-2_Ben_MDL	SS-3_Ben
C_s	ASU	***0.42***	0.35	**0**	*0.38*	***0.37***
C_s-	ASU	***0.84***	0.35	***0.64***	0.4	***0.65***
C_s+	ASU	**0**	*0.39*	**0**	*0.39*	***0.58***

Calculation	Building	SS-1_Ben	SS-1_Ben_MDL	SS-2_Ben	SS-2_Ben_MDL	SS-3_Ben
C_s	Moffett	***0.98***	0.73	***0.42***	0.37	***2.7***
C_s-	Moffett	***0.75***	0.4	***0.45***	0.41	***2***
C_s+	Moffett	***0.75***	0.42	***0.83***	0.41	***1.5***

Roadmap of variable names						
C_s	Building	**1-BL-SS-VOC-1**	1-BL-SS-VOC-1_MDL	**1-BL-SS-VOC-2**	1-BL-SS-VOC-2_MDL	**1-BL-SS-VOC-3**
C_s-	Building	**1-NP-SS-VOC-1**	1-NP-SS-VOC-1_MDL	**1-NP-SS-VOC-2**	1-NP-SS-VOC-2_MDL	**1-NP-SS-VOC-3**
C_s+	Building	**1-PP-SS-VOC-1**	1-PP-SS-VOC-1_MDL	**1-PP-SS-VOC-2**	1-PP-SS-VOC-2_MDL	**1-PP-SS-VOC-3**
Units						
µg/m3	none	µg/m3	µg/m3	µg/m3	µg/m3	µg/m3

reported value < MDL

italics: data used in calcs

Red text: can leak; deviation 3

bold text: deviation 5

orange text: ADQ observations

Table A4. Data used to verify model assumption $C_s = C_s^-$ (Continued)

						excluding SS-1	
Calculation	Building	SS-3_Ben_MDL	C_s_Ben	delta_C_s_Ben	C_s/C_i_Ben	C_s_Ben	delta_C_s_Ben
C_s	ASU	0.37	0.39	0.03	0.85	0.38	0.01
C_s-	ASU	0.39	0.71	0.11	1.55	0.65	0.01
C_s+	ASU	0.35	0.45	0.11	0.79	0.49	0.13

Calculation	Building	SS-3_Ben_MDL	C_s_Ben	delta_C_s_Ben	C_s/C_i_Ben	C_s_Ben	delta_C_s_Ben
C_s	Moffett	0.39	1.37	1.19	1.24	1.61	1.61
C_s-	Moffett	0.42	1.07	0.82	0.68	1.10	1.10
C_s+	Moffett	0.52	1.03	0.41	0.67	0.47	0.47

Roadmap of variable names

C_s	Building	1-BL-SS-VOC-3_MDL	C_s	std_dev_C_s	C_s/C_i	C_s	std_dev_C_s
C_s-	Building	1-NP-SS-VOC-3_MDL	C_s-	std_dev_C_s-	C_s-/C_i-	C_s-	std_dev_C_s-
C_s+	Building	1-PP-SS-VOC-3_MDL	C_s+	std_dev_C_s+	C_s+/C_i+	C_s+	std_dev_C_s+
Units							
µg/m3	none	µg/m3	µg/m3	µg/m3	unitless	µg/m3	µg/m3
reported value < MDL						omit SS-1	

italics: data used in calcs

Red text: can leak; deviation 3

bold text: deviation 5

orange text: ADQ observations

Table A4. Data used to verify model assumption $C_s = C_s^-$ (Continued)

		Tol=toluene				
Calculation	Building	SS-1_Tol	SS-1_Tol_MDL	SS-2_Tol	SS-2_Tol_MDL	SS-3_Tol
C_s	ASU	***3.8***	1.8	**0**	*1.9*	***2.4***
C_s-	ASU	***12***	1.8	**0**	*2*	**0**
C_s+	ASU	**0**	*1.9*	**0**	*2*	***3.7***

Calculation	Building	SS-1_Tol	SS-1_Tol_MDL	SS-2_Tol	SS-2_Tol_MDL	SS-3_Tol
C_s	Moffett	**0**	*3.7*	**0**	*1.8*	***7.1***
C_s-	Moffett	***3.3***	2	**0**	*2.1*	***5.8***
C_s+	Moffett	***3.5***	2.1	***4***	2.1	***4.8***

Roadmap of variable names						
C_s	Building	**1-BL-SS-VOC-1**	1-BL-SS-VOC-1_MDL	**1-BL-SS-VOC-2**	1-BL-SS-VOC-2_MDL	**1-BL-SS-VOC-3**
C_s-	Building	**1-NP-SS-VOC-1**	1-NP-SS-VOC-1_MDL	**1-NP-SS-VOC-2**	1-NP-SS-VOC-2_MDL	**1-NP-SS-VOC-3**
C_s+	Building	**1-PP-SS-VOC-1**	1-PP-SS-VOC-1_MDL	**1-PP-SS-VOC-2**	1-PP-SS-VOC-2_MDL	**1-PP-SS-VOC-3**
Units						
µg/m3	none	µg/m3	µg/m3	µg/m3	µg/m3	µg/m3

reported value < MDL

italics: data used in calcs

Red text: can leak; deviation 3

bold text: deviation 5

orange text: ADQ observations

Table A4. Data used to verify model assumption $C_s = C_s^-$ (Continued)

						excluding SS-1	
Calculation	Building	SS-3_Tol_MDL	C_s_Tol	delta_C_s_Tol	C_s/C_i_Tol	C_s_Tol	delta_C_s_Tol
C_s	ASU	1.9	2.7	1.0	0.7	2.2	0.4
C_s-	ASU	*2*	5.3	5.8	1.7	2.0	0.0
C_s+	ASU	1.8	2.5	1.0	1.1	2.9	1.2

Calculation	Building	SS-3_Tol_MDL	C_s_Tol	delta_C_s_Tol	C_s/C_i_Tol	C_s_Tol	delta_C_s_Tol
C_s	Moffett	2	4.2	2.7	1.1	4.5	3.7
C_s-	Moffett	2.1	3.7	1.9	0.4	4.0	2.6
C_s+	Moffett	2.6	4.1	0.7	0.5	4.4	0.6

Roadmap of variable names

C_s	Building	1-BL-SS-VOC-3_MDL	C_s	std_dev_C_s	C_s/C_i	C_s	std_dev_C_s
C_s-	Building	1-NP-SS-VOC-3_MDL	C_s-	std_dev_C_s-	C_s-/C_i-	C_s-	std_dev_C_s-
C_s+	Building	1-PP-SS-VOC-3_MDL	C_s+	std_dev_C_s+	C_s+/C_i+	C_s+	std_dev_C_s+

Units							
µg/m3	none	µg/m3	µg/m3	µg/m3	unitless	µg/m3	µg/m3
reported value < MDL							omit SS-1

italics: data used in calcs

Red text: can leak; deviation 3

bold text: deviation 5

orange text: ADQ observations

Table A5. Data used to verify Mosley Model assumptions $R_s = R_s^-$, $R_a << R_s$, $R_a^- << R_s^-$, and $R_a^+ << R_s^+$

Calculation	Building	SS-1_1_Rn	SS-1_1_Rn_SD	SS-1_1_Rn_MDL	SS-1_2_Rn	SS-1_2_Rn_SD	SS-1_2_Rn_MDL
R_s,R_a	ASU	*404*	42	115	*488*	46	127
R_s-,R_a-	ASU	*429*	43	119	*425*	43	118
R_s+,R_a+	ASU	*376*	40	111	*447*	44	122

Calculation	Building	SS-1_1_Rn	SS-1_1_Rn_SD	SS-1_1_Rn_MDL	SS-1_2_Rn	SS-1_2_Rn_SD	SS-1_2_Rn_MDL
R_s,R_a	Moffett	*147*	26	71	*166*	27	76
R_s-,R_a-	Moffett	*175*	28	77	*185*	29	79
R_s+,R_a+	Moffett	*81*	20	54	*107*	22	62

Variable names

R_s,R_a	Building	BL-SS-1_1_Rn	BL-SS-1_1_Rn_SD	BL-SS-1_1_Rn_MDL	BL-SS-1_2_Rn	BL-SS-1_2_Rn_SD	BL-SS-1_2_Rn_MDL
R_s-,R_a-	Building	NP-SS-1_1_Rn	NP-SS-1_1_Rn_SD	NP-SS-1_1_Rn_MDL	NP-SS-1_2_Rn	NP-SS-1_2_Rn_SD	NP-SS-1_2_Rn_MDL
R_s+,R_a+	Building	PP-SS-1_1_Rn	PP-SS-1_1_Rn_SD	PP-SS-1_1_Rn_MDL	PP-SS-1_2_Rn	PP-SS-1_2_Rn_SD	PP-SS-1_2_Rn_MDL

Units							
pCi/L	none	pCi/L	pCi/L	pCi/L	pCi/L	pCi/L	pCi/L

reported value < MDL

italicized text: data used in calcs

Table A5. Data used to verify Mosley Model assumptions $R_s = R_s^-$, $R_a << R_s$, $R_a^- << R_s^-$, and $R_a^+ << R_s^+$ (Continued)

Calculation	Building	SS-1_3_Rn	SS-1_3_Rn_SD	SS-1_3_Rn_MDL	SS-2_1_Rn	SS-2_1_Rn_SD	SS-2_1_Rn_MDL
R_s,R_a	ASU	*419*	42	117	*76*	19	53
R_s-,R_a-	ASU	*446*	44	121	*118*	23	65
R_s+,R_a+	ASU	*410*	42	116	*58*	17	48

Calculation	Building	SS-1_3_Rn	SS-1_3_Rn_SD	SS-1_3_Rn_MDL	SS-2_1_Rn	SS-2_1_Rn_SD	SS-2_1_Rn_MDL
R_s,R_a	Moffett	*180*	28	79	*72*	19	51
R_s-,R_a-	Moffett	*209*	30	84	*246*	33	91
R_s+,R_a+	Moffett	*108*	22	62	*18*	10	29

Variable names

R_s,R_a	Building	BL-SS-1_3_Rn	BL-SS-1_3_Rn_SD	BL-SS-1_3_Rn_MDL	BL-SS-2_1_Rn	BL-SS-2_1_Rn_SD	BL-SS-2_1_Rn_MDL
R_s-,R_a-	Building	NP-SS-1_3_Rn	NP-SS-1_3_Rn_SD	NP-SS-1_3_Rn_MDL	NP-SS-2_1_Rn	NP-SS-2_1_Rn_SD	NP-SS-2_1_Rn_MDL
R_s+,R_a+	Building	PP-SS-1_3_Rn	PP-SS-1_3_Rn_SD	PP-SS-1_3_Rn_MDL	PP-SS-2_1_Rn	PP-SS-2_1_Rn_SD	PP-SS-2_1_Rn_MDL
Units							
pCi/L	none	pCi/L	pCi/L	pCi/L	pCi/L	pCi/L	pCi/L

reported value < MDL

italicized text: data used in calcs

Table A5. Data used to verify Mosley Model assumptions $R_s = R_s^-$, $R_a << R_s$, $R_a^- << R_s^-$, and $R_a^+ << R_s^+$ (Continued)

Calculation	Building	SS-2_2_Rn	SS-2_2_Rn_SD	SS-2_2_Rn_MDL	SS-2_3_Rn	SS-2_3_Rn_SD	SS-2_3_Rn_MDL
R_s,R_a	ASU	*88*	21	57	*77*	20	54
R_s-,R_a-	ASU	*112*	23	64	*86*	21	57
R_s+,R_a+	ASU	*41.1*	15	41.2	*37*	14	*40*

Calculation	Building	SS-2_2_Rn	SS-2_2_Rn_SD	SS-2_2_Rn_MDL	SS-2_3_Rn	SS-2_3_Rn_SD	SS-2_3_Rn_MDL
R_s,R_a	Moffett	*81*	20	54	*93*	21	58
R_s-,R_a-	Moffett	*249*	33	92	*278*	35	97
R_s+,R_a+	Moffett	*19*	11	29	*18*	10	*29*

Variable names

R_s,R_a	Building	BL-SS-2_2_Rn	BL-SS-2_2_Rn_SD	BL-SS-2_2_Rn_MDL	BL-SS-2_3_Rn	BL-SS-2_3_Rn_SD	BL-SS-2_3_Rn_MDL
R_s-,R_a-	Building	NP-SS-2_2_Rn	NP-SS-2_2_Rn_SD	NP-SS-2_2_Rn_MDL	NP-SS-2_3_Rn	NP-SS-2_3_Rn_SD	NP-SS-2_3_Rn_MDL
R_s+,R_a+	Building	PP-SS-2_2_Rn	PP-SS-2_2_Rn_SD	PP-SS-2_2_Rn_MDL	PP-SS-2_3_Rn	PP-SS-2_3_Rn_SD	PP-SS-2_3_Rn_MDL
Units							
pCi/L	none	pCi/L	pCi/L	pCi/L	pCi/L	pCi/L	pCi/L

reported value < MDL

italicized text: data used in calcs

Table A5. Data used to verify Mosley Model assumptions $R_s = R_s^-$, $R_a << R_s$, $R_a^- << R_s^-$, and $R_a^+ << R_s^+$ (Continued)

Calculation	Building	SS-3_1_Rn	SS-3_1_Rn_SD	SS-3_1_Rn_MDL	SS-3_2_Rn	SS-3_2_Rn_SD	SS-3_2_Rn_MDL
R_s,R_a	ASU	*15*	11	30	*18*	11	31
R_s-,R_a-	ASU	*101*	22	61	*105*	22	62
R_s+,R_a+	ASU	*4.8*	7.3	20	*4.8*	8.5	24

Calculation	Building	SS-3_1_Rn	SS-3_1_Rn_SD	SS-3_1_Rn_MDL	SS-3_2_Rn	SS-3_2_Rn_SD	SS-3_2_Rn_MDL
R_s,R_a	Moffett	*528*	47	132	*587*	50	139
R_s-,R_a-	Moffett	*592*	50	139	*648*	53	146
R_s+,R_a+	Moffett	*613*	51	141	*633*	52	144

Variable names

R_s,R_a	Building	BL-SS-3_1_Rn	BL-SS-3_1_Rn_SD	BL-SS-3_1_Rn_MDL	BL-SS-3_2_Rn	BL-SS-3_2_Rn_SD	BL-SS-3_2_Rn_MDL
R_s-,R_a-	Building	NP-SS-3_1_Rn	NP-SS-3_1_Rn_SD	NP-SS-3_1_Rn_MDL	NP-SS-3_2_Rn	NP-SS-3_2_Rn_SD	NP-SS-3_2_Rn_MDL
R_s+,R_a+	Building	PP-SS-3_1_Rn	PP-SS-3_1_Rn_SD	PP-SS-3_1_Rn_MDL	PP-SS-3_2_Rn	PP-SS-3_2_Rn_SD	PP-SS-3_2_Rn_MDL
Units							
pCi/L	none	pCi/L	pCi/L	pCi/L	pCi/L	pCi/L	pCi/L

reported value < MDL

italicized text: data used in calcs

Table A5. Data used to verify Mosley Model assumptions $R_s = R_s^-$, $R_a << R_s$, $R_a^- << R_s^-$, and $R_a^+ << R_s^+$ (Continued)

Calculation	Building	SS-3_3_Rn	SS-3_3_Rn_SD	SS-3_3_Rn_MDL	SS-1_Rn_AVG	std_dev_SS-1_Rn
R_s,R_a	ASU	*15*	11	31	437	45
R_s-,R_a-	ASU	*135*	25	70	433	11
R_s+,R_a+	ASU	*8.6*	7.9	22	411	36

Calculation	Building	SS-3_3_Rn	SS-3_3_Rn_SD	SS-3_3_Rn_MDL	SS-1_Rn_AVG	std_dev_SS-1_Rn
R_s,R_a	Moffett	*549*	48	134	164	16
R_s-,R_a-	Moffett	*684*	54	150	190	18
R_s+,R_a+	Moffett	*611*	51	141	99	15

Variable names

R_s,R_a	Building	BL-SS-3_3_Rn	BL-SS-3_3_Rn_SD	BL-SS-3_3_Rn_MDL	BL-SS-1_Rn_AVG	std_dev_BL-SS-1_Rn
R_s-,R_a-	Building	NP-SS-3_3_Rn	NP-SS-3_3_Rn_SD	NP-SS-3_3_Rn_MDL	NP-SS-1_Rn_AVG	std_dev_NP-SS-1_Rn
R_s+,R_a+	Building	PP-SS-3_3_Rn	PP-SS-3_3_Rn_SD	PP-SS-3_3_Rn_MDL	PP-SS-1_Rn_AVG	std_dev_PP-SS-1_Rn

Units

pCi/L	none	pCi/L	pCi/L	pCi/L	pCi/L	pCi/L

reported value < MDL

italicized text: data used in calcs

Table A5. Data used to verify Mosley Model assumptions $R_s = R_s^-$, $R_a << R_s$, $R_a^- << R_s^-$, and $R_a^+ << R_s^+$ (Continued)

Calculation	Building	SS-2_Rn_AVG	std_dev_SS-2_Rn	SS-3_Rn_AVG	std_dev_SS-3_Rn	R_s	std_dev_R_s
R_s,R_a	ASU	80	7.0	16	1.7	178	227
R_s-,R_a-	ASU	106	17	113	18	218	187
R_s+,R_a+	ASU	46	11	6.0	2.2	154	223

Calculation	Building	SS-2_Rn_AVG	std_dev_SS-2_Rn	SS-3_Rn_AVG	std_dev_SS-3_Rn	R_s	std_dev_R_s
R_s,R_a	Moffett	82	11	555	30	267	253
R_s-,R_a-	Moffett	258	18	641	47	363	243
R_s+,R_a+	Moffett	18	0.5	619	12	245	326

Variable names

R_s,R_a	Building	BL-SS-2_Rn_AVG	std_dev_BL-SS-2_Rn	BL-SS-3_Rn_AVG	std_dev_BL-SS-3_Rn	R_s	std_dev_R_s
R_s-,R_a-	Building	NP-SS-2_Rn_AVG	std_dev_NP-SS-2_Rn	NP-SS-3_Rn_AVG	std_dev_NP-SS-3_Rn	R_s-	std_dev_R_s-
R_s+,R_a+	Building	PP-SS-2_Rn_AVG	std_dev_PP-SS-2_Rn	PP-SS-3_Rn_AVG	std_dev_PP-SS-3_Rn	R_s+	std_dev_R_s+
Units							
pCi/L	none	pCi/L	pCi/L	pCi/L	pCi/L	pCi/L	pCi/L

reported value < MDL

italicized text: data used in calcs

Table A5. Data used to verify Mosley Model assumptions $R_s = R_s^-$, $R_a << R_s$, $R_a^- << R_s^-$, and $R_a^+ << R_s^+$ (Continued)

		excluding SS-1							
Calculation	Building	R_s	std_dev_R_s	R_a	R_a_MDL	delta_R_a	R_s/R_i	R_s/R_a	delta_(R_s/R_a)
R_s,R_a	ASU	48	45	*0.104*	0.289	0.038	472	1703	2258
R_s-,R_a-	ASU	110	5	*0.026*	0.220	0.028	116	8215	11239
R_s+,R_a+	ASU	26	28	*0.069*	0.055	0.052	1686	2232	3642

Calculation	Building	R_s	std_dev_R_s	R_a	R_a_MDL	delta_R_a	R_s/R_i	R_s/R_a	delta_(R_s/R_a)
R_s,R_a	Moffett	N/A	N/A	*0.177*	0.175	0.008	278	1507	1427
R_s-,R_a-	Moffett	N/A	N/A	*0.256*	0.237	0.066	589	1416	1017
R_s+,R_a+	Moffett	N/A	N/A	*0.328*	0.165	0.107	811	748	1024

Variable names

R_s,R_a	Building	R_s	std_dev_R_s	R_a	R_a_MDL	delta_R_a	R_s/R_i	R_s/R_a	delta_(R_s/R_a)
R_s-,R_a-	Building	R_s-	std_dev_R_s-	R_a-	R_a-_MDL	delta_R_a-	R_s-/R_i-	R_s-/R_a-	delta_(R_s-/R_a-)
R_s+,R_a+	Building	R_s+	std_dev_R_s+	R_a+	R_a+_MDL	delta_R_a+	R_s+/R_i+	R_s+/R_a+	delta_(R_s+/R_a+)
Units									
pCi/L	none	pCi/L	pCi/L	pCi/L	pCi/L	pCi/L	unitless	unitless	unitless

reported value < MDL

italicized text: data used in calcs

Table A5. Data used to verify Mosley Model assumptions $R_s = R_s^-$, $R_a << R_s$, $R_a^- << R_s^-$, and $R_a^+ << R_s^+$ (Continued)

		excluding SS-1	
Calculation	Building	R_s/R_a	delta_(R_s/R_a)
R_s,R_a	ASU	463	466
R_s-,R_a-	ASU	4137	4407
R_s+,R_a+	ASU	373	492

Calculation	Building	R_s/R_a	delta_(R_s/R_a)
R_s,R_a	Moffett	N/A	N/A
R_s-,R_a-	Moffett	N/A	N/A
R_s+,R_a+	Moffett	N/A	N/A

Variable names

R_s,R_a	Building	R_s/R_a	delta_(R_s/R_a)
R_s-,R_a-	Building	R_s-/R_a-	delta_(R_s-/R_a-)
R_s+,R_a+	Building	R_s+/R_a+	delta_(R_s+/R_a+)

Units			
pCi/L	none	unitless	Unitless

reported value < MDL

italicized text: data used in calcs

Table A6. Data used to verify $Q_i >> \lambda V$, $Q_i^- >> \lambda V$, $Q_i^+ >> \lambda V$

Calculation	Building	Q_i	delta_Q_i	lambda	delta_lambda	V	delta_V	lambda*V	delta_(lambda*V)
Q_i,lamda*V	ASU	54	14	0.0075546	1%	273.5	30%	2.07	0.62
Q_i-,lamda*V	ASU	384	351	0.0075546	1%	273.5	30%	2.07	0.62
Q_i+,lamda*V	ASU	364	342	0.0075546	1%	273.5	30%	2.07	0.62

Calculation	Building	Q_i	delta_Q_i	lambda	delta_lambda	V	delta_V	lambda*V	delta_(lambda*V)
Q_i,lamda*V	Moffett	105	13	0.0075546	1%	364.8	30%	2.76	0.83
Q_i-,lamda*V	Moffett	592	256	0.0075546	1%	364.8	30%	2.76	0.83
Q_i+,lamda*V	Moffett	634	542	0.0075546	1%	364.8	30%	2.76	0.83

Roadmap of variable names

Q_i,lamda*V	Building	Q_i	delta_Q_i	lambda	delta_lambda	V	delta_V	lambda*V	delta_(lambda*V)
Q_i-,lamda*V	Building	Q_i-	delta_Q_i-	lambda	delta_lambda	V	delta_V	lambda*V	delta_(lambda*V)
Q_i+,lamda*V	Building	Q_i+	delta_Q_i+	lambda	delta_lambda	V	delta_V	lambda*V	delta_(lambda*V)
Units									
m3/h	none	m3/h	m3/h	/h	%	m3	%	m3/h	m3/h

Table A6. Data used to verify $Q_i >> \lambda V$, $Q_i^- >> \lambda V$, $Q_i^+ >> \lambda V$ (Continued)

Calculation	Building	Q_i/(lambda*V)	delta_[Q_i/(lambda*V)]
Q_i,lamda*V	ASU	26	10
Q_i-,lamda*V	ASU	186	179
Q_i+,lamda*V	ASU	176	174

Calculation	Building	Q_i/(lambda*V)	delta_[Q_i/(lambda*V)]
Q_i,lamda*V	Moffett	38	12
Q_i-,lamda*V	Moffett	215	113
Q_i+,lamda*V	Moffett	230	209

Roadmap of variable names

Q_i,lamda*V	Building	Q_i/(lambda*V)	delta_[Q_i/(lambda*V)]
Q_i-,lamda*V	Building	Q_i-/(lambda*V)	delta_[Q_i+/(lambda*V)]
Q_i+,lamda*V	Building	Q_i+/(lambda*V)	delta_[Q_i+/(lambda*V)]

Units			
m3/h	None	unitless	unitless

Table A7. Indoor air, ambient air, and sub-slab SF_6 data

Calculation	Building	AA_SF_6	AA_SF_6_MDL	SS-1_SF_6	SS-1_SF_6 _MDL	SS-2_SF_6
T_s,T_i/T_s	ASU	0	*8.8*	*290*	17	*260*
T_s-,T_i-/T_s-	ASU	*12*	9.4	*120*	8	*14*
T_s+,T_i+/T_s+	ASU	0	*10*	*370*	9	*1,000*

Calculation	Building	AA_SF_6	AA_SF_6_MDL	SS-1_SF_6	SS-1_SF_6 _MDL	SS-2_SF_6
T_s,T_i/T_s	Moffett	*18*	8.7	*1,800*	110	*1,700*
T_s-,T_i-/T_s-	Moffett	*16*	7.9	*200*	10	*86*
T_s+,T_i+/T_s+	Moffett	*18*	9.1	*570*	10	*750*

Roadmap of variable names

Q_i*R_i	Building	1-BL-AA-VOC-1	1-BL-AA-VOC-1_MDL	1-BL-SS-VOC-1	1-BL-SS-VOC-1_MDL	1-BL-SS-VOC-2
Q_i-*R_i-	Building	1-NP-AA-VOC-1	1-NP-AA-VOC-1_MDL	1-NP-SS-VOC-1	1-NP-SS-VOC-1_MDL	1-NP-SS-VOC-2
Q_i+*R_i+	Building	1-PP-AA-VOC-1	1-PP-AA-VOC-1_MDL	1-PP-SS-VOC-1	1-PP-SS-VOC-1_MDL	1-PP-SS-VOC-2
Units						
pCi/h	none	µg/m3	µg/m3	µg/m3	µg/m3	µg/m3

reported value < MDL

italicized text: data used in calcs

Table A7. Indoor air, ambient air, and sub-slab SF_6 data (Continued)

							excluding SS-1	
Calculation	Building	SS-2_SF_6 MDL	SS-3_SF_6	SS-3_SF_6 MDL	T_s	std_dev_T_s	T_s	std_dev_T_s
T_s,T_i/T_s	ASU	9	*1,700*	88	750	823	980	1018
T_s-,T_i-/T_s-	ASU	10	*24*	9.4	53	59	19	7
T_s+,T_i+/T_s+	ASU	19	*1,600*	84	990	615	1300	424

Calculation	Building	SS-2_SF_6 MDL	SS-3_SF_6	SS-3_SF_6 MDL	T_s	delta_T_s	T_s	std_dev_T_s
T_s,T_i/T_s	Moffett	88	*100*	9	1,200	954	N/A	N/A
T_s-,T_i-/T_s-	Moffett	10	*72*	10	119	70	N/A	N/A
T_s+,T_i+/T_s+	Moffett	10	*90*	10	470	341	N/A	N/A

Roadmap of variable names

Q_i*R_i	Building	1-BL-SS-VOC-2_MDL	1-BL-SS-VOC-3	1-BL-SS-VOC-3_MDL	T_s	std_dev_T_s	T_s	std_dev_T_s
Q_i-*R_i-	Building	1-NP-SS-VOC-2_MDL	1-NP-SS-VOC-3	1-NP-SS-VOC-3_MDL	T_s-	std_dev_T_s-	T_s-	std_dev_T_s-
Q_i+*R_i+	Building	1-PP-SS-VOC-2_MDL	1-PP-SS-VOC-3	1-PP-SS-VOC-3_MDL	T_s+	std_dev_T_s+	T_s+	std_dev_T_s+
Units								
pCi/h	none	µg/m3	µg/m3	µg/m3	µg/m3	µg/m3	µg/m3	µg/m3

reported value < MDL

italicized text: data used in calcs

Table A7. Indoor air, ambient air, and sub-slab SF_6 data (Continued)

							excluding SS-1	
Calculation	Building	T_i	std_dev_T_i	T_i/T_a	T_s/T_i	delta_(T_s/T_i)	T_s/T_i	delta_(T_s/T_i)
T_s,T_i/T_s	ASU	5200	1253	591	0.14	0.16	0.19	0.20
T_s-,T_i-/T_s-	ASU	780	710	65	0.07	0.10	0.02	0.02
T_s+,T_i+/T_s+	ASU	867	810	87	1.1	1.3	1.5	1.5

Calculation	Building	T_i	std_dev_T_i	T_i/T_a	T_s/T_i	delta_(T_s/T_i)	T_s	std_dev_T_s
T_s,T_i/T_s	Moffett	3300	265	183	0.36	0.29	N/A	N/A
T_s-,T_i-/T_s-	Moffett	563	237	35	0.21	0.15	N/A	N/A
T_s+,T_i+/T_s+	Moffett	530	450	29	0.89	1.0	N/A	N/A

Roadmap of variable names

Q_i*R_i	Building	T_i	std_dev_T_i	T_i/T_a	T_s/T_i	delta_(T_s/T_i)	T_s/T_i	delta_(T_s/T_i)
Q_i-*R_i-	Building	T_i-	std_dev_T_i-	T_i-/T_a-	T_s-/T_i-	delta_(T_s-/T_i-)	T_s-/T_i-	delta_(T_s-/T_i-)
Q_i+*R_i+	Building	T_i+	std_dev_T_i+	T_i+/T_a+	T_s+/T_i+	delta_(T_s+/T_i+)	T_s+/T_i+	delta_(T_s+/T_i+)
Units								
pCi/h	none	µg/m3	µg/m3	unitless	unitless	unitless	unitless	unitless

reported value < MDL

italicized text: data used in calcs

Table A8. Calculation of Mass Discharges

						Radon			TCE	
Pressure	Building	Q_i	R_i	R_a	Q_i·R_i	Q_i·R_a	Q_i·(R_i-R_a)	Q_i·C_i_TCE	Q_i·C_a_TCE	Q_i·(C_i_TCE-C_a_TCE)
BL	ASU	54	377	104	20520	5690	14830	1017	9.3	1008
NP	ASU	384	1868	26	716388	10157	706231	3631	58	3574
PP	ASU	364	91	69	33310	25167	8143	53	31	23
BL/BL	ASU	N/A	N/A	N/A	1.0	0.28	0.72	1.0	0.01	0.99
NP/BL	ASU	N/A	N/A	N/A	35	0.49	34.4	3.6	0.06	3.5
PP/BL	ASU	N/A	N/A	N/A	1.6	1.2	0.40	0.05	0.03	0.02

Pressure	Building	Q_i	R_i	R_a	Q_i·R_i	Q_i·R_a	Q_i·(R_i-R_a)	Q_i·C_i_TCE	Q_i·C_a_TCE	Q_i·(C_i_TCE-C_a_TCE)
BL	Moffett	105	961	177	101219	18663	82556	519	8.8	511
NP	Moffett	592	617	256	365347	151855	213492	1856	71	1785
PP	Moffett	634	302	328	191721	207874	-16153	74	56	18
BL/BL	Moffett	N/A	N/A	N/A	1.0	0.18	0.82	1.0	0.02	0.98
NP/BL	Moffett	N/A	N/A	N/A	3.6	1.5	2.1	3.6	0.14	3.4
PP/BL	Moffett	N/A	N/A	N/A	1.9	2.1	-0.16	0.14	0.11	0.03

Values highlighted in green are plotted in Figures 16 and 17.

Table A8. Calculation of Mass Discharges (Continued)

		1,1-DCE			PCE		
Pressure	Building	Q_i·C_i_DCE	Q_i·C_a_DCE	Q_i·(C_i_DCE-C_a_DCE)	Q_i·C_i_PCE	Q_i·C_a_PCE	Q_i·(C_i_PCE-C_a_PCE)
BL	ASU	6.7	2.0	4.7	N/A	N/A	N/A
NP	ASU	2391	15	2376	N/A	N/A	N/A
PP	ASU	15.4	15.3	0.12	N/A	N/A	N/A
BL/BL	ASU	1.0	0.30	0.70	N/A	N/A	N/A
NP/BL	ASU	356	2.2	354	N/A	N/A	N/A
PP/BL	ASU	2.3	2.3	0.02	N/A	N/A	N/A

Pressure	Building	Q_i·C_i_DCE	Q_i·C_a_DCE	Q_i·(C_i_DCE-C_a_DCE)	Q_i·C_i_PCE	Q_i·C_a_PCE	Q_i·(C_i_PCE-C_a_PCE)
BL	Moffett	N/A	N/A	N/A	298	13	286
NP	Moffett	N/A	N/A	N/A	1185	124	1060
PP	Moffett	N/A	N/A	N/A	266	564	-298
BL/BL	Moffett	N/A	N/A	N/A	1.0	0.04	0.96
NP/BL	Moffett	N/A	N/A	N/A	4.0	0.42	3.6
PP/BL	Moffett	N/A	N/A	N/A	0.89	1.89	-1.00

Table A8. Calculation of Mass Discharges (Continued)

			SF6			Benzene			Toluene	
Pressure	Building	Q_i·T_i	Q_i·T_a	Q_i·(T_i-T_a)	Q_i·C_i_Ben	Q_i·C_a_Ben	Q_i·(C_i_Ben-C_a_Ben)	Q_i·C_i_Tol	Q_i·C_a_Tol	Q_i·(C_i_Tol-C_a_Tol)
BL	ASU	283293	479	282814	24.9	21.2	3.6	203	212	-9
NP	ASU	299201	4603	294598	175	161	14	1176	729	448
PP	ASU	315823	3641	312182	209	164	45	825	546	279
BL/BL	ASU	1.0	0.00	1.00	1.0	0.85	0.15	1.0	1.04	-0.04
NP/BL	ASU	1.06	0.02	1.04	7.0	6.5	0.6	5.8	3.6	2.2
PP/BL	ASU	1.11	0.01	1.10	8.4	6.6	1.8	4.1	2.7	1.4

Pressure	Building	Q_i·T_i	Q_i·T_a	Q_i·(T_i-T_a)	Q_i·C_i_Ben	Q_i·C_a_Ben	Q_i·(C_i_Ben-C_a_Ben)	Q_i·C_i_Tol	Q_i·C_a_Tol	Q_i·(C_i_Tol-C_a_Tol)
BL	Moffett	347459	1895	345564	115.8	116	0.0	411	369	42
NP	Moffett	333696	9478	324219	928	889	39	5667	5568	99
PP	Moffett	336020	11412	324608	972	888	85	5389	6340	-951
BL/BL	Moffett	1.0	0.01	0.99	1.0	1.00	0.00	1.0	0.90	0.10
NP/BL	Moffett	0.96	0.03	0.93	8.0	7.7	0.3	13.8	13.6	0.24
PP/BL	Moffett	0.97	0.03	0.93	8.4	7.7	0.7	13.1	15.4	-2.3